To Mr. Patrick T. Chiarito

STRUCTURES RESEARCH 42

SHEAR LAG IN Box BEAMS
Kuhn, Chiarito
TR 739

RESTRICTED

NATIONAL ADVISORY COMMITTEE FOR AERONAUTICS

CLASSIFIED DOCUMENT

This document contains classified information affecting the National Defense of the United States within the meaning of the Espionage Act, USC 50:31 and 32. Its transmission or the revelation of its contents in any manner to an unauthorized person is prohibited by law. Information so classified may be imparted only to persons in the military and naval Services of the United States, appropriate civilian officers and employees of the Federal Government who have a legitimate interest therein, and to United States citizens of known loyalty and discretion who of necessity must be informed thereof.

# SHEAR LAG IN BOX BEAMS

## METHODS OF ANALYSIS AND EXPERIMENTAL INVESTIGATIONS

By Paul Kuhn and Patrick T. Chiarito
Langley Memorial Aeronautical Laboratory

T.R. 739

68

FOR REFERENCE

NOT TO BE TAKEN FROM THIS ROOM

May 1941

# SHEAR LAG IN BOX BEAMS

## METHODS OF ANALYSIS AND EXPERIMENTAL INVESTIGATIONS

By Paul Kuhn and Patrick T. Chiarito

## SUMMARY

The bending stresses in the covers of box beams or wide-flange beams differ appreciably from the stresses predicted by the ordinary bending theory on account of shear deformation of the flanges. The problem of predicting these differences has become known as the shear-lag problem.

The first part of the paper deals with methods of shear-lag analysis suitable for practical use. The basic elements of these methods have been published in previous papers, but the treatment of these methods presented in this paper is consolidated and improved in several respects. The methods are sufficiently general to cover any arbitrary spanwise variation of cross section and loading as well as chordwise variations of stringer area, stringer spacing, and sheet thickness. Methods of analyzing the effects of cut-outs are also given.

The second part of the paper describes strain-gage tests made by the NACA to verify the theory. Three tests were made on axially loaded panels of variable cross section, six were made on beams of variable cross section, and three were made on beams of constant cross section for extreme or limiting cases. Three tests published by other investigators are also analyzed by the proposed method.

In order to make the test of the theory as severe as possible, the NACA specimens were designed to show larger shear-lag effects than may be expected in typical present-day construction. The agreement was quite satisfactory even in extreme cases such as very short, wide beams. Satisfactory agreement was also found in tests on the limiting case of a cover without stiffeners; this agreement shows that the theory is applicable to the case of heavy cover plates used without stiffening or to cases in which continuous stiffening in the form of corrugated sheet is used.

The third part of the paper gives numerical examples illustrating the methods of analysis. An appendix gives

comparisons with other methods, particularly with the method of Ebner and Koller.

## INTRODUCTION

The bending stresses in box beams do not always conform very closely to the predictions of the engineering theory of bending. The deviations from the theory are caused chiefly by the shear deformations in the cover of the box that constitutes the flange of the beam. The problem of analyzing these deviations from the engineering theory of bending has become known as the shear-lag problem, a term that is convenient although not very descriptive.

The most important case of shear-lag action occurs in the wing structure. The cross section of the wing usually varies considerably along the span; analytical solutions based on the assumption of constant cross section are therefore of little practical value, and methods of analysis have had to be developed to cope with the conditions found in actual structures. The development of such methods has been continued over a period of several years (references 1 to 3) and it is now possible to give a reasonably well-rounded presentation of practical methods of analysis.

The paper is divided into three parts. The first part discusses the methods of analysis. The second part describes tests made by the NACA and shows comparisons between experimental and calculated results for the NACA tests as well as for tests made elsewhere. Numerical examples to illustrate the methods of analysis are presented in the third part.

The method of presentation chosen is intended to meet the needs of the practicing stress analyst. The paper contains the information actually needed in stress analysis; detailed derivations and discussions have been omitted, but they may be found in several of the cited references.

# I. METHODS OF ANALYSIS

## DEFINITION OF THE PROBLEM AND BASIC ASSUMPTIONS

Reduced to its simplest form the problem may be stated as follows: A sheet, stiffened or unstiffened, is fastened to a foundation along one edge and loaded along the two edges perpendicular to the foundation by distributed or concentrated forces as indicated in figure 1. The sheet may be a structure in itself (fig. 2(a)) or it may be the cover of a box beam (fig. 2(b)). The problem is to find the stresses in the sheet.

As shown in figure 1, stiffeners are theoretically necessary along the loaded edges if concentrated forces P are introduced because the stresses would otherwise become infinite. These edge stiffeners will be referred to throughout this paper as "corner flanges" or simply "flanges." Other stiffeners parallel to the loaded edges will be referred to as "longitudinals" or "stringers"; these stiffeners may or may not exist in any given case and may or may not be attached to the foundation.

It will be assumed that the structure is always symmetrical about a longitudinal plane ($y = 0$). This assumption materially simplifies the problem without decreasing the practical usefulness of the theory very much because most practical structures are at least approximately symmetrical. On account of the symmetry, it will be sufficient to consider one-half of the structure in all derivations and computations.

It will be assumed that infinitely many ribs of infinite extensional (chordwise) stiffness are distributed along the span. An equivalent assumption is frequently made in theoretical solutions of stress problems. The assumption is plausible in this case because it is fairly obvious that the extensional stiffness of the ribs together with the lateral bending stiffness of the flanges between the ribs is sufficient to take care of such transverse stresses as might arise from longitudinal forces and stresses. The final proof that the assumption of rigid ribs is admissible must, of course, be furnished by experiments like those described in the second part of this paper.

The field of shear-lag analysis is very extensive; it was therefore considered advisable to confine the discus-

sion, in general, to beams with flat covers. The most general method of analysis given in this paper can be very readily extended to beams with cambered covers and this extension is therefore given. An approximate method for dealing with moderate amounts of camber is given in reference 2.

## ANALYSIS OF SINGLE-STRINGER STRUCTURES

Structures like those shown in figure 2, having but a single stringer, are rarely encountered in practice. Nevertheless, the analysis of single-stringer structures will be fully discussed for several reasons. The immediate reason is that the fundamental relations as well as all the methods of analysis can be easily demonstrated on this type of structure. A more important reason is the fact that the most rapid method of analyzing multistringer structures is based on the temporary reduction of the multistringer structure to a single-stringer structure.

### Sign Conventions

The sign conventions adopted are as follows: Normal stresses and strains in the stringers and the flanges are positive when they are tensile. Shear stresses and strains in the cover sheet are positive when they are caused by positive strains in the flange. Shear stresses in the web are positive when they are causing positive strains in the flange.

The compression side of the beam is analyzed independently of the tension side. It is therefore permissible and convenient to retain the sign convention just given for the analysis of the compression side, changing only the definition of stringer stresses to positive when compressive.

In general, the positive directions of the coordinate axes will be taken as shown in figure 3. In some cases, particularly for analytical solutions, it is more convenient to use the opposite direction for the positive x-direction because the resulting formulas are simpler. (See, for instance, formulas for axially loaded panels, references 1 and 2.)

## Fundamental Equations and Analytical Solutions

For purposes of shear-lag analysis, all structures are idealized in a manner familiar, for instance, from the design of plate girders. Stringers are assumed to be concentrated at their centroids; the idealized sheet is assumed to carry only shear, but the fact that the actual sheet carried longitudinal stresses in addition to the shear is taken into account by adding the well-known effective width of the sheet to the stringers. The participation of the shear web in the bending action is expressed by adding $1/6\ ht_W$ to $A_F$, which makes the section modulus of the idealized section equal to that of the actual section. Figure 4 shows the idealized cross sections of a single-stringer panel and of a single-stringer beam; the standard basic symbols used in this paper are indicated in this figure. A complete list of symbols is given in appendix A.

Figure 5 shows an idealized single-stringer beam of constant cross section subjected to a transverse load at the tip. Inspection of the free-body diagrams in figure 5(b) shows that there are two equations of static equilibrium,

$$dF_F = S_W \frac{dx}{h} - dS_C \tag{1a}$$

$$dF_L = dS_C \tag{1b}$$

where $S_W$ is the shear force in the web, in this case equal to $P$; and $dS_C = \tau\, t\, dx$, where $\tau$ denotes the shear stress in the cover sheet.

Under the assumption of infinite transverse stiffness, the relative longitudinal displacement $(u_F - u_L)$ of two corresponding points on the flange and on the longitudinal divided by the width $b$ defines the shear strain $\gamma$ and therefore the shear stress $\tau$ (fig. 5(c)). Because the displacements $u$ are given by the expression $u = \int_{x=L}^{x=x} \frac{\sigma}{E}\, dx$, differentiation gives the basic elastic relation

$$d\tau = -\frac{G}{Eb} (\sigma_F - \sigma_L)\, dx \tag{1c}$$

where G is the effective shear modulus, which takes into account the effects of buckling when necessary. Equations (1a), (1b), and (1c) can be combined to form a differential equation, and this equation can be solved for simple cases. A number of solutions are given in references 1 and 2; similar solutions have been given by other authors. These analytical solutions are of some value in making comparative studies and in studying various aspects of the shear-lag problem. For practical stress analysis, however, numerical methods capable of dealing with arbitrary variations of cross section and loading are required. Two such methods will be described: the solution by means of a recurrence formula and the solution by successive shear-fault reduction.

## Analysis of Single-Stringer Structures by the Recurrence Formula

Principle and scope of method.- The principle of analyzing a beam of variable cross section is as follows: The beam is divided into a convenient number of bays in such a way that the cross section and the running shear in the web $S_w/h$ may be assumed to be constant within each bay. The shear deformation in the cover sheet of each bay is computed in terms of the unknown forces acting between bays. Application of the principle of consistent deformations then gives a set of equations, similar in form to three-moment equations, for the unknown forces.

Theoretically, the method permits taking into account any variation of cross section and loading along the span. The limitations are similar to those encountered in other problems of stress distribution in cases of variable cross section and loading.

Recurrence formula for shear lag.- As stated in the preceding section, the beam is divided into a number of bays; the cross section and the web shear $S_w/h$ are assumed to be constant within each bay. The lengths of the bays need not be equal nor need they be small, as is often required in similar methods. In the limit, a single bay may span the entire length of the beam. The system of numbering the stations and the bays between stations is shown in figure 6.

Each individual bay can now be treated as a free body subjected to certain forces (fig. 7). These forces can be

split into two groups (fig. 8): one group consists of the forces calculated by the ordinary bending theory, which assumes no shear deformation; the other group represents the differences between the actual forces and the forces of the first group or, in other words, the changes in forces caused by the shear deformation of the cover sheet.

The first group of forces will be designated P-forces to indicate that they are calculated by the theory that assumes plane sections to remain plane. Individual forces and stresses belonging to this group will be denoted by a superscript P. The calculation of these forces and stresses is familiar to every engineer and consequently need not be discussed in detail.

The second group of forces will be designated X-forces. Because the P-forces on any one bay are in static equilibrium, the X-forces on any one bay must be a self-equilibrated group longitudinally; that is, at any given station the force $X_F$ acting on the flange must be equal and opposite to the force $X_L$ acting on the longitudinal. This conclusion was anticipated in figure 8 by writing X without subscripts F and L.

The shear deformation of the cover sheet can now be calculated in terms of the known P-forces and the unknown X-forces; the details of this calculation are given in reference 3. Equating the deformations at the adjoining ends of successive bays yields the recurrence formula

$$X_{n-1}\, q_n - X_n(p_n + p_{n+1}) + X_{n+1}\, q_{n+1} = -\gamma_n + \gamma_{n+1} \qquad (2)$$

where

$$p_n = \frac{K}{Gt \tanh KL} \qquad (3a)$$

$$q_n = \frac{K}{Gt \sinh KL} \qquad (3b)$$

$$\gamma_n = \frac{S_W A_L}{htA_T G} = \frac{S Q_L}{G_e I t} \qquad (3c)$$

K is a shear-lag parameter appearing in all analytical solutions for single-stringer structures (references 1 and 2) and is defined by

$$K^2 = \frac{Gt}{Eb}\left(\frac{1}{A_F} + \frac{1}{A_L}\right) \qquad (4)$$

In equations (3a) to (3c), each individual quantity should be understood to have a subscript n, indicating the average value for the bay in question. Note should be taken that this statement applies to L, which is to be taken as the length of the individual bay in question, not as the length of the entire beam.

Strictly speaking, all coefficients $\gamma$ appearing in this paper should have a superscript P. These superscripts have been omitted because they are not needed in the actual use of the equations; they are needed only in the derivation of the equations (reference 3).

Written in more explicit form, the equations are

$$\left.\begin{aligned}
X_0 q_1 - X_1(p_1 + p_2) + X_2 q_2 &= -\gamma_1 + \gamma_2 \\
X_1 q_2 - X_2(p_2 + p_3) + X_3 q_3 &= -\gamma_2 + \gamma_3 \\
&\cdots \\
X_{n-1} q_n - X_n(p_n + p_{n+1}) + X_{n+1} q_{n+1} &= -\gamma_n + \gamma_{n+1} \\
&\cdots \\
X_{r-1} q_r - X_r(p_r + p_{r+1}) &= -\gamma_r + \gamma_{r+1}
\end{aligned}\right\} \qquad (5)$$

It will be noted that the externally applied load appears only in the coefficients $\gamma$; for any given beam, then, the left-hand side of the equations remains unchanged if changes occur in the loading.

Boundary conditions.- Before the system of equations (5) can be solved, the boundary conditions at the tip and at the root must be defined. At the tip, the following cases may arise:

(1) Only a transverse force is applied (fig. 9(a)). In this case, $X_0 = 0$.

(2) A longitudinal force P may be introduced (fig. 9(b)). In this case

$$X_0 = P\frac{A_L}{A_T} \qquad (6)$$

When the longitudinal force P is the only force applied to the beam, the idealized shear web is inactive, and the problem is that of an axially loaded panel.

At the root, the following cases may arise:

1. The flange and the longitudinal are connected to a rigid foundation.

2. The flange and the longitudinal are connected to a foundation that deforms under load.

3. The flange is connected to the foundation; the longitudinal is not connected.

This system of classifying the possible cases is based on the convention of defining the foundation as the station where the vertical shear is taken out.

Case 1 at the root arises in practice when a wing is continuous from tip to tip. The plane of symmetry is equivalent to a rigid foundation. Case 2 arises in practice when a wing is joined to carry-through members passing through the fuselage. Case 3 has been used in practical design to facilitate the assembly of the wing to the fuselage by reducing the number of bolts to a minimum.

The foundation may be considered as bay r+1. In case 1 there is no shear deformation of bay r+1, and $p_{r+1}$ as well as $\gamma_{r+1}$ equal zero. In case 2, $\gamma_{r+1}$ equals zero, because no shear is carried in bay r+1; the deformation of the bay depends only on the axial stiffnesses of the flange and the longitudinal passing through the fuselage, and

$$p_{r+1} = \left(\frac{1}{A_F} + \frac{1}{A_L}\right) \frac{L}{bE} \tag{7}$$

where L is the distance from the wing root to the plane of symmetry of the airplane.

In case 3 the last equation of the system cannot be used, and $X_r$ is found by inspection to be

$$X_r = \frac{M}{h_W} \frac{A_L}{A_T} \tag{8}$$

Calculation of stresses from X-forces.- After the system of equations (5) has been solved, the longitudinal stresses are found by superposing on the stresses calculated by the ordinary bending formula the stresses calculated from the X-forces

$$\sigma_F = \sigma_F^P + X/A_F \tag{9a}$$

and

$$\sigma_L = \sigma_L^P - X/A_L \tag{9b}$$

where $\sigma^P$ is the stress calculated by the ordinary bending formula. In the case under discussion, where the beam has no camber,

$$\sigma_F^P = \sigma_L^P = \frac{M}{h\,A_T} \tag{10}$$

The running shear in the cover sheet of bay n close to the inboard end of the bay, that is, close to station n, is given by the formula

$$(\tau t)_{n_i} = \left(\frac{SA_L}{h\,A_T}\right)_n + X_{n-1}\,\frac{K_n}{\sinh K_n L_n} - X_n\,\frac{K_n}{\tanh K_n L_n} \tag{11a}$$

Near the outboard end of bay n, that is, near station n - 1, the running shear in the cover sheet is

$$(\tau t)_{n_o} = \left(\frac{SA_L}{h\,A_T}\right)_n + X_{n-1}\,\frac{K_n}{\tanh K_n L_n} - X_n\,\frac{K_n}{\sinh K_n L_n} \tag{11b}$$

For some applications it is desired to compute the average running shear in a bay. If the bay is not too long, this average shear may be obtained by averaging the shears at the two ends of the bay computed by the formulas just given. The result is

$$(\tau t_m)_{av} = \left(\frac{SA_L}{h\,A_T}\right)_n - \frac{1}{2}\,Gt\,(X_n - X_{n-1})\,(p_n + q_n) \tag{11c}$$

An alternative way to compute the average shear is to use the basic static relation (1b)

$$(\tau t L)_n = F_{L_n} - F_{L_{n-1}} \qquad (11d)$$

Formula (11d) gives the true average, while formula (11c) is approximate.

Influence of taper in depth and width.- When a beam is tapered in depth, it is necessary to remember that part of the vertical shear is carried by the inclined flanges and longitudinals, so that

$$S_W = S_E - \frac{M}{h} \tan i \qquad (12)$$

where $i$ is the inclination of the tension flange with respect to the compression flange.

When a beam is tapered in width, neither the ordinary bending theory nor the shear-lag theory is strictly applicable. The error caused by applying the ordinary bending theory, however, is small for normal angles of taper; to a similar degree of approximation, the following approximate method of shear-lag calculation may be used.

Assume that the taper is removed by making the widths $b$ at all stations equal to the width $b_r$ at the root. At the same time, increase the sheet thicknesses in the ratio $b_r/b$. The result will be an untapered beam that has the same shear stiffness $Gt/b$ at any station as the actual beam. This method of procedure assumes that transverse components of longitudinal forces can be neglected; this assumption is in keeping with the assumption of rigid ribs.

It should be noted that the parameter $K$ (equation (4)) in any bay of the fictitious untapered beam is equal to the corresponding parameter $K$ of the actual tapered beam, but the coefficients $p$, $q$, and $\gamma$ of the fictitious beam differ from those of the actual beam by the ratio $b/b_r$. It is stated in reference 3 that the effect of taper in plan form might be more pronounced than is indicated by the method just given. Re-examination of the test data in the light of the additional test experience gained since reference 3 was written tends to show that the method given here is sufficiently accurate for the taper ratios likely to be encountered on wings.

## Analysis of Single-Stringer Structures by Successive Shear-Fault Reduction

Principle and scope of method.- The principle of the method of successive shear-fault reduction is as follows.

An estimate is made of the stresses $\sigma_F$ in the flange; the stresses $\sigma_L$ in the longitudinal are calculated by statics. By the application of the basic equation (1c) and a process of numerical integration, the spanwise distribution of shear force in the sheet can then be calculated. On the other hand, application of the basic equation (1b) also gives a spanwise curve of shear force in the sheet. The two curves will not agree except by accident because the estimated values of $\sigma_F$ and $\sigma_L$ will not fulfill the elastic relations and the boundary conditions except by accident. The difference between the two curves will be referred to as the curve of "shear faults."

The existence of shear faults in the calculation proves that the assumed stresses $\sigma_F$ do not constitute the true solution of the stress problem for the specified external loads. The assumed stresses $\sigma_F$ constitute, however, the true solution for a closely related problem, namely, the structure subjected to the specified external loads and, in addition, subjected to a system of external loads equal to the shear faults. Obviously, then, the desired solution can be obtained from the assumed solution by deducting the effects of the shear faults. This deduction is effected by superposing the effects of corrective external shear forces that are assumed to be applied in opposite direction to the shear faults.

If the magnitudes of the corrections were made equal to the faults, the basic static equation (1b) would be fulfilled at each station but the basic elastic relation (1c) would be upset. As a compromise between these conflicting requirements, the correction is made equal to one-half of the fault.

Because transverse forces are absorbed by the rib system and are not considered, the introduction of an external shear is equivalent to the introduction of a pair of equal and opposite forces. By St. Venant's principle, the influence of such a combination of forces is felt over only a limited distance. In order to simplify the computa-

tion, it will be assumed that the influence of each corrective force decreases to zero at the next station. Errors introduced by this simplification will be small and will eventually be eliminated by repeating the process of correction.

Application of the corrective forces to the initially assumed values of $\sigma_F$ and $\sigma_L$ yields a new set of values for $\sigma_F$ and $\sigma_L$, and the entire process is repeated. It will be found that the corrective forces are becoming smaller with each repetition of the process, so that the solution will be obtained by a sufficient number of repetitions. In theory, the computation is finished when the corrections to $\sigma_F$ and $\sigma_L$ are reduced to one unit of the last significant figure of $\sigma_F$ or $\sigma_L$. In practice, the computation will often be finished sooner at the discretion of the analyst.

For single-stringer structures, the method of successive shear-fault reduction is unlikely to be favored over the recurrence formula because the time required for a solution depends very much on the ability of the analyst to make a good initial estimate of $\sigma_F$ and $\sigma_L$. The time required for a solution by means of the recurrence formula, on the other hand, is almost independent of the skill and the experience of the analyst because the only item left to his choice is the number of bays. The method of shear-fault reduction for single-stringer structures, however, is the direct basis of the most general method for analyzing multistringer structures, and this fact justifies the description of the method.

Method of successive shear-fault reduction.- In order to apply the method of shear-fault reduction, the beam is divided into a convenient number of bays. Because the computation involves numerical integration and differentiation, the lengths $\Delta x$ of these bays must be chosen fairly small so that no appreciable error is made by assuming the stresses to vary linearly in each bay. Five bays may be considered as the minimum. In order to reduce the time required for computation and the possibility of errors, the bays should be made of equal lengths whenever feasible.

The computation is started by tabulating for each station the given magnitudes of $A_F$, $A_L$, t, G, and M/h (or P) if they vary along the span. If the beam tapers in

width, a fictitious beam of constant width is used, as previously discussed.

The magnitudes just enumerated should be separately tabulated because they will remain constant; whereas, the main part of the calculation is repeated a number of times. The details of the procedure are learned most easily by following column for column the numerical example given in part III, table X.

Column 1 in table X gives assumed values for $\sigma_F$. In assuming these stress values, the analyst must be guided by previous experience. It is possible to use any arbitrary values whatever but, if the assumed values differ too much from the true ones, a large number of cycles of the computation will be required. The simplest procedure for general use is to multiply the stresses obtained from the ordinary bending theory by a factor slightly larger than unity. With some experience, this factor can be estimated reasonably well from a knowledge of the average of the shear-lag parameter KL and the loading condition.

Column 2 gives the forces $F_F = \sigma_F A_F$.

Column 3 gives the forces $F_L = M/h - F_F$ in the case of a beam or $F_L = P - F_F$ in the case of an axially loaded panel.

Column 4 gives the stresses $\sigma_L = F_L/A_L$.

Column 5 gives the differences between columns 1 and 4 $(\sigma_F - \sigma_L)$.

Column 6 gives the increments of shear stress obtained from the basic relation (1c),

$$\Delta\tau = -\frac{G\Delta x}{Eb}(\sigma_F - \sigma_L) \qquad \text{(SS-1)}$$

It will be noted that the values of $\Delta\tau$ in column 6 are positive. This sign arises from the fact that the integration of the shear stress increments proceeds from the root to the tip so that the increments $\Delta x$ are negative.

Column 7 gives the shear stresses $\tau$ in each bay. These stresses are obtained by adding up the increments

given in column 6, starting at the root where $\tau = 0$. It should be noted that the values of $\Delta\tau$ represent the increments of shear stress for intervals of length $\Delta x$ along the span; the distance between the root and the middle of bay r is, however, only half an interval $\Delta x$, so that the value of $\tau$ in the root bay is $\tau = \frac{1}{2} \Delta \tau$. From here on, the full value of $\Delta\tau$ is added each time, unless the value of $\tau$ at the tip is to be calculated when a one-half step would be used again. (The value of $\tau$ at the tip is needed for the calculation of the margin of safety, but it is not needed for the calculations indicated in table X. Consequently, this value is calculated only after the last cycle has been completed.)

Column 8 gives the increments of shear force

$$\Delta S_{CE} = \tau t \Delta x \qquad (SS-2)$$

Column 9 gives the increments $\Delta F_L$, obtained by subtracting the value of $F_L$ at the outboard end of the bay from the value of $F_L$ at the inboard end of the bay.

According to the basic relation (1c), $\Delta F_L$ should equal $\Delta S_{CE}$ in each bay. The differences in each bay constitute the shear faults

$$SF = \Delta S_{CE} - \Delta F_L \qquad (SS-3)$$

and the shear faults SF are given in column 10.

Consider now figure 10(a), which shows one bay with a positive shear fault SF and the corresponding shear-fault correction SFC; SFC is in the form of external forces distributed uniformly along the bay.

The length of a bay is small compared with the length of the structure; it may therefore be assumed that the properties of the structure just outboard and just inboard of the bay considered are the same. Under this assumption, one-half of the shear-fault correction SFC will be absorbed by the structure outboard of the bay; the other half will be absorbed by the structure inboard of the bay. As previously stated, the total shear-fault corrective force will be taken as one-half of the shear fault

$$\text{Total SFC} = -\frac{1}{2} SF \qquad (SS-4)$$

Therefore the corrective force at the outboard end of the bay will be

$$SFC_o = -\frac{1}{2} SFC = \frac{1}{4} SF \qquad (SS-5a)$$

and the corrective force at the inboard end of the bay will be

$$SFC_i = \frac{1}{2} SFC = -\frac{1}{4} SF \qquad (SS-5b)$$

The corrective stresses $\Delta\sigma_F$ and $\Delta\sigma_L$ are found by dividing the corrective forces $SFC_o$ and $SFC_i$ by the areas $A_F$ or $A_L$ and are shown in figure 10(b). The signs of the corrective stress $\Delta\sigma_F$ are the signs given in formulas (SS-5a) and (SS-5b), while the signs of the corrective stresses $\Delta\sigma_L$ are opposite to those given in formulas (SS-5a) and (SS-5b) (fig. 10(b)).

At the tip station there is no outboard structure to develop any resistance to the shear-fault correction force. Consequently, for the tip bay

$$SFC_o = 0 \qquad (SS-5c)$$

$$SFC_i = SFC = \frac{1}{2} SF \qquad (SS-5d)$$

In the numerical example, table X, it will be seen that column 11 lists the values of $SFC_o$ and column 12 lists the values of $SFC_i$. At each station there is one value of $SFC_o$ and one value of $SFC_i$. The sum of the two values is the final value of the shear-fault corrective force and is tabulated in column 13.

Column 14 gives $\Delta\sigma_F = SFC/A_F$, and column 15 gives $\Delta\sigma_L = -SFC/A_L$.

The addition of the corrections $\Delta\sigma_F$ to the initially assumed values of $\sigma_F$ and of the corrections $\Delta\sigma_L$ to the initial values of $\sigma_L$ gives a new set of values for $\sigma_F$ and $\sigma_L$. The entire process is then repeated as indicated in table XI but the column giving $F_F$ is no longer needed.

The entire calculation as shown in table XI is repeated

again and again until successive sets of values of $\sigma_F$ and $\sigma_L$ are judged to agree with sufficient accuracy. The limit of possible accuracy is reached when the values of $\Delta\sigma_F$ or $\Delta\sigma_L$ become equal to unity in the last significant figure of $\sigma_F$ or $\sigma_L$.

In order to avoid carrying along errors, $F_L$ should be obtained from the static equation $F_L = M/h - F_F$ every second or third cycle instead of from $\Delta\sigma_L$.

The sum of the shear faults may be used as an indication that correct sign conventions have been used; the sum of the faults in any given cycle must be smaller than the sum of the faults in the preceding cycle. This criterion is not sufficiently sensitive to prove the absence of any numerical error, but it is sometimes a welcome help when starting calculations.

A complication arises when the longitudinal is not connected at the root. In this case, the stress $\sigma_L$ is equal to zero at the root but the shear stress $\tau$ is not equal to zero. It is therefore impossible to proceed directly with the summation of the increments $\Delta\tau$. In order to overcome this difficulty, a trial value $\tau_o$ for $\tau$ at $x = 0$ is assumed, and the summation proceeds from this trial value. From statics, it is evident that

$$S_{CE} = \sum_{x=0}^{x=L} \Delta S_{CE} = 0$$

The trial value $\tau_o$ must therefore be negative, so that the summation of the increments $\Delta S_{CE}$ along the entire span may be equal to zero. On the first trial, this condition will not be met except by accident, and the trial value for $\tau_o$ must be adjusted until the given condition is met. Speaking graphically, the process consists in finding the area between a curve (the $\tau t$-curve) and an arbitrary horizontal line, and then shifting the horizontal line until the area becomes zero. After the first cycle has been completed, the value $\tau_o$ obtained can be used as a trial value for the second cycle, and it will be so close that the necessary adjustment will be small.

When the longitudinal is discontinuous at some point

other than the root, the summation of the increments $\Delta\tau$ may be performed in the usual manner for the region between the root and the inboard end of the break. The region from the outboard end of the break to the tip is treated in a manner analogous to that just discussed for a longitudinal discontinuous at the root.

In a cambered beam, the basic equation (1c) must be modified to read

$$d\tau = -\frac{G}{Eb'}\left[(\sigma_F - \sigma_L) - (\sigma_F{}^P - \sigma_L{}^P)\right] dx \qquad (1c')$$

as shown in reference 2. In this equation, $\sigma_F{}^P$ is the stress in the flange calculated by the usual $Mc/I$ formula, and $\sigma_L{}^P$ is the stress in the longitudinal calculated by the $Mc/I$ formula. In the case of a flat cover, $\sigma_F{}^P$ equals $\sigma_L{}^P$ and they cancel, reducing equation (1c') to equation (1c). When a cambered beam is analyzed by the shear-fault-reduction method, formula (SS-1) must be modified to conform with formula (1c'). An additional column will therefore be required after column 5 in table X.

## ANALYSIS OF MULTISTRINGER STRUCTURES

Two methods will be given for the analysis of multistringer structures. The first method consists in reducing the problem to that of a fictitious single-stringer structure that can be analyzed by the recurrence formula. The final step of transferring back to the actual multistringer structure can be made only under the assumption that the chordwise distribution of material - stringers and sheet - is uniform and that the moduli E and G are constant along the chord. Small variations from uniformity can be disregarded but, when large variations exist, it is desirable to have a more general method available. For such cases, a method of successive shear-fault reduction is described that is an extension of the method of successive shear-fault reduction described for single-stringer structures. This method permits taking into account arbitrary chordwise variations of stringer size, stringer spacing, sheet thickness, and elastic moduli.

## Substitute Single-Stringer Method

Principle of method.- The transverse bending loads acting on a box beam are taken up first by the shear webs. The shear stresses in the web are partly converted into normal stresses at the flange; the rest of the stresses becomes shear in the cover sheet, which is gradually converted into normal stresses in the longitudinals as the longitudinal plane of symmetry is approached. It may be said, therefore, that the most important physical action centers around the flange because the conversion of shear stress into bending stress begins here.

This consideration leads to a very convenient method of analyzing a multistringer structure by substituting temporarily a fictitious single-stringer structure. This fictitious structure retains without change those parts of the actual structure in which the primary and the most important action takes place, namely, the shear web, the corner flange, and the sheet adjacent to it. The longitudinals, however, are combined into a single fictitious stringer, the "substitute single stringer," located at the centroid of the internal forces in the stringers. The analysis of the resulting single-stringer structure can be performed by the methods described previously and gives the actual stress in the flange (equation (9a)) as well as the actual shear stress in the cover sheet next to the flange (equations (11)). For the stress in the longitudinals, only an average value is obtained by the analysis of the fictitious single-stringer structure. The stresses in the individual longitudinals of the actual structure are calculated at any given station along the span by assuming that the average stress just calculated is distributed chordwise according to the hyperbolic-cosine law found in such analytical solutions as have been published.

The validity of the substitution method outlined can be made plausible in a general way by reference to St. Venant's principle. A much more convincing proof, however, will be given by the comparisons between experimental and calculated results in the second part of this paper.

Determination of the substitute single-stringer structure (first approximation).- A typical cross section of a multistringer structure is shown in figure 11(a). This cross section is idealized as indicated in figure 11(b). It should be noted that the effective width of skin adjacent to the flange is considered as a longitudinal distinct

from the flange. The adoption of this rule makes it feasible to cover all possible cases with a single rule because in a limiting case such as shown in figure 1, for instance, obviously the entire sheet should be considered as constituting the longitudinals. Incidentally, this rule tends to reduce the error due to the finite number of stringers that will be discussed.

The width d of the idealized sheet between longitudinals depends on the spacing $b_1$ between rivet rows and on the type of the stiffeners. Open-section stiffeners (fig. 12(a)) do not contribute to the shear stiffness of the cover; therefore, $d = b_1$. Closed-section stiffeners (fig. 12(b)) contribute to the shear stiffness of the cover. If this contribution is taken into account, the idealized width for shear deformation is $d = b_1 + b_{2e}$, in which

$$b_{2e} = \frac{b_2}{1 + \frac{t_{st} b_2}{t_p}} \qquad (13)$$

where $t_{st}$ is the thickness of the stiffener and p the perimeter, or developed width, of the stiffener between rivet rows.

The idealized multistringer structure (fig. 11(b)) is now converted into a single-stringer structure by combining all idealized longitudinals into a single longitudinal located at the force centroid of the longitudinals. Because the actual stresses are not known at this stage, the stresses computed by the ordinary bending theory are used to obtain a first approximation. For the flat covers under consideration, the force centroid will then be the centroid of the cross-sectional areas of the stringers, the Mc/I stress being the same in all stringers. The distance of this centroid from the flange is the width $b_S$ of the substitute structure (fig. 11(c)). The substitute structure can be analyzed by the recurrence formula or by any other method if desired. If a second approximation is to be made, the calculations made for the first approximation can be confined to finding the stresses $\sigma_F$ in the flange and $\sigma_L$ in the longitudinal of the single-stringer structure.

Chordwise distribution of stresses.- The analysis of the substitute single-stringer structure furnishes the

flange stress $\sigma_F$ and the chordwise average of the stresses in the longitudinals for all stations along the span. The actual chordwise distribution of the stresses may be obtained in the following manner, as explained in reference 1.

For the limiting case of infinitely many stringers, some analytical solutions have been obtained in the form of solutions for the continuous cover sheet. These solutions show that the chordwise distribution of the stringer stresses at any given station follows a hyperbolic-cosine law. The stress at a distance $y$ from the center line may therefore be written as

$$\sigma = \sigma_{CL} \cosh Yy \qquad (14)$$

where $Y$ is an auxiliary parameter and $\sigma_{CL}$ is the value of $\sigma$ at $y = 0$. In this equation, both the stress $\sigma_{CL}$ in the longitudinal at the center line and the auxiliary parameter $Y$ are unknown. Two conditions are available to determine these unknowns: (1) The average of the stresses $\sigma$ between $y = 0$ and $y = b$ must be equal to the stress $\sigma_L$ of the substitute single stringer, and (2) at the flange $y = b$, the stress $\sigma$ must equal the stress $\sigma_F$. The result is a transcendental equation for $Yb$,

$$\frac{\tanh Yb}{Yb} = \frac{\sigma_L}{\sigma_F} \qquad (15)$$

In order to facilitate the determination of $Yb$, figure 13 has been prepared. With the help of this figure, $Yb$ can be determined by inspection after computing the ratio $\sigma_L/\sigma_F$. The stress at the center line is then computed by the formula

$$\sigma_{CL} = \sigma_F/\cosh Yb \qquad (16)$$

In order to compute the stress in any stringer at a given distance $y$ from the center line, it is only necessary to compute $Yy = (Yb) \times (y/b)$ and to apply formula (14).

Formulas (14) to (16) apply only when $0 < \sigma_L/\sigma_F < 1$. In regions critical for design work, this condition is probably always fulfilled. For certain purposes such as checking the theory against experimental results, however, it may be desired to calculate the chordwise stress distribu-

tion at stations where the ratio $\sigma_L/\sigma_F$ falls outside of this range. It was proposed in reference 1 to replace formulas (14) to (16) for such cases by

$$\sigma = \sigma_{CL}(2-\cosh Yy) \tag{14a}$$

$$\frac{2 - \frac{\sinh Yb}{Yb}}{2 - \cosh Yb} = \frac{\sigma_L}{\sigma_F} \tag{15a}$$

$$\sigma_{CL} = \sigma_F/(2 - \cosh Yb) \tag{16a}$$

Formula (15a) was used instead of formula (15) to extend the range of the Yb-curve in figure 13. It will be noted in figure 13 that the Yb-curve for very small negative values of $\sigma_L/\sigma_F$ does not become infinite as would be expected by analogy with small positive values. This peculiarity is caused by the approximate nature of equation (14a) and is of no practical importance.

Correction of chordwise stress distribution for finite number of stringers.- The method of computing stringer stresses by using formula (14) is based on the assumption that the stringers are infinitely closely spaced. If the spacing of the stiffeners is finite, the total internal force will be found by a summation instead of an integration, and the internal force will differ somewhat from the external force. The magnitude of the error depends on the number of stringers and on the curvature of the chordwise stress plot, which is characterized by the ratio $\sigma_L/\sigma_F$ or by the parameter Yb.

The sign of the error depends on the location of the first stringer near the flange. Under the rules given for idealizing the multistringer cross section, the first full-size stringer is located at $y = b(1 - 1/n)$, where $n$ is the number of stringers (arrangement A, fig. 14). For this case the summation of the stringer forces will yield a smaller force than is necessary to balance the external load. If a full-size stringer were located at the edge $y = b$ (arrangement B, fig. 14), the summation of the stringer forces would yield too large a value. As long as Yb is less than about 1.5, the errors for these two cases are numerically equal and are shown in figure 14.

The rule that the effective width of skin adjacent to the flange should be considered as a stringer (fig. 11(b)) helps to reduce the error by bringing the actual case between the two extreme arrangements A and B of figure 14. In practice, the ratio of the actual force to the summation of the calculated stringer forces may be applied as a correction factor to the calculated stringer stresses as illustrated by the numerical example in part III. This method of correction was used in the analysis of all NACA tests described in part II with very satisfactory results, even in some quite extreme cases; it was also used with very satisfactory results in making comparisons with the Ebner-Koller method. (See appendix B.) If the results obtained by this method should be considered as too inaccurate, the method of successive shear-fault reduction may be resorted to for improving the accuracy of the results.

Successive approximations for substitute width.- By definition, the substitute width is the distance from the flange to the force centroid of the stringers. For infinitely many stringers, the centroid can be found by integration (reference 2), and its location is shown graphically in figure 15. The substitute width is given by the expression

$$b_S = \left(1 - \frac{y_L}{b}\right) b \qquad (17)$$

In any given case, the factor $1 - (y_L/b)$ is taken from figure 15, and $b$ is the effective width for shear deformation as defined by figure 11(b).

In order to use figure 15 it is necessary to know the parameter Yb; for this reason it is necessary to make successive approximations. In the first approximation it is assumed that there is no shear lag; in this case $Yb = 0$ and $1 - (y_L/b) = 0.5$. The first approximation to the substitute width is therefore $b_{S_1} = \frac{b}{2}$, and with this width the first analysis is carried out as previously discussed. The stresses $\sigma_F$ and $\sigma_L$ are calculated for the substitute single-stringer structure, and for each station the ratio $\sigma_L/\sigma_F$ is calculated and used to determine the value of Yb from figure 14. The spanwise average of Yb is then calculated and the corresponding value of $1 - (y_L/b)$ is found from figure 15. This new value of $1 - (y_L/b)$ is inserted in formula (17) to obtain the second approximation to $b_S$, and

the analysis of the substitute single-stringer structure is repeated with the changes necessitated by changing the substitute width.

If the stresses $\sigma_F$ and $\sigma_L$ obtained in the second approximation differ very much from the stresses obtained in the first approximation, a third approximation may be made. On account of the rapid convergence of the process, the difference between the first and the second approximations need not be very small to insure that the second approximation may be taken as final. It is suggested that the stress analyst work some examples by means of the analytical formulas given in reference 2. As a rough guide, it may be stated that, if the accuracy of the 10-inch slide rule is used as a criterion, the second approximation may be considered as the final one when the shear-lag parameter KL for the entire beam is greater than 4 in the first approximation. When KL is about 7 or greater than 7 in the first approximation, the first approximation is sufficiently accurate. These relations are also influenced to some extent by the ratio $A_F/A_L$.

The outlined procedure should be slightly modified for axially loaded panels. In such panels, the value of Yb becomes infinite at the station where the axial load is introduced. In order to avoid this difficulty, the spanwise average of the ratios $\sigma_L/\sigma_F$ should be found and Yb for the average ratio $\sigma_L/\sigma_F$ should be determined. This method may be applied to beams in many cases and the final results obtained by the two methods will be the same, at least for practical purposes. It is preferable, however, to use the two distinct methods to avoid uncertainties in procedure.

The method given for finding successive approximations to $b_S$ applies directly only when there are infinitely many stringers. When there are only a few stringers, the first approximation $b_{S_1}$ is not equal to $b/2$ but is determined by the centroid of the areas of the stringers as discussed in connection with figures 11(b) and 11(c). In such cases, it may be assumed that the ratio of a higher-order approximation of $b_S$ to the first approximation $b_{S_1}$ is the same as though there were many stringers; any higher-order approximation to the substitute width is then given by the expression

$$b_S = 2b_{S_1}\left(1 - \frac{y_L}{b}\right) \qquad (17a)$$

where the factor $1 - (y_L/b)$ is determined as before from figure 15.

Method of Successive Shear-Fault Reduction

Principle and scope of method.- The analysis of multistringer structures by successive shear-fault reduction employs the same basic procedure that is used for the analysis of single-stringer structures. Some modifications and additional concepts are, of course, required to adapt the method to the much more complicated problem of analyzing multistringer structures.

The process of successive shear-fault reduction in a single-stringer structure consists in a repetition of adjustments on a spanwise sequence of elements. It is obviously not feasible to carry on such a process of adjustments at the same time on chordwise sequences of elements. In order to overcome this difficulty, a concept will be introduced that has become quite familiar through the Cross method of moment distribution, namely, the concept of locking parts of the structure in place to isolate the part being adjusted from the rest of the structure. The particular method of locking employed herein consists in locking certain stringers at a given state of longitudinal strain or, to use a descriptive expression, in imagining them to be frozen solid. The stringers locked at any given time are the stringers to either side of the one being adjusted. The stringers are adjusted in sequence, starting from the flange and proceeding to the center-line stringer. The process is repeated until the agreement between successive cycles of the computation is considered satisfactory.

The method is obviously more laborious than the substitute single-stringer method. It is very general, however, being capable of taking into account chordwise variations of stringer spacing, stringer area, sheet thickness, and shear modulus; it can also deal more successfully with structures having a very small number of stringers (two or three).

In practice, it will probably be found advantageous, in general, to use the substitute single-stringer method to obtain a first approximation, average values being used wherever necessary. The method of shear-fault reduction

can then be used to improve the accuracy of the results.

The method of shear-fault reduction has one advantage that may be helpful at times. After the constants have been computed and the first cycle has been completed, the work involved in succeeding cycles is so simple that it can be handled by computers with little engineering training.

Procedure for computation.- The computation is started by assuming initial values for the stresses in all stringers A to F (fig. 16), taking care that at each station the summation of the internal forces equals the external force M/h or P.

The flange A is adjusted first. In order to effect this adjustment, the stringer B is locked at the state of stress initially assumed. The computation then proceeds in practically the same manner as described for single-stringer structures; the only difference is that the values of $\sigma_L$ (in this case $\sigma_B$) are not changed but remain the same for all cycles. After a number of cycles - say five cycles - the adjustment of stringer A is stopped, and stringer A is locked at the state of stress just computed.

Before the adjustment of stringer A was started, static equilibrium existed between the internal stringer stresses and the external load at each cross section. After the adjustment, equilibrium no longer exists; before the adjustment of stringer B is started, it will be necessary to restore this equilibrium. To this end, the stresses in stringer B are increased or decreased so that the summation of the internal forces at each station again equals the external force.

With these corrected stresses acting in stringer B, the adjustment of stringer B is started. Stringer A is locked at the stresses obtained from the first process of adjustment; stringer C is locked at the stresses initially assumed. The detailed form of the computation is shown in table XII of part III and differs from that used for single-stringer structures only insofar as necessary to take into account the fact that there is a sheet and a stringer on either side of the stringer being adjusted instead of only one sheet and stringer on one side.

Columns 1, 2, and 3 of table XII give the values of the stringer stresses $\sigma_A$, $\sigma_C$, and $\sigma_B$. They are listed in this sequence so as to separate the values of $\sigma_A$ and $\sigma_C$, which remain constant during the adjustment of stringer B, from the stresses $\sigma_B$ and the other quantities that change during the adjustment.

Columns 4 to 7 give the computation of the shear force in the panel between stringers A and B; all properties of this panel are denoted by the superscript AB.

Columns 8 to 11 give the computation of the shear force in the panel between the stringers B and C; all properties of this panel are denoted by the superscript BC.

Column 12 gives the difference between the shear forces in the two panels for each bay

$$D = \Delta S^{AB}_{CE} - \Delta S^{BC}_{CE}$$

Column 13 gives the force $F_B = \sigma_B A_B$.

Column 14 gives the increments $\Delta F_B$.

Column 15 gives the shear fault

$$SF = D - \Delta F_B$$

Columns 16 to 19 give the shear-fault correction stress $\Delta\sigma_B$ in analogy with the columns 11 to 15 of the single-stringer computation.

After several cycles - say five cycles - the adjustment of stringer B is stopped, and the stringer is locked at the stresses thus obtained. The process of adjustment has again upset the static equilibrium; that is, the external force at any cross section will not be exactly balanced by the summation of the internal stringer forces assumed to exist at this stage. Static equilibrium is restored as before by increasing the stresses in the stringer that will be adjusted next, namely, stringer C.

Stringer C is now unlocked and adjusted, and the procedure of adjusting and restoring equilibrium is con-

tinued until the center stringer is reached. The entire process is then repeated several times until successive values of all stringer stresses in the structure are in sufficiently close agreement.

In the case of a cambered cover, it is necessary to introduce the same modification as discussed for single-stringer beams, based on the modified basic equation (1c'). After column 4 of table XII a column must be added for $\left[(\sigma_A - \sigma_B) - (\sigma_A{}^P - \sigma_B{}^P)\right]$; similarly, after column 8 a column must be added for $\left[(\sigma_B - \sigma_C) - (\sigma_B{}^P - \sigma_C{}^P)\right]$.

## Analysis of Cut-Out Effects

Principle and scope of method.- The most convenient and the most rapid method of analyzing structures with cut-outs is the indirect, or inverse, method. The analysis by the indirect method is made in two steps. First, the structure is analyzed for the basic condition that exists before the cut-out is made. The results of this basic analysis are used to calculate the internal forces that exist along the boundary of the proposed cut-out. External forces equal and opposite to these internal forces are then introduced; these external forces reduce the stresses to zero along the boundary of the proposed cut-out, and consequently the cut-out can now be made without disturbing the stresses.

The external forces introduced to reduce the stresses along the boundary of the cut-out to zero will be called the "liquidating" forces, a term used by R. V. Southwell in a somewhat different meaning. In general, it will be impossible to calculate accurately the stresses that these liquidating forces set up at a distance from the cut-out. Some simplification of the problem is permissible because the liquidating forces form self-equilibrated systems so that, by St. Venant's principle, their effects become negligible at some distance from the cut-out. In order to obtain numerical answers, however, it is necessary to make very stringent simplifying assumptions, and the method can therefore be applied only to reasonably small cut-outs.

The treatment given here is confined to structures having distinct stringers. For cases in which the stringers and the skin are fused into a homogeneous unit, it is preferable to use the standard methods of the theory of

elasticity, and some solutions of the cut-out problem for such cases may be found in publications on the theory of elasticity.

Effects of removing a skin panel.- Figure 17(a) shows the internal shear forces that exist along the edges of a skin panel bounded by two stringers and two ribs. The directions of the force arrows are the positive directions in accordance with the general sign conventions. In order to reduce the shear stresses along the edges of the panel to zero, external or liquidating shear forces are introduced as shown in figure 17(b), which are equal and opposite to the internal shear forces; only the forces acting on the main structure are shown in figure 17(b) because the stresses in the skin panel itself are of no interest.

In most practical cases, the stringer areas and the skin thicknesses just outboard of the cut-out are the same as those just inboard of the cut-out. The stress-distribution set up by the liquidating forces will then be symmetrical about a chordwise line bisecting the cut-out. Figure 17(c) shows schematically the stresses set up in the stringers with the signs appropriate to the case where the basic stresses are positive. The figure indicates stresses only for the two stringers bordering the cut-out; the stresses in the other stringers are small enough (as will be shown experimentally in pt. III) to be neglected in view of the fact that the changes in stress distribution caused by a small cut-out are small compared with the basic stresses.

The assumption that the liquidating forces of figure 17(b) set up stresses only in stringers C and D is equivalent to assuming that the skin panels BC and DE are rendered inoperative by slotting them lengthwise. Under this assumption, the problem becomes identical with the problem of the free panel shown in figure 18. The analytical solution for the free panel is given in reference 1; for the present purpose it can be simplified by assuming that the structure is very long on either side of the cut-out. The forces in the stringers inboard and outboard of the cut-out are then given by the formula

$$P = \pm \frac{1}{2} \tau_o \, t \, L e^{-Kx} \qquad (18a)$$

where $\tau_o$ is the basic shear stress existing in the panel before the cut-out is made. $t$ is the thickness of the

panel, L is the length of the cut-out panel, and K is the shear-lag parameter defined by

$$K^2 = \frac{Gt}{Ed}\left(\frac{1}{A_C} + \frac{1}{A_D}\right) \qquad (18b)$$

The signs of the stringer stresses set up by the liquidating forces P are indicated in figure 17(c) for the case of a positive basic shear stress $\tau_o$. The shear stresses set up by the liquidating forces are given by

$$\tau = \frac{1}{2}\,\tau_o\,KLe^{-Kx} \qquad (18c)$$

and are of such a direction as to increase the basic shear stresses. Within the region of the cut-out, the stringer forces vary linearly between the maximum values obtained by setting $x = 0$ in formula (18a). The convention for measuring x in formulas (18a) and (18c) is shown in figure 17(a).

The shear stresses given by formula (18c) are probably conservative because some of the shear load is taken by the adjoining panels, which are assumed to be inoperative in this simplified theory. Conversely, allowance must be made for increased shear stresses in the adjoining panels. Considerations of continuity indicate that, in the immediate vicinity of the corners of the cut-out, the maximum shear stresses in the adjoining panels BC and DE of figure 17 should be taken as equal to the maximum stresses given by formula (18c).

Effects of cutting stringers.- Figure 19(a) shows a cut-out obtained by removing three skin panels and cutting two stringers. The effects of removing the skin panels can be calculated by the method described in the preceding section. The effects of cutting the stringers are represented by the liquidating forces P shown in figure 19(a). The liquidating forces cause compressive stresses in the cut stringers and tensile reactions in the uncut stringers if the basic stresses are positive, that is, tensile. By analogy with the preceding case of the skin panel, it may be assumed that the tensile reaction to the liquidating forces is entirely furnished by the two stringers bordering the cut-out; the stress system shown in figure 19(b) is based on this assumption, and the numerical solution is obtained by considering one cut stringer and the adjacent continuous stringer to work together as a free panel.

The solution for the free panel (fig. 18) of infinite length is

$$P_1 = P_2 = Pe^{-Kx} \tag{19a}$$

$$\sigma_1 = P_1/A_1 \qquad \sigma_2 = P_2/A_2 \tag{19b}$$

$$\tau = PKe^{-Kx}/t \tag{19c}$$

with K defined by

$$K^2 = \frac{Gt}{Ed_e}\left(\frac{1}{A_1} + \frac{1}{A_2}\right) \tag{19d}$$

$d_e$ = distance between result. forces in cut & uncut stringers

If symmetry about a longitudinal line through the center of the cut-out is assumed, the numerical solution for the cut-out is obtained in the first approximation by setting in formulas (19b) and (19d)

$$A_1 = A_E = A_F \quad A_2 = A_D = A_G \quad d = b \tag{20}$$

where b denotes temporarily the effective half-width of the cut-out. The tests to be described in part III indicate, however, that, even when only one stringer is cut, it is justifiable to assume that several of the continuous stringers participate in furnishing the reaction to the liquidating forces. The simplest assumption that can be made about the participation of other stringers is expressed by setting

$$A_2 = A_G + A_H e^{-d/b} + A_I e^{-2d/b} + \ldots \tag{21}$$

when formulas (19) are used. The stresses caused by the liquidating forces are then

$$\sigma_G = \sigma_2 = P_2/A_2$$

$$\sigma_H = \sigma_2\, e^{-d/b} \tag{22}$$

$$\sigma_I = \sigma_2\, e^{-2d/b}$$

When only one stringer is interrupted, half of it is considered as constituting $A_1$. When n stringers are interrupted, the n/2 stringers on each side of the cut-out are considered to constitute $A_1$, and they are assumed to be concentrated at their common centroid to determine b.

It is apparent that the use of formula (20) will be conservative for stringers D and G and the skin panels between them but somewhat unconservative for stringers and panels distant from the cut-out.

At present, insufficient theoretical or experimental knowledge is available to define the limits within which the method presented here may be safely used. It would seem advisable to consider this method as giving only a first approximation when more than three stringers are interrupted by the cut-out. The method of shear-fault reduction must be resorted to in such cases to improve the accuracy of the results.

## II. EXPERIMENTAL VERIFICATION OF THE THEORY OF SHEAR LAG

### TEST OBJECTS AND TEST PROCEDURE

New NACA tests.- Previous experimental investigations on shear lag have been generally confined to panels and beams of constant cross section; it was therefore considered desirable to obtain experimental verification on a beam with a variable cross section. Although the cross section can be varied in a number of ways, it was deemed most important and instructive to verify the influence of tapering the cross-sectional area of the stringers.

A skin-stringer panel was therefore built as shown in figure 20 and tested in three different set-ups. A photograph of the second set-up is shown in figure 21. In order to obtain a sensitive check on the theory, the panel was designed for large shear-lag effects by using a large ratio of stringer area to sheet area.

The tension panel was then converted into a beam by adding shear webs; a cross section of the beam is shown in figure 22, and figure 23 shows the inside of the beam with strain gages set up at one station. This beam is designated beam 1. Beam 1 was also tested with two small cut-outs and two large cut-outs located symmetrically to the longitudinal axis. Figure 24 shows a strain-gage set-up on the beam with the large cut-outs.

After the cut-out tests were completed, the beam was

cut off just outboard of the first bulkhead, producing a very short, wide beam designated beam 2. The test set-up for this short beam is shown in figure 25.

It was also considered desirable to verify the validity of the theory in the limiting case of a beam without stiffeners. The dimensions of a beam built for this purpose, designated beam 3, are given in figure 26, and the test set-up is shown in figure 27. In order to obtain a sensitive check on the theory, the beam was made quite short.

As indicated in figure 26, beam 3 was tested in two conditions: first without corner flanges (original cross section) and then with corner flanges consisting of flat strips riveted to the cover as close to the corner as possible (modified cross section).

The beam was built and loaded symmetrically about a transverse plane; it was thus possible to realize the condition of a built-in end and at the same time to measure strains directly at the root section.

All strain readings were taken with 2-inch Tuckerman gages. These gages were always used in pairs on opposite sides of the sheet or the stringer to eliminate as far as possible the effects of local bending. Temperature variations during the tests were confined to $1^{\circ}$ F, limiting the error in stresses to about 50 pounds per square inch.

The load was applied in four equal steps in all of the cases except one, in which case three steps were used (beam 1, case 4). The stress readings plotted correspond to the highest test load used but were obtained by drawing the best-fitting straight lines through the load-strain plots and correcting for zero shift when necessary. The friction of the loading apparatus was measured several times during the tests and was found to be 2 percent, unless otherwise noted on the spanwise stress plots. Corrections have been applied for friction.

Young's moduli for the stringers were determined from several specimens cut from the beams after the tests had been completed. For the sheet used to manufacture beam 3, the modulus was determined from several test coupons cut from the same sheet from which the beam was fabricated. The moduli obtained are noted on the drawings of the specimens.

In all these tests the buckling stress of the sheet was never exceeded enough to cause an appreciable reduction in the average shear modulus. In many tests there was no visible buckling at all.

Old tests reanalyzed.- Because the methods of analysis proposed in this paper are relatively new, it seems desirable to buttress them with as many experimental verifications as possible. An effort was therefore made to secure all available test results and to analyze them by the proposed methods. It was found, however, that many published tests were of doubtful value for furnishing quantitative checks because very thin sheet that buckled at low loads had been used in these tests; the effective shear modulus could not, therefore, be calculated with sufficient accuracy for a quantitative check. The tests considered usable were a test on a compression panel made by White and Antz (reference 4) and two beam tests made by Schapitz (reference 5). The beam tested by Schapitz is shown schematically in figure 28.

## TEST RESULTS AND COMPARISONS WITH THEORY

Methods of analysis used.- All calculations were made by analyzing the substitute single-stringer structure by means of the recurrence formula. The stresses in the stringers were computed by using the method of chordwise distribution as described in part I of this paper, including the correction for a finite number of stringers. Unless otherwise noted the calculated results shown as curves in the figures are those obtained with the second approximation for the substitute width.

Part I does not give explicit rules for determining the width $b_3$ of the idealized sheet between stringers when the stringers are arranged as in beam 1. The sheet was assumed to be clamped between the opposing stringers with an effectiveness of 50 percent; in other words, the calculations were made as though the stringers were attached by two rows of rivets separated by half the width of the stringers.

New NACA tests.- The panel was tested under three conditions, as schematically indicated in figure 29. Figures 30 to 32 show the experimental and the calculated results in the form of spanwise plots of stress. Figures 33 and 34

show the corresponding chordwise plots for the first two cases.

The agreement between experiment and theory is very satisfactory except near the root in cases 1 and 2. The experimental points in this region scatter badly about a mean line (figs. 33 and 34). Integration of the measured stresses over the cross section gives internal forces that agree within about 5 percent with the external load, indicating that the strain measurements are fairly accurate but that there was some irregular behavior of the structure. It was thought that this irregularity might be caused by play in the bolt holes at the root; several holes were therefore carefully reamed out for the next larger size of bolts before making the beam tests, and the chordwise plots of stresses for the beams were much more regular.

Beam 1 was tested under the four loading conditions shown in figure 35. The spanwise stress plots are shown in figures 36 to 39. The agreement between tests and theory is very satisfactory for the most highly stressed stringers near the flange and for the flanges themselves, except for the fact that the experimental stress in the flange at the station nearest the root is slightly high in cases 1 and 4. In the stringers near the center line, the experimental stresses are higher than the calculated stresses near the root in cases 1, 3, and 4. It is believed that the discrepancy can probably be charged to the assumption that the sheet was 100 percent effective in contributing to the stiffener area. There are fairly consistent indications from a number of tests that this assumption is too optimistic when the ratio $\sigma_F/\sigma_L$ is large. A similar observation was made in reference 6. This remark applies both to the compression side when the stresses are below the buckling stresses for the sheet and to the tension side. On the compression side, the well-known effective width of the sheet must be used when the sheet has buckled.

The results on beam 2 are shown in figure 40. In view of the fact that this beam has an extremely small ratio of length to width as well as a small shear-lag parameter K, the agreement is excellent.

Figure 41 shows the results of test 1 on beam 3. Because the beam is symmetrical about the longitudinal axis as well as the transverse axis, there are four stress values for each station. It will be noted that in most cases the four values agree very closely, which indicates that the beam

showed excellent symmetry of strain about both axes.

This test is a rather crucial test on the range of validity of the theory. It has been held by some investigators that the theory of shear lag as developed in this paper would not apply to the limiting case where the elements of the cover-carrying shear (the sheet panels) and the elements carrying normal stresses (the stringers) are merged into a single unit, namely, a sheet. Figure 41 shows that this opinion is too pessimistic; the agreement is not perfect, but the maximum flange stresses, which are of paramount interest for design, are predicted fairly well.

The main difficulty in applying the theory to the case just discussed lies in the fact that $A_F$ becomes very small compared with $A_L$; the flange area consists only of the area 1/6 ht, which expresses the participation of the shear web in the bending action. For small ratios of $A_F$ to $A_L$, the shear-lag parameter K becomes very large and sensitive to errors in $A_F$. The difficulty is obviated when a corner flange of reasonable area is provided; in built-up structures, such a corner flange is usually provided in the form of an angle for riveting the cover to the shear web. In beam 3, a corner flange was provided by riveting flat strips along the edges, as shown on the second cross section in figure 26. The test results for this condition are plotted in figure 42 and show excellent agreement with the theory.

Old tests.- Figure 43 shows the experimental and the calculated results for the compression panel described in reference 4.

Figure 44 shows the results of the test on the beam described in reference 5 for a load applied at the tip. Figure 45 shows the test results for the same beam under loads distributed as indicated in figure 28. The agreement is fairly satisfactory.

Cut-out tests.- The approximate method of analyzing cut-outs described in this paper is based on the assumption that a pair of equal and opposite forces applied to adjacent stringers does not affect other stringers very much. A special test was made on beam 1 to verify directly the validity of this assumption. Two equal and opposite forces of P = 1162 pounds were applied to bolts at the intersections of the rib at midspan with stringers D and E.

Figure 46 shows the experimental stresses and the stresses calculated under the assumption that only stringers D and E are stressed.

Figure 47 shows the results of the test on beam 1 with small cut-outs located as shown by the sketch; only the skin was cut out in this case.

Figure 48 shows the results of the test on beam 1 with large cut-outs located as shown by the sketch and in figure 24. The agreement between theory and experiments for the cut-out tests is very satisfactory except for the discrepancies already noted in the tests on the same beam without cut-outs.

## III. NUMERICAL EXAMPLES

### IDEALIZATION OF CROSS SECTIONS

Problem 1.- To find the idealized cross section of a beam with open-section stiffeners:

The actual cross section of the beam is shown in figure 49(a). The effective width of the sheet for normal stresses is to be taken as $w = 20t$.

The idealized width $d$ for shear deformation (fig. 11) is equal to the width between rivet rows, that is, 4 inches.

The area of the idealized flange is obtained by adding the following areas:

| | (sq in.) |
|---|---|
| Corner angle . . . . . | 0.300 |
| Skin from corner to rivet line (0.375 x 0.040) . . . . . | .015 |
| Equivalent of web (1/6 x 6.00 x 0.065) . . | .065 |
| Area of idealized flange . . . . . | 0.380 |

The first stringer ~~immediately adjacent to~~ adjoining the flange consists of only the effective width of skin; the area is

$$20 \times 0.040 \times 0.040 = 0.032 \text{ square inch}$$

Each of the next two stringers consists of a stiffener and a double strip of skin; the area of each idealized stringer is therefore

$$A = 0.200 + 2 \times 20 \times 0.040 \times 0.040 = 0.264 \text{ square inch}$$

The stringer at the center line has one-half of this area, or 0.132 square inch.

The total area of the longitudinals is

$$A_L = 0.032 + 0.264 + 0.264 + 0.132 = 0.692 \text{ square inch}$$

The idealized cross section is shown in figure 49(b).

Problem 2.- To find the idealized cross section of a beam with closed-section stiffeners:

The actual cross section of the beam is shown in figure 49(c). The effective width of the sheet is to be taken as $w = 20t$.

The effective width $b_2$ for shear deformation is, by formula (13),

$$b_{2_e} = \frac{1.50}{1 + \frac{0.080 \times 1.50}{0.040 \times 3.00}} = 0.75 \text{ inch}$$

The idealized width from the flange to the first stringer is therefore

$$d = 3.25 + \frac{1}{2} \times 0.75 = 3.63 \text{ inches}$$

and the idealized width of the second and third panel is

$$d = 2.50 + 0.75 = 3.25 \text{ inches}$$

The areas of the flange $A_F$ and of the first small stringer are the same as in problem 1.

The area of the second as well as of the third idealized stringer is obtained by adding the following areas

| | (sq in.) |
|---|---|
| Hat section | 0.260 |
| Skin between rivets (1.5 x 0.040) | .060 |
| Two strips of skin (2 x 20 x 0.040 x 0.040) | .064 |
| Area of idealized stringer | 0.384 |

The stringer at the center line has one-half of this area, or 0.192 square inch.

The total area of the longitudinals is

$$A_L = 0.032 + 0.384 + 0.384 + 0.192 = 0.992 \text{ square inch}$$

The idealized cross section is shown in figure 49(d).

## ANALYSIS OF A MULTISTRINGER BEAM, OBTAINED BY THE USE OF THE SUBSTITUTE SINGLE-STRINGER METHOD AND THE RECURRENCE FORMULA

Given data.- Figure 50 shows the idealized form of a beam; the problem is to find the stresses in this beam under the load indicated by the use of the substitute single-stringer method and the recurrence formula.

This idealized beam is very nearly identical with the idealized form of beam 1 discussed in part II. The following simplifications have been made: The slightly tapering effective width of beam 1 has been replaced by a constant width; the slightly tapering effective depth, with a discontinuity at the midspan, has been replaced by a constant depth; the load has been located exactly at the tip instead of at the actual location of 0.56 inch from the tip. None of these deviations amounts to more than 2 percent at any point, so that the results obtained in these numerical examples can be compared quite closely with the corresponding calculated curves shown in part II.

From the data given in figure 50, table I has been prepared to give the data in the form required for the analysis.

First approximation to substitute single-stringer structures.- The first approximation to the substitute single-stringer structure is obtained by combining the stringers constituting $A_L$ into a single stringer located at the centroid of $A_L$. As indicated in figure 50, this centroid is located 6.28 inches from the flange, and this distance is by definition the substitute width in the first approximation.

The computation of the coefficients required for the analysis of the substitute beam is shown in table II. The values of $A_F$ and $A_L$ are the same as for the actual structure and are obtained from table I. The shear-lag parameter K is calculated by formula (4). The substitute width $b_S$ just found is used where b appears in this formula, so that

$$\frac{Gt}{Eb_S} = \frac{0.40 \times 0.015}{6.28} = 0.000956$$

The coefficients p, q, and $\gamma$ are calculated by formulas (3a), (3b), and (3c); because G and t are constant in this particular beam, the common factor Gt has been omitted from all coefficients.

With the coefficients computed in table II, the system of equations for the X-forces (first approximation) is written in conformance with equations (5). The boundary conditions are $X_0 = 0$ and $\gamma_{r+1} = 0$.

$$-X_1(0.1400 + 0.1388) + X_2(0.1182) = -66.7 + 66.5$$

$$X_1(0.1182) - X_2(0.1388 + 0.1376) + X_3(0.1190) = -66.5 + 66.3$$

$$X_2(0.1190) - X_3(0.1376 + 0.1362) + X_4(0.1191) = -66.3 + 66.1$$

$$X_3(0.1191) - X_4(0.1362 + 0.1358) + X_5(0.1200) = -66.1 + 66.0$$

$$X_4(0.1200) - X_5(0.1358 + 0.1347) + X_6(0.1201) = -66.0 + 66.0$$

$$X_5(0.1201) - X_6(0.1347) = -66.0$$

These equations are then solved, and table III gives the final computation of the stresses in the substitute beam as obtained by formulas (9a) and (9b).

Second approximation to substitute single-stringer structure.- The calculation of the second approximation begins with the last two columns of table III. The parameter Yb is obtained from figure 13 for each station, and the average value of Yb is computed. From figure 15, the value of $1 - (y_L/b)$ corresponding to this average value of Yb is read, and the second approximation to the substitute width is obtained by formula (17a). Actually it is not necessary to compute the second approximation of $b_S$; it is possible to proceed directly to the new values of the shear-lag parameter K by dividing the values of K given in table II by the expression $\sqrt{2[1 - (y_L/b)]}$. Table IV gives the new values of K and the computation of the new set of coefficients p and q for the recurrence formula. Table V gives the values of the X-forces and the final stresses in the beam for the second approximation. As a check, the average value of Yb is again computed, and the corresponding value of $1 - (y_L/b)$ is found. The factor $\sqrt{2[1 - (y_L/b)]}$ differs by only 1 percent from the factor obtained in the first approximation; the second approximation may therefore be considered the final approximation.

Calculation of chordwise distribution of stresses.- After the final approximation to the stresses in the substitute beam has been computed, the chordwise distribution of the stresses in the actual beam can be found. As an example, the calculation will be shown in detail for station 5.

According to table V, $\sigma_F = 5000$ pounds per square inch and $\sigma_L = 2673$ pounds per square inch for station 5; the ratio $\sigma_L/\sigma_F = 0.535$, and the corresponding value of Yb = 1.760 from figure 13. This value of Yb is entered in table VI, and the values of Yy for the two intermediate stringers B and C are calculated by proportion and entered in column 2. Next, the hyperbolic cosines are entered in column 3. The stress in the center stringer D is now calculated by formula (16).

$$\sigma_{CL} = \frac{5000}{2.992} = 1673 \text{ pounds per square inch}$$

and entered in column 4. The stresses in the stringers B

and C are then calculated by formula (14) and entered in column 4.

Column 5 gives the cross-sectional areas of the stringers $A_{st}$, and column 6 gives the internal forces $\sigma A_{st}$. The sum of these forces will not equal the force $\sigma_L A_L$ on account of the finite number of stringers, and a correction must be applied to all of the stresses $\sigma$ except to the stress in stringer A; the stress in stringer A must necessarily remain equal to $\sigma_F$.

The correction is made as follows: The force $F_L$ is $\sigma_L A_L = 2673 \times 0.771 = 2060$ pounds. The force in stringer A is 140 pounds, as shown in column 6; the total force that must be applied by the center stringer D and the two intermediate stringers B and C is therefore 2060 - 140 = 1920 pounds. The summation of the internal forces in the three stringers B, C, and D as given in column 6 is only 1715 pounds; the stresses $\sigma$ given in column 4 must therefore be multiplied by the factor 1920/1715 = 1.120 to obtain the final values of the stresses $\sigma$, which are listed in column 7. As a check, the internal forces are again computed with the corrected values of $\sigma$; the summation checks exactly with the force $F_L = 2060$ pounds.

The calculation of the chordwise distribution of stresses is made in the same manner for each station; the results of the calculations are given in table VII.

## ANALYSIS OF MULTISTRINGER BEAM WITH CUT-OUT

It will be assumed for the example of a multistringer beam with cut-out that a cut-out is made in the beam shown in figure 50 and analyzed in the preceding example; the skin panels AB and BC and the stringer B are removed between stations 3 and $4\frac{1}{2}$, corresponding to the large cut-out in beam 1 described in part II. The effects of making this cut-out are to be found.

Effects of removing skin panel AB.- The total shear force in the skin panel AB between stations 3 and $4\frac{1}{2}$ is found by statics with the stresses given in table VII; it is equal to the sum of the forces in stringers B, C, and D at station $4\frac{1}{2}$ minus the sum of the forces in the same stringers at station 3. The result of the simple calcula-

tion is $\tau_o tL = 484$ pounds. The next step is the calculation of the parameter K by formula (18b). In this case, the cut panel is bounded by stringers A and B; the areas $A_C$ and $A_D$ of formula (18b) are therefore replaced by $A_A$ and $A_B$. In order to be consistent with the assumption that the structure is the same at the two ends of the cut-out, the values of $A_A$ and $A_B$ used will be those valid for the middle of the cut-out. Formula (18b) gives therefore

$$K^2 = \frac{0.4 \times 0.015}{3.625}\left(\frac{1}{0.355} + \frac{1}{0.271}\right) = 0.01078$$

$$K = 0.1038$$

After these preliminary calculations, the solution can be carried out in tabular form as shown in table VIII. The value of P at stations 3 and $4\frac{1}{2}$ is $\frac{1}{2}\tau_o tL = 242$ pounds; at the other stations $P = 242e^{-Kx}$ pounds according to formula (18a). The calculation of the stresses $P/A_A$ and $P/A_B$ is self-explanatory.

Effects of removing skin panel BC.- For panel BC, the shear force is found by subtracting the internal forces in stringers C and D at station 3 from the forces at station $4\frac{1}{2}$; the result is

$$\tau_o tL = 195 \text{ pounds}$$

The value of K is found from

$$K^2 = \frac{0.40 \times 0.015}{3.625}\left(\frac{1}{0.271} + \frac{1}{0.271}\right) = 0.0122$$

$$K = 0.1104$$

Table VIII shows the details of computing the stresses $P/A_B$ and $P/A_C$ caused by removing the skin panel BC. The last four rows of the table give the stringer stresses in the beam, obtained by superposing on the stresses of table VII the stresses caused by removing the two skin panels AB and BC. The signs of the stresses are determined by comparison with figure 17(c); at station 3, for instance,

$$\sigma_B = 2370 + 945 - 381 = 2934 \text{ pounds per square inch}$$

where 945 pounds per square inch is the stress caused by removing panel AB, and 381 pounds per square inch is the stress caused by removing panel BC.

Effect of cutting stringer.- According to the stresses listed in table VIII, the stress in stringer B at station 3 is $\sigma_B = 2934$ pounds per square inch. The internal force at the outboard end of the cut-out is therefore $2934 \times 0.256 = 752$ pounds. At the inboard end of the cut-out, the force is $2614 \times 0.287 = 750$ pounds. The region around the cut-out is now divided into four free panels so that formulas (19) can be used. Two of these panels are inboard of the cut-out; for the first panel

$$A_1 = \frac{1}{2} A_B \quad \text{and} \quad A_2 = A_A$$

for the second panel

$$A_1 = \frac{1}{2} A_B \quad \text{and} \quad A_2 = A_C + e^{-1} A_D$$

by formula (21), all areas being those at station $4\frac{1}{2}$. For simplicity, it will be assumed that the two panels have the same shear-lag parameter K, and K will be computed by using the average of the two given values of $A_2$. The result is

$$K^2 = \frac{0.40 \times 0.015}{3.625} \left( \frac{1}{0.358} + \frac{1}{0.1435} \right) = 0.01618$$

$$K = 0.127$$

for the inboard panels.

The other two free panels are outboard of the cut-out and are defined in the same manner; the calculations are made with the areas at station 3. The shear-lag parameter is given by

$$K^2 = \frac{0.40 \times 0.015}{3.625} \left( \frac{1}{0.318} + \frac{1}{0.128} \right) = 0.01813$$

$$K = 0.1347$$

The calculation itself is given in table IX. The stresses caused by cutting stringer B shown in this table are superposed on the final stresses shown in table VIII to

obtain the final stresses in the stringers. The stresses in stringer D caused by cutting stringer B are obtained by formula (22) as $e^{-1} P/A_2$.

When the results of this computation are compared with the curves in figure 48, it should be borne in mind that an additional small correction must be made for the actual test because removal of the skin panels reduces the areas $A_A$ and $A_D$ in the region of the cut-out.

## ANALYSIS BY SUCCESSIVE SHEAR-FAULT REDUCTION

Analysis of single-stringer beam.- The method of analyzing a single-stringer beam by successive shear-fault reduction will be demonstrated on the substitute single-stringer beam analyzed previously by the recurrence formula. The basic data for the beam are those given in table I; for the substitute width, the second approximation $b_S = 6.28 \times 1.090 = 6.85$ inches was used. As the initial assumption, the stresses in the flange were arbitrarily assumed to be 1.40 times the stresses given by the Mc/I formula. Table X gives the first cycle of the computation; a comment on the form of the computations is given in part I of this paper. Table XI gives the second cycle of the computation, starting with the values of $\sigma_F$ found at the end of the first cycle. As a general check on the computations, the sum of the shear faults is shown for both cycles; it will be noted that it has decreased from 843 to 764 pounds.

Analysis of multistringer beam.- As an example for the analysis of a multistringer beam, the beam of figure 50 is again used, and a typical cycle of adjustment for stringer B is shown in table XII. Because the example is illustrative, the stress values $\sigma_A$, $\sigma_B$, and $\sigma_C$ were not assumed arbitrarily but were taken from table VII, the final result of the previous analysis. The shear faults are therefore very small, and the adjusted stresses $\sigma_B$ are practically identical with the initial stresses. The small differences that exist arise from two reasons. The first reason is the limited numerical accuracy of the process. This numerical accuracy is determined by two factors: the number of bays used and the accuracy of multiplication and division. These operations were carried out with a 10-inch

slide rule in all numerical examples given in this report. The second reason for the failure of table XII to show exact agreement between the initial and the final values of $\sigma_B$ lies in the slight differences between the basic assumptions. The recurrence formula is based on the assumption that the cross section is constant in each bay, but the stresses vary nonlinearly in each bay. The shear-fault reduction method, on the other hand, assumes that all stresses vary linearly in each bay.

## CONCLUSION

The theory of shear-lag action presented in this paper is based on the concept of idealized structures consisting of stringers carrying longitudinal stresses, of sheet carrying shear stresses, and of transverse ribs infinitely closely spaced and of infinite stiffness. The test results indicate that this theory is acceptable as a basis for practical stress analysis, because, in general, the differences between test results and calculated results in the critical regions are smaller than occasional scatter of test results caused by uncontrollable irregularities in the behavior of the structure.

Langley Memorial Aeronautical Laboratory,
National Advisory Committee for Aeronautics,
Langley Field, Va.

# APPENDIX A

## SYMBOLS

| | |
|---|---|
| A | cross-sectional area, sq in. |
| E | Young's modulus, lb/sq in. |
| F | internal force, lb |
| G | effective shear modulus, lb/sq in. |
| I | geometric moment of inertia, $in.^4$ |
| K | shear-lag parameter (equation (4)) |
| L | length, in. |
| M | bending moment, in.-lb |
| P | external load, lb |
| S | shear force, lb |
| SF | shear fault (equation (SS-3)) |
| SFC | shear-fault correction (equation (SS-4)) |
| Y | auxiliary parameter (equation (14)) |
| b | half-width of structure, in.; with numerical subscripts, distance between stringers (fig. 12), in. |
| b′ | developed width, in. |
| h | depth of beam, in. between centroids |
| t | thickness, in. |
| w | effective width |
| x | distance parallel to center line |
| y | distance from center line |
| $\gamma$ | shear strain |

$\sigma$ direct (normal) stress, lb/sq in.

$\tau$ shear stress, lb/sq in.

$\tau_o$ basic shear stress existing before a cut-out is made, lb/sq in.

Superscripts have the following significance:

P theoretical values based on the assumption that plane cross sections remain plane

Subscripts have the following significance:

C cover sheet

E external (applied)

F flange

L longitudinal

S substitute

st stringer

T total

W shear web

CE occurring in the cover sheet and obtained by the elastic relation.

CL center line

i inboard

o outboard

av average

e effective

# APPENDIX B

## COMPARISON BETWEEN DIFFERENT SOLUTIONS OF THE SHEAR-LAG PROBLEM

The basic shear-lag problem is the problem of a box beam with constant cross section. In 1930 Younger published a solution of this problem (reference 7). In 1937 the author published a slightly different solution, the constant-stress solution (reference 1). In 1938 Reissner published a third solution (reference 8). If the flange efficiency $\eta$ of a box beam is defined by the ratio of the $Mc/I$ stress to the actual flange stress, all three solutions can be reduced to the same form, namely,

$$\eta = \frac{\tanh F}{F}$$

where $F$ is a function of the geometrical and the physical properties of the box. This function $F$ is defined as follows:

$$F = 1.571\ b/L \sqrt{\frac{E}{G}} \qquad \text{(Younger, reference 7)}$$

$$F = 1.414\ b/L \sqrt{\frac{E}{G}} \qquad \text{(Kuhn, reference 1)}$$

$$F = 1.732\ b/L \sqrt{\frac{E}{G}} \qquad \text{(Reissner, reference 8)}$$

It will be seen that the three solutions are identical in form and differ only slightly in the numerical constant.

All three solutions involve some simplifying assumptions, and any one of the three could be used equally well as a basis for building up approximate solutions for beams of variable cross section. All three solutions, however, lead to the result that the flange efficiency is constant along the span. A glance at figures 41 and 42 indicates that this result cannot be more than a rough approximation; the flange stresses on these figures are not straight lines. For this reason, the treatment of the beam with variable cross section as presented in this paper was not based on any of these solutions.

Of the three basic solutions given, only Reissner's solution is of such a nature that the underlying assumptions can be physically realized without difficulty (constant cross section, concentrated load at tip). At the time of publication, it was stated that the solution is applicable only when the cover consists of corrugated sheet (reference 8); it was stated later (reference 9) that the solution applies also when the cover consists of a flat sheet. Reissner's solution is therefore shown in figure 41; it will be seen that, at some distance from the root, it is a fair approximation, but at the root the experimental shear-lag effect is nearly twice as large as that predicted by Reissner's solution.

The series solution given by Winny (reference 10) is based on the same principles as the solutions listed and is therefore open to the same objection in that it cannot give more than a very rough approximation. In view of this fact, the labor of using a solution by series is hardly justifiable.

The solution given by Goodey (reference 11) is identical with the solution of the single-stringer beam given in reference 1. Goodey also gives one case not included in reference 1, namely, the case of uniformly distributed loading.

A very complete and elaborate method of shear-lag analysis has been presented by Ebner and Köller (reference 12). The idealized structure consists of stringers, sheet, and transverse ribs. The transverse ribs are finite in number and of finite stiffness; the method is therefore more complete than the methods presented in this paper. Comparative calculations made in reference 12, however, show that the rib stiffness has only a small influence on the stringer stresses so that the simplifying assumption of infinite number and stiffness of the ribs results only in very small errors. This conclusion drawn by Ebner and Köller from their theory is amply confirmed by the good agreement between the experiments and the analyses presented in this paper.

The method of reference 12 is rather difficult to follow; comparisons have therefore been confined to the analysis of numerical examples given therein by the methods presented in this paper. The dimensions of the structure analyzed in reference 12 are given in figure 51.

Figure 52 shows the results for load case 1, which is the case of an axially loaded panel. It will be noted that in reference 12 there is given an "exact" method as well as an approximate one, the approximate method being recommended for practice because the exact method is quite cumbersome. The solution made by the substitute single-stringer method agrees with the exact method of reference 12 at all of the stations except one to the accuracy of reading the values from a small graph. The maximum difference between the exact method and the present single-stringer method is only slightly larger than the difference between the two methods of reference 12 and is unimportant for design purposes.

Figure 53 shows the results for the beam. The agreement between the solution of reference 12 and the single-stringer solution of this paper is very close except at the root, where there is a difference of 3 percent on the flange stress and a difference of 20 percent on the stress in the center stringer. The agreement between the solution of reference 12 and the solution by successive shear-fault reduction is good.

It should be pointed out that this numerical example represents the most severe test that can possibly be made of the powers of the substitute single-stringer method. The chordwise distribution method, which is an integral part of this method, is based on the assumption that there are infinitely many stringers; the half structure analyzed here has only two stringers, which is not a very close approximation to infinitely many stringers.

The example may serve as a warning, therefore, that in such extreme cases, the method of shear-fault reduction should be used to refine the approximation obtained by the single-stringer method. From a practical point of view, the discrepancy found here between the method of reference 12 and the substitute single-stringer method is of little interest because structures with only two stringers are not likely to be encountered in practice.

## REFERENCES


1. Kuhn, Paul: Stress Analysis of Beams with Shear Deformation of the Flanges. Rep. No. 608, NACA, 1937.

2. Kuhn, Paul: Approximate Stress Analysis of Multi-stringer Beams with Shear D formation of the Flanges. Rep. No. 636, NACA, 1938.

3. Kuhn, Paul: A Recurrence Formula for Shear-Lag Problems. T.N. No. 739, NACA, 1939.

4. White, Roland J., and Antz, Hans M.: Tests on the Stress Distribution in Reinforced Panels. Jour. Aero. Sci., vol. 3, no. 6, April 1936, pp. 209-212.

5. Schapitz, E., Feller, H., and Köller, H.: Experimental and Analytical Investigation of a Monocoque Wing Model Loaded in Bending. T.M. No. 915, NACA, 1939.

6. Schapitz, E., and Krümling, G.: Load Tests on a Stiffened Circular Cylindrical Shell. T.M. No. 864, NACA, 1938.

7. Younger, John E.: Metal Wing Construction. Part II - Mathematical Investigations. A.C.T.R. ser. no. 3288, Matériel Div., Army Air Corps, 1930.

8. Reissner, Eric: On the Problem of Stress Distribution in Wide-Flanged Box Beams. Jour. Aero. Sci., vol. 5, no. 8, June 1938, pp. 295-299.

9. Reissner, E.: Letter to the Editor. Jour. Aero Sci., vol. 5, no. 9, July 1938, p. 368.

10. Winny, H. F.: The Distribution of Stress in Monocoque Wings. R. & M. No. 1756, British A.R.C., 1937.

11. Goodey, W. J.: A Stressed-Skin Problem. Aircraft Engineering, vol. X, no. 107, Jan. 1938, pp. 11-13.

12. Ebner, H., and Köller, H.: Über den Kraftverlauf in längs- und querversteiften Scheiben. Luftfahrtforschung, Bd. 15, Lfg. 10, 10 Oct. 1938, pp. 527-542.

TABLE I

BASIC DATA FOR ANALYSIS OF BEAM

[G/E = 0.40; h = 6.18 in.; b = 10.875 in.;
t = 0.015 in.; P = 600 lb;]

| Station | x (in.) | $A_F$ (sq in.) | $A_L$ (sq in.) | $A_T$ (sq in.) | M (lb-in.) | $\frac{M}{h}$ (lb) | $\sigma \frac{P}{F}$ (lb/sq in.) |
|---|---|---|---|---|---|---|---|
| 0 | 0 | 0.229 | 0.502 | 0.731 | 0 | 0 | 0 |
| 1 | 8 | .256 | .556 | .812 | 4,800 | 777 | 956 |
| 2 | 16 | .283 | .610 | .893 | 9,600 | 1554 | 1740 |
| 3 | 24 | .310 | .663 | .973 | 14,400 | 2331 | 2395 |
| 4 | 32 | .337 | .717 | 1.054 | 19,200 | 3108 | 2947 |
| 5 | 40 | .364 | .771 | 1.135 | 24,000 | 3885 | 3420 |
| 6 | 48 | .392 | .825 | 1.217 | 28,800 | 4662 | 3835 |

TABLE IV

Coefficients for Recurrence Formula (Second Approximation)

| Bay | K | KL | tanh KL | sinh KL | p | q |
|---|---|---|---|---|---|---|
| 1 | 0.0826 | 0.661 | 0.579 | 0.710 | 0.1425 | 0.1163 |
| 2 | .0786 | .629 | .557 | .671 | .1410 | .1172 |
| 3 | .0750 | .600 | .537 | .637 | .1396 | .1176 |
| 4 | .0718 | .574 | .518 | .606 | .1336 | .1184 |
| 5 | .0690 | .552 | .502 | .580 | .1374 | .1190 |
| 6 | .0665 | .532 | .487 | .557 | .1366 | .1195 |

COMPUTATION OF COEFFICIFNTS FOR RECURRENCE FORMULA (FIRST APPROXIMATION)

$\left[K^2 = 0.000956 \left(\frac{1}{A_F} + \frac{1}{A_L}\right);\quad L = 8.00 \text{ in.}\right]$

TABLE II

| Bay | $A_F$ (sq in.) | $A_L$ (sq in.) | $\frac{1}{A_F}$ | $\frac{1}{A_L}$ | $\frac{1}{A_F} + \frac{1}{A_L}$ | $K^2$ | K | KL | tanh KL | sinh KL | p | q | $\frac{A_L}{A_T}$ | Y |
|---|---|---|---|---|---|---|---|---|---|---|---|---|---|---|
| 1 | 0.242 | 0.529 | 4.13 | 1.89 | 6.02 | 0.00575 | 0.0758 | 0.607 | 0.542 | 0.645 | 0.1400 | 0.1177 | 0.687 | 66.7 |
| 2 | .269 | .583 | 3.72 | 1.72 | 5.44 | .00520 | .0721 | .577 | .520 | .610 | .1388 | .1192 | .685 | 66.5 |
| 3 | .296 | .636 | 3.38 | 1.57 | 4.95 | .00473 | .0688 | .550 | .500 | .578 | .1376 | .1190 | .683 | 66.3 |
| 4 | .323 | .690 | 3.10 | 1.45 | 4.55 | .00435 | .0659 | .528 | .484 | .553 | .1362 | .1191 | .681 | 66.1 |
| 5 | .350 | .744 | 2.86 | 1.34 | 4.20 | .00402 | .0633 | .506 | .467 | .528 | .1358 | .1200 | .680 | 66.0 |
| 6 | .378 | .798 | 2.65 | 1.25 | 3.90 | .00373 | .0610 | .488 | .453 | .508 | .1347 | .1201 | .680 | 66.0 |

STRESSES IN SUBSTITUTE SINGLE-STRINGER BEAM (FIRST APPROXIMATION)

$\left[Yb = 1.54,\ \left(1 - \frac{y_L}{b}\right) = 0.420 \text{ from fig. 15}\right.$

$\left.\frac{1}{\sqrt{2\left(1 - \frac{y_L}{b}\right)}} = \frac{1}{\sqrt{0.840}} = 1.090\right]$ ← for correcting K

TABLE III

| Station | $\sigma^P$ (lb/sq in.) | X (lb) | $\frac{X}{A_F}$ (lb/sq in.) | $\sigma_F$ (lb/sq in.) | $\frac{X}{A_L}$ (lb/sq in.) | $\sigma_L$ (lb/sq in.) | $\frac{\sigma_L}{\sigma_F}$ | Yb |
|---|---|---|---|---|---|---|---|---|
| 1 | 956 | 48 | 188 | 1144 | 86 | 870 | 0.760 | 1.00 |
| 2 | 1740 | 113 | 400 | 2140 | 186 | 1554 | .725 | 1.10 |
| 3 | 2395 | 212 | 684 | 3079 | 320 | 2075 | .675 | 1.25 |
| 4 | 2947 | 373 | 1107 | 4054 | 520 | 2427 | .600 | 1.50 |
| 5 | 3420 | 633 | 1740 | 5160 | 822 | 2598 | .504 | 1.90 |
| 6 | 3835 | 1054 | 2690 | 6525 | 1278 | 2557 | .392 | 2.50 |
| | | | | | | Total | | 9.25 |
| | | | | | | Average | | 1.54 |

Table IV ←

TABLE V

STRESSES IN SUBSTITUTE SINGLE-STRINGER BEAM (SECOND APPROXIMATION)

$\left[\left(1 - \frac{y_L}{b}\right) = 0.429 \quad \text{from fig. 15.}\right.$

$\left.\frac{1}{\sqrt{2\left(1 - \frac{y_L}{b}\right)}} = \frac{1}{\sqrt{0.858}} = 1.079\right]$

| Station | $\sigma^P$ (lb/sq in.) | X (lb) | $\frac{X}{A_F}$ (lb/sq in.) | $\sigma_F$ (lb/sq in.) | $\frac{X}{A_L}$ (lb/sq in.) | $\sigma_L$ (lb/sq in.) | $\frac{\sigma_L}{\sigma_F}$ | Yb | |
|---|---|---|---|---|---|---|---|---|---|
| 1 | 956 | 40 | 156 | 1112 | 72 | 884 | 0.795 | 0.90 | |
| 2 | 1740 | 96 | 339 | 2079 | 157 | 1583 | .761 | 1.00 | |
| 3 | 2395 | 187 | 603 | 2998 | 282 | 2113 | .704 | 1.16 | |
| 4 | 2947 | 335 | 994 | 3941 | 468 | 2479 | .629 | 1.40 | |
| 5 | 3420 | 576 | 1580 | 5000 | 747 | 2673 | .535 | 1.76 | |
| 6 | 3835 | 987 | 2520 | 6355 | 1195 | 2640 | .416 | 2.40 | |
| | | | | | | | Total | 8.62 | |
| | | | | | | | Average | 1.44 | |

TABLE VI

COMPUTATION OF CHORDWISE DISTRIBUTION

OF STRESSES AT STATION 5

| Stringer | y | Yy | cosh Yy | $\sigma$ [1] (lb/sq in) | $A_{St}$ (sq in.) | $\sigma A_{St}$ [1] (lb) | $\sigma$ [2] (lb/sq in) | $\sigma A_{St}$ [2] (lb) |
|---|---|---|---|---|---|---|---|---|
| ℄ D | 0 | 0 | 1.000 | 1673 | 0.149 | 249 | 1873 | 279 |
| C | $\frac{1}{3}$ b | .587 | 1.177 | 1968 | .297 | 585 | 2203 | 655 |
| B | $\frac{2}{3}$ b | 1.174 | 1.772 | 2965 | .297 | 881 | 3320 | 986 |
| A | b | 1.760 | 2.992 | 5000 | .028 | (140) | 5000 | 140 |
| | | | | | .771 | 1715 | | 2060 |

$\left[\sigma_L A_L = 2673 \times 0.771 = 2060 - \frac{140}{1920}\ \text{lb}\right.$ $\left.\text{Correction factor} = \frac{1920}{1715} = 1.120\right]$

[1] Uncorrected values.

[2] Corrected values.

TABLE VII

Chordwise Distribution of Stresses in Beam

| Station | $\sigma_A$ (lb/sq in.) | $\sigma_B$ (lb/sq in.) | $\sigma_C$ (lb/sq in.) | $\sigma_D$ (lb/sq in.) |
|---|---|---|---|---|
| 1 | 1112 | 952 | 840 | 800 |
| 2 | 2079 | 1774 | 1518 | 1440 |
| 3 | 2998 | 2370 | 1936 | 1790 |
| 4 | 3941 | 2875 | 2200 | 1985 |
| 5 | 5000 | 3320 | 2203 | 1873 |
| 6 | 6355 | 3399 | 2020 | 1630 |

TABLE VIII

EFFECT OF REMOVING SKIN PANELS

| Station x | 6<br>12 | 5<br>4 | 4½<br>0 | 3<br>0 | 2<br>8 | 1<br>16 |
|---|---|---|---|---|---|---|
| **Effect of removing panel AB** | | | | | | |
| Kx | 1.247 | 0.415 | 0 | 0 | 0.830 | 1.660 |
| $e^{-Kx}$ | .287 | .647 | 1.000 | 1.000 | .436 | .190 |
| P (lb) | 69.5 | 156.7 | 242.0 | 242.0 | 105.6 | 46.0 |
| $A_A$ (sq in.) | .422 | .392 | .377 | .334 | .305 | .276 |
| $P/A_A$ | 165 | 400 | 642 | 725 | 346 | 167 |
| $A_B$ (sq in.) | .318 | .297 | .286 | .256 | .235 | .215 |
| $P/A_B$ | 219 | 527 | 847 | 945 | 450 | 214 |
| **Effect of removing panel BC** | | | | | | |
| Kx | 1.325 | 0.442 | 0 | 0 | 0.883 | 1.766 |
| $e^{-Kx}$ | .266 | .643 | 1.00 | 1.00 | .414 | .170 |
| P(lb) | 25.9 | 62.7 | 97.5 | 97.5 | 40.4 | 16.6 |
| $P/A_B$ | 81 | 211 | 341 | 381 | 172 | 77 |
| $P/A_C$ | 81 | 211 | 341 | 381 | 172 | 77 |
| **Stringer stresses after removing panels AB and BC** | | | | | | |
| $\sigma_A$ (lb/sq in.) | 6515 | 5400 | 5092 | 2275 | 1744 | 1193 |
| $\sigma_B$ (lb/sq in.) | 3262 | 2984 | 2614 | 2934 | 2048 | 1097 |
| $\sigma_C$ (lb/sq in.) | 1949 | 1989 | 1899 | 2331 | 1672 | 927 |
| $\sigma_D$ (lb/sq in.) | 1650 | 1870 | 1970 | 1800 | 1430 | 820 |

TABLE IX

EFFECT OF CUTTING STRINGER
FINAL STRINGER STRESSES

| Station x | 6<br>12 | 5<br>4 | 4½<br>0 | 3<br>0 | 2<br>8 | 1<br>16 |
|---|---|---|---|---|---|---|
| **Effect of cutting stringer B** | | | | | | |
| K | 0.1270 | 0.1270 | 0.1270 | 0.1347 | 0.1347 | 0.1347 |
| Kx | 1.525 | .508 | 0 | 0 | 1.077 | 2.155 |
| $e^{-Kx}$ | .217 | .601 | 1.000 | 1.000 | .340 | .116 |
| P (lb) | 81 | 226 | 375 | 376 | 128 | 44 |
| $P/A_A$ | 193 | 576 | 995 | 1127 | 420 | 158 |
| $P/A_1$ | 512 | 1522 | 2614 | 2934 | 1090 | 406 |
| $P/A_2$ | 218 | 642 | 1107 | 1240 | 460 | 171 |
| $e^{-1}P/A_2$ | 80 | 236 | 407 | 456 | 169 | 63 |
| **Final stringer stresses** | | | | | | |
| $\sigma_A$ (lb/sq in.) | 6708 | 5976 | 6087 | 3402 | 2164 | 1351 |
| $\sigma_B$ (lb/sq in.) | 2750 | 1462 | 0 | 0 | 958 | 691 |
| $\sigma_C$ (lb/sq in.) | 2167 | 2631 | 3006 | 3571 | 2132 | 1098 |
| $\sigma_D$ (lb/sq in.) | 1730 | 2106 | 2377 | 2256 | 1599 | 883 |

NACA

Tables 10, 11, 12

ANALYSIS OF SINGLE-STRINGER BEAM BY SUCCESSIVE SHEAR-FAULT REDUCTION - First Cycle

TABLE X $\quad \frac{G\,\Delta x}{E\,b} = \frac{0.40 \times 8}{6.85} = 0.467 \qquad t\,\Delta x = 0.015 \times 8 = 0.120$ sq in.

| | | 1 | 2 | 3 | 4 | 5 | 6 | 7 | 8 | 9 | 10 | 11 | 12 | 13 | 14 | 15 | 16 | 17 |
|---|---|---|---|---|---|---|---|---|---|---|---|---|---|---|---|---|---|---|
| Bay | Station | $\sigma_F$ (lb/sq in.) | $F_F$ (lb) | $F_L$ (lb) | $\sigma_L$ (lb/sq in.) | $\sigma_F-\sigma_L$ (lb/sq in.) | $\Delta\tau$ (lb/sq in.) | $\tau$ (lb/sq in.) | $\Delta S_{CE}$ (lb) | $\Delta F_L$ (lb) | SF (lb) | $SFC_o$ (lb) | $SFC_i$ (lb) | SFC (lb) | $\Delta\sigma_F$ (lb/sq in.) | $\Delta\sigma_L$ (lb/sq in.) | $\sigma_F$ (lb/sq in.) | $\sigma_L$ (lb/sq in.) |
| | 0 | 0 | 0 | 0 | 0 | | | | | | | | | | | | | |
| 1 | | | | | | | | 3663 | 440 | 435 | + 5 | | | | | | | |
| | 1 | 1338 | 342 | 435 | 783 | 555 | 259 | | | | | - 6 | - 3 | - 9 | - 35 | + 16 | 1303 | 799 |
| 2 | | | | | | | | 3404 | 408 | 430 | - 22 | | | | | | | |
| | 2 | 2435 | 689 | 865 | 1420 | 1015 | 474 | | | | | - 19 | + 6 | - 13 | - 46 | + 21 | 2389 | 1441 |
| 3 | | | | | | | | 2930 | 352 | 426 | - 74 | | | | | | | |
| | 3 | 3350 | 1040 | 1291 | 1950 | 1400 | 654 | | | | | - 38 | + 19 | - 19 | - 61 | + 29 | 3289 | 1979 |
| 4 | | | | | | | | 2276 | 273 | 425 | - 152 | | | | | | | |
| | 4 | 4130 | 1392 | 1716 | 2400 | 1730 | 807 | | | | | - 62 | + 38 | - 24 | - 71 | + 34 | 4059 | 2366 |
| 5 | | | | | | | | 1469 | 176 | 424 | - 248 | | | | | | | |
| | 5 | 4790 | 1745 | 2140 | 2780 | 2010 | 939 | | | | | - 88 | + 62 | - 26 | - 71 | + 34 | 4719 | 2814 |
| 6 | | | | | | | | 530 | 64 | 416 | - 352 | | | | | | | |
| | 6 | 5370 | 2106 | 2556 | 3100 | 2270 | 1060 | | | | | | + 88 | + 88 | + 224 | - 107 | 5594 | 2993 |
| | | | | | | | | | | $\Sigma$ = -843 | | | | | | | | |

ANALYSIS OF SINGLE-STRINGER BEAM BY SUCCESSIVE SHEAR-FAULT REDUCTION - 2nd Cycle

TABLE XI $\quad \frac{G\,\Delta x}{E\,b} = \frac{0.40 \times 8}{6.85} = 0.467 \qquad t\,\Delta x = 0.015 \times 8 = 0.120$ sq in.

| | | 1 | 2 | 3 | 4 | 5 | 6 | 7 | 8 | 9 | 10 | 11 | 12 | 13 | 14 | 15 | 16 |
|---|---|---|---|---|---|---|---|---|---|---|---|---|---|---|---|---|---|
| Bay | Station | $\sigma_F$ (lb/sq in.) | $F_L$ (lb) | $\sigma_L$ (lb/sq in.) | $\sigma_F-\sigma_L$ (lb/sq in.) | $\Delta\tau$ (lb/sq in.) | $\tau$ (lb/sq in.) | $\Delta S_{CE}$ (lb) | $\Delta F_L$ (lb) | SF (lb) | $SFC_o$ (lb) | $SFC_i$ (lb) | SFC (lb) | $\Delta\sigma_F$ (lb/sq in.) | $\Delta\sigma_L$ (lb/sq in.) | $\sigma_F$ (lb/sq in.) | $\sigma_L$ (lb/sq in.) |
| | 0 | 0 | 0 | 0 | 0 | | | | | | | | | | | | |
| 1 | | | | | | | 3578 | 429 | 444 | - 15 | | | | | | | |
| | 1 | 1303 | 444 | 799 | 504 | 235 | | | | | - 9 | + 8 | - 1 | - 4 | + 2 | 1299 | 801 |
| 2 | | | | | | | 3343 | 401 | 435 | - 34 | | | | | | | |
| | 2 | 2389 | 879 | 1441 | 948 | 443 | | | | | - 22 | + 9 | - 13 | - 46 | + 21 | 2343 | 1462 |
| 3 | | | | | | | 2900 | 348 | 434 | - 86 | | | | | | | |
| | 3 | 3289 | 1313 | 1979 | 1310 | 612 | | | | | - 27 | + 22 | - 5 | - 16 | + 8 | 3273 | 1987 |
| 4 | | | | | | | 2288 | 275 | 383 | - 108 | | | | | | | |
| | 4 | 4059 | 1696 | 2366 | 1693 | 791 | | | | | - 72 | + 27 | - 45 | - 133 | + 63 | 3926 | 2429 |
| 5 | | | | | | | 1497 | 180 | 469 | - 289 | | | | | | | |
| | 5 | 4719 | 2165 | 2814 | 1905 | 890 | | | | | - 77 | + 72 | - 5 | - 14 | + 6 | 4705 | 2820 |
| 6 | | | | | | | 607 | 73 | 305 | - 232 | | | | | | | |
| | 6 | 5594 | 2470 | 2993 | 2601 | 1213 | | | | | | + 77 | + 77 | + 197 | - 93 | 5781 | 2900 |
| | | | | | | | | | | $\Sigma$ = -764 | | | | | | | |

ANALYSIS OF MULTISTRINGER BEAM BY SUCCESSIVE SHEAR-FAULT REDUCTION
Typical Cycle for Adjustment of Stringer B

TABLE XII $\quad \frac{G\,\Delta x}{E\,b} = \frac{0.40 \times 8}{3.625} = 0.883 \qquad t\,\Delta x = 0.015 \times 8 = 0.120$ sq in.

| | | 1 | 2 | 3 | 4 | 5 | 6 | 7 | 8 | 9 | 10 | 11 | 12 | 13 | 14 | 15 | 16 | 17 | 18 | 19 | 20 |
|---|---|---|---|---|---|---|---|---|---|---|---|---|---|---|---|---|---|---|---|---|---|
| Bay | Station | $\sigma_A$ (lb/sq in.) | $\sigma_C$ (lb/sq in.) | $\sigma_B$ (lb/sq in.) | $\sigma_A-\sigma_B$ (lb/sq in.) | $\Delta\tau^{AB}$ (lb/sq in.) | $\tau^{AB}$ (lb/sq in.) | $\Delta S_{CE}^{AB}$ (lb) | $\sigma_B-\sigma_C$ (lb/sq in.) | $\Delta\tau^{BC}$ (lb/sq in.) | $\tau^{BC}$ (lb/sq in.) | $\Delta S_{CE}^{BC}$ (lb) | D (lb) | $F_B$ (lb) | $\Delta F_B$ (lb) | SF (lb) | $SFC_o$ (lb) | $SFC_i$ (lb) | SFC (lb) | $\Delta\sigma_B$ (lb/sq in.) | $\sigma_B$ (lb/sq in.) |
| | 0 | 0 | 0 | 0 | 0 | | | | | | | | | | | | | | | | |
| 1 | | | | | | | 4696 | 564 | | | 2901 | 348 | 216 | | 204 | +12 | | | | | |
| | 1 | 1112 | 840 | 952 | 160 | 141 | | | 112 | 99 | | | | 204 | | | -1 | -6 | -7 | +33 | 985 |
| 2 | | | | | | | 4555 | 547 | | | 2802 | 336 | 211 | | 213 | - 2 | | | | | |
| | 2 | 2079 | 1518 | 1774 | 305 | 269 | | | 256 | 226 | | | | 417 | | | +4 | +1 | +5 | -21 | 1753 |
| 3 | | | | | | | 4286 | 515 | | | 2576 | 310 | 205 | | 189 | +16 | | | | | |
| | 3 | 2998 | 1936 | 2370 | 628 | 555 | | | 434 | 384 | | | | 606 | | | -1 | -4 | -5 | +20 | 2390 |
| 4 | | | | | | | 3731 | 448 | | | 2192 | 263 | 185 | | 189 | -4 | | | | | |
| | 4 | 3941 | 2200 | 2875 | 1066 | 942 | | | 675 | 596 | | | | 795 | | | -12 | +1 | -11 | +40 | 2915 |
| 5 | | | | | | | 2789 | 335 | | | 1596 | 192 | 143 | | 191 | -48 | | | | | |
| | 5 | 5000 | 2203 | 3320 | 1680 | 1484 | | | 1117 | 986 | | | | 986 | | | -3 | +12 | +9 | -30 | 3290 |
| 6 | | | | | | | 1305 | 157 | | | 610 | 73 | 84 | | 94 | -10 | | | | | |
| | 6 | 6355 | 2020 | 3399 | 2956 | 2610 | | | 1379 | 1220 | | | | 1080 | | | | +3 | +3 | - 9 | 3390 |
| | | | | | | | | | | | | | | | $\Sigma$ = -36 | | | | | | |

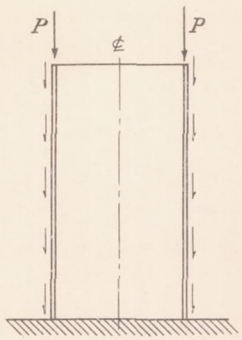



Figure 1.

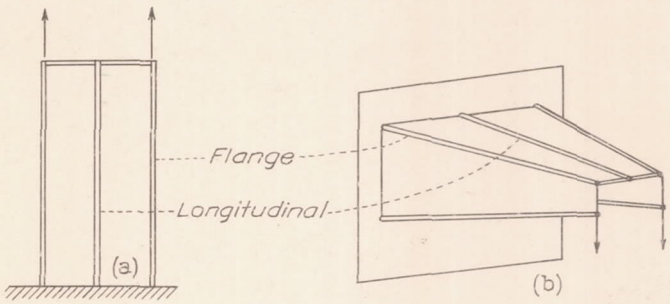



Figure 2.

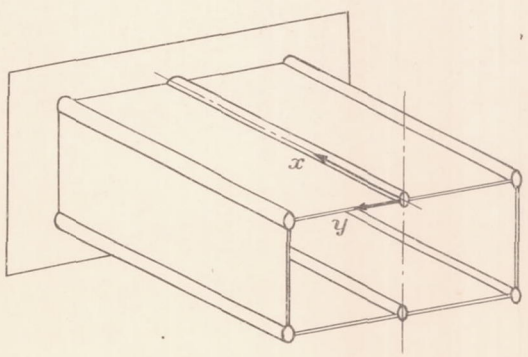



Figure 3.- Convention for coordinate axes.

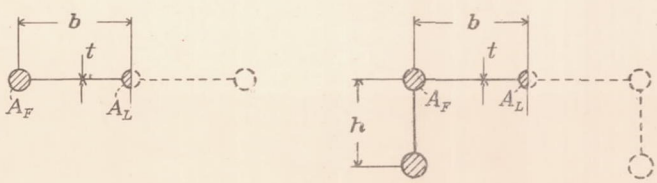



Figure 4.- Convention for symbols on cross sections.

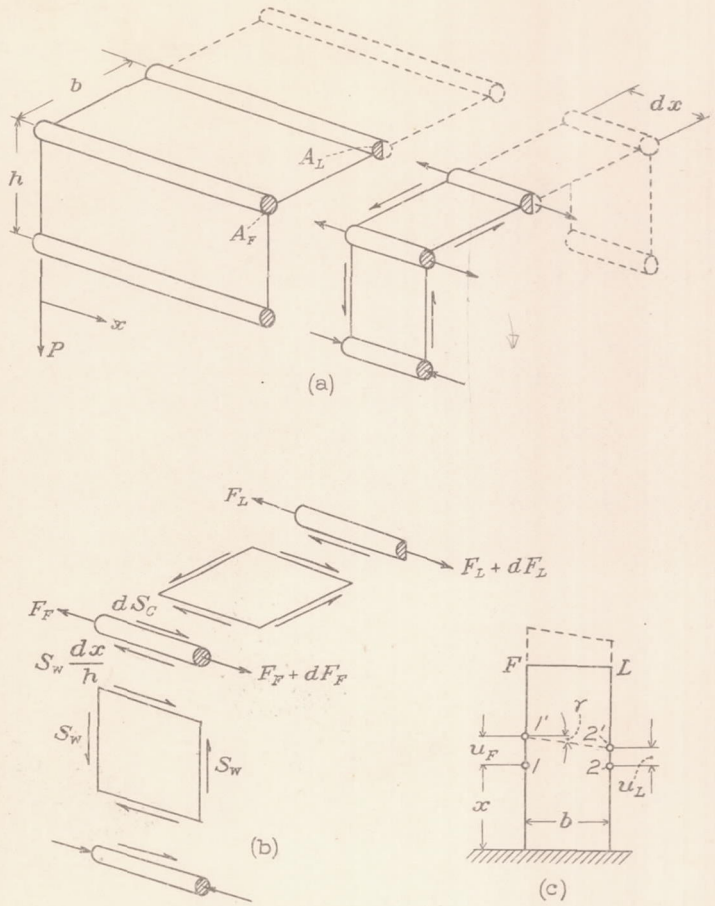



Figure 5.- Free-body diagrams of beam.

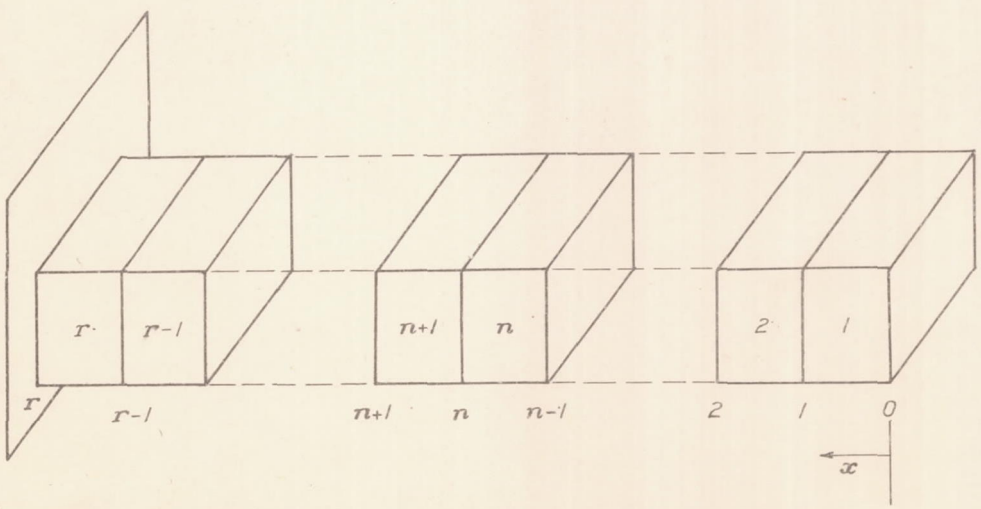



Figure 6.- Convention for numbering bays and stations of a beam.

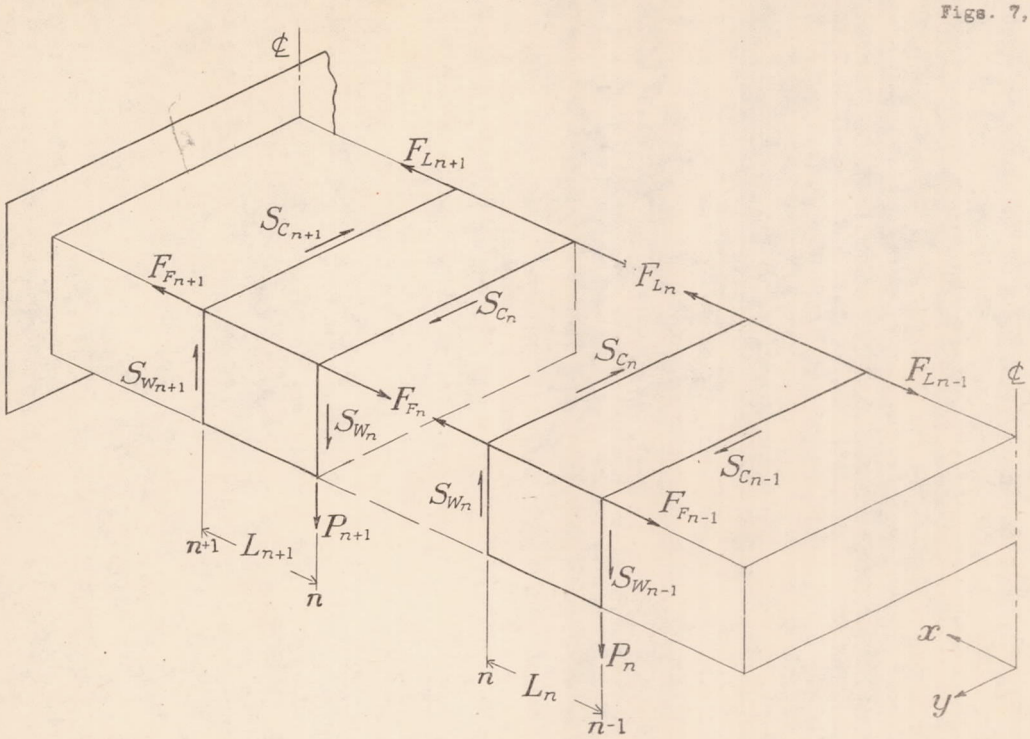
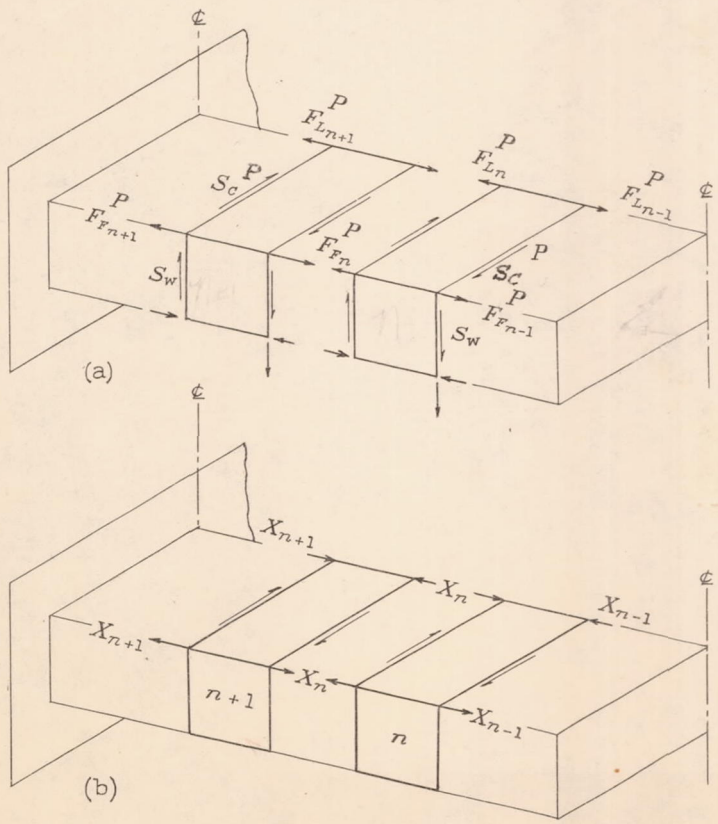



Figure 7.- Free-body diagrams of bays.




(a) P-forces (b) X-forces

Figure 8.- Separation of forces acting on bays.

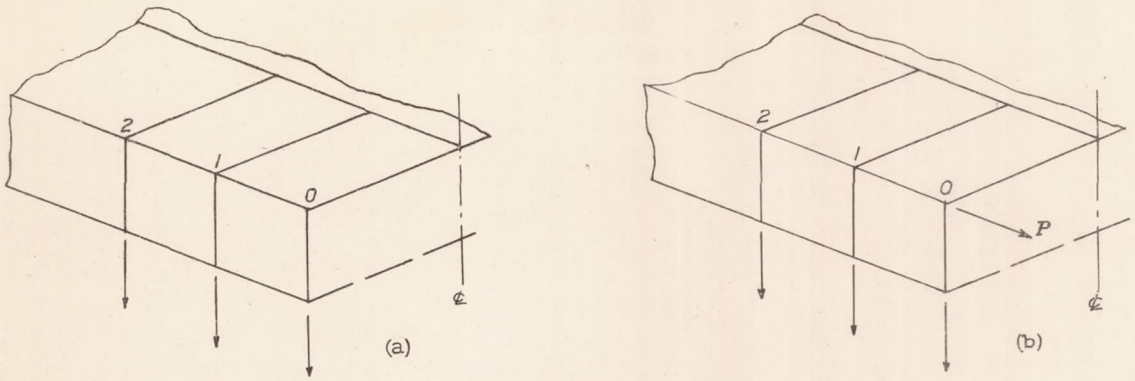



Figure 9.- Boundary conditions at tip.

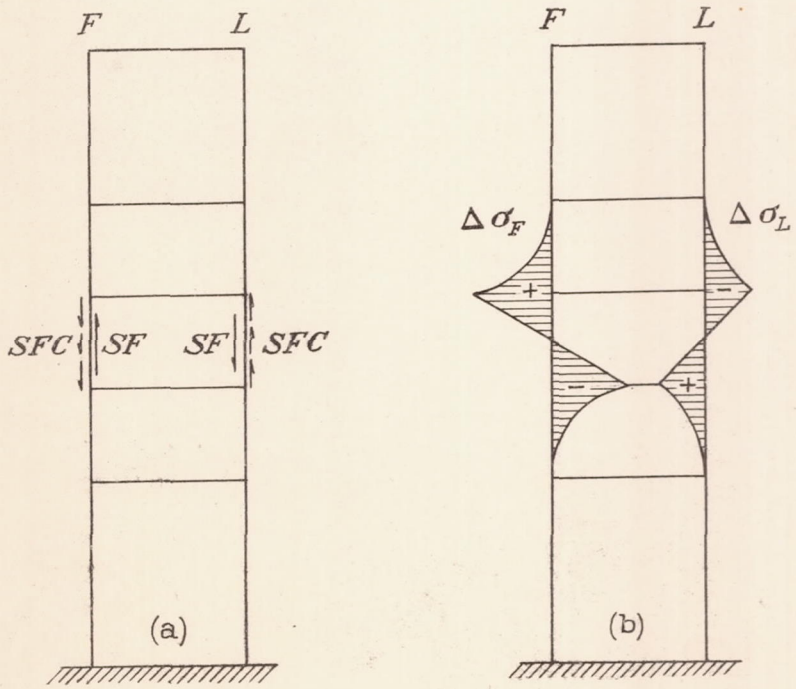



Figure 10.- Shear fault and shear-fault correction.

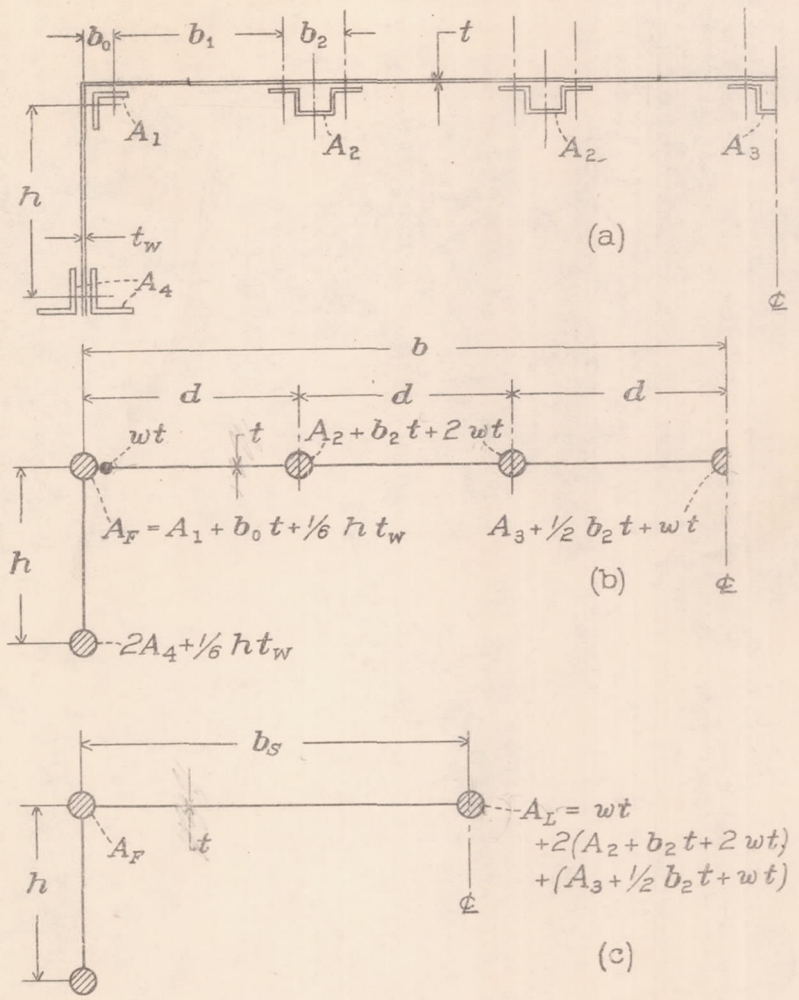



Figure 11.- Idealization of multistringer cross section.

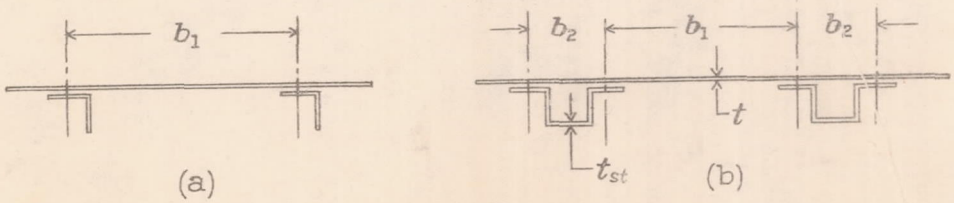



Figure 12.- Standard symbols for width of panels.

Based on assumption that $A_L$ is uniformly distributed over width b.

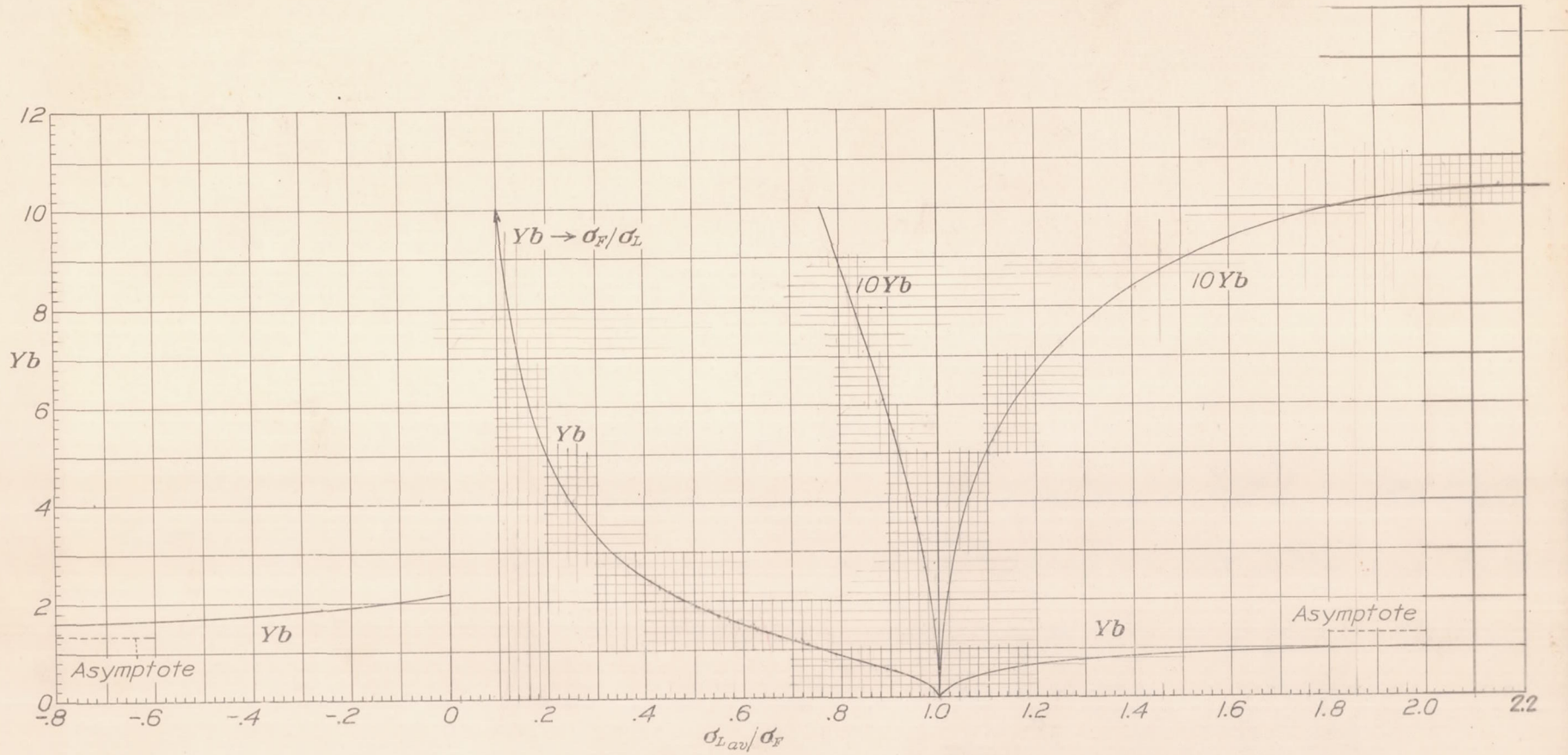
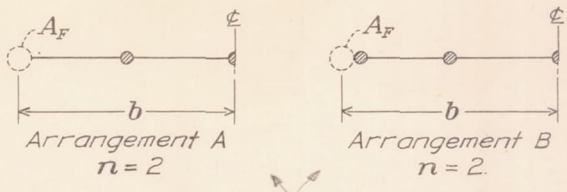



Figure 13.- Auxiliary graph for determining chordwise distribution of stresses.




Extreme arrangements

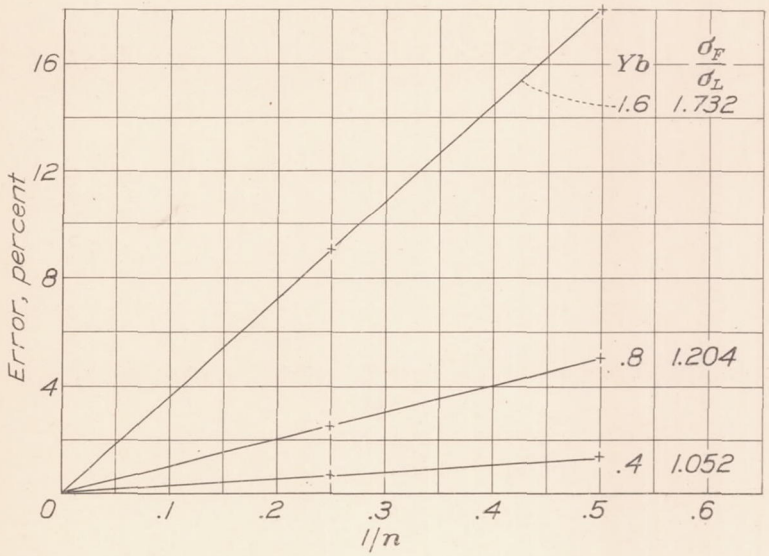



Figure 14.- Error in total force caused by finite number of stringers. n, number of stringers, except stringer contiguous to flange.

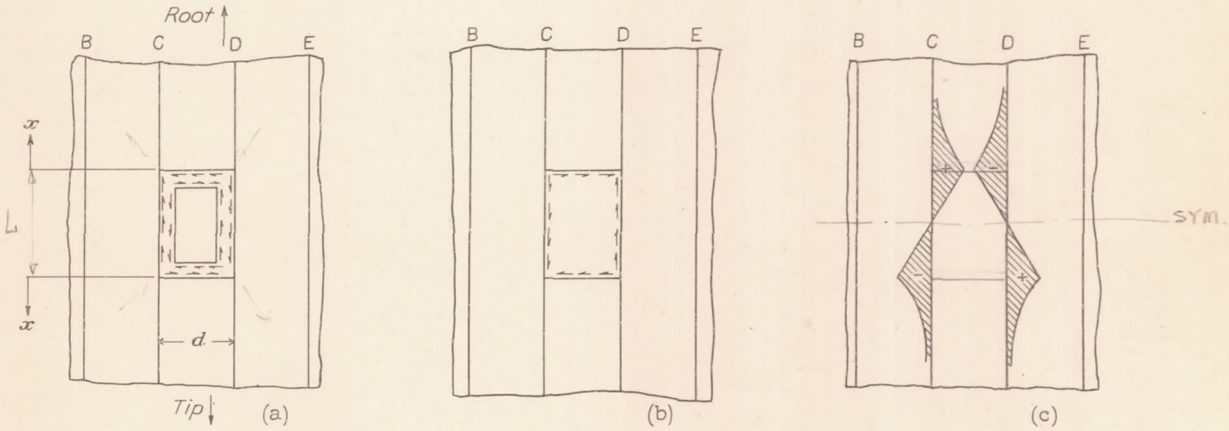



Figure 17.- Effects of removing a skin panel.

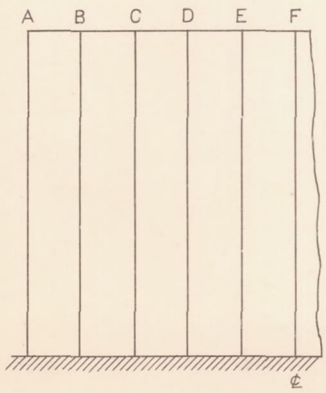



Figure 16.

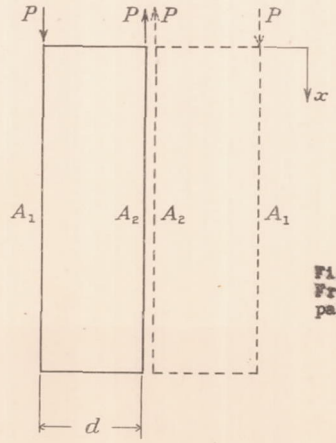



Figure 18.- Free panel.

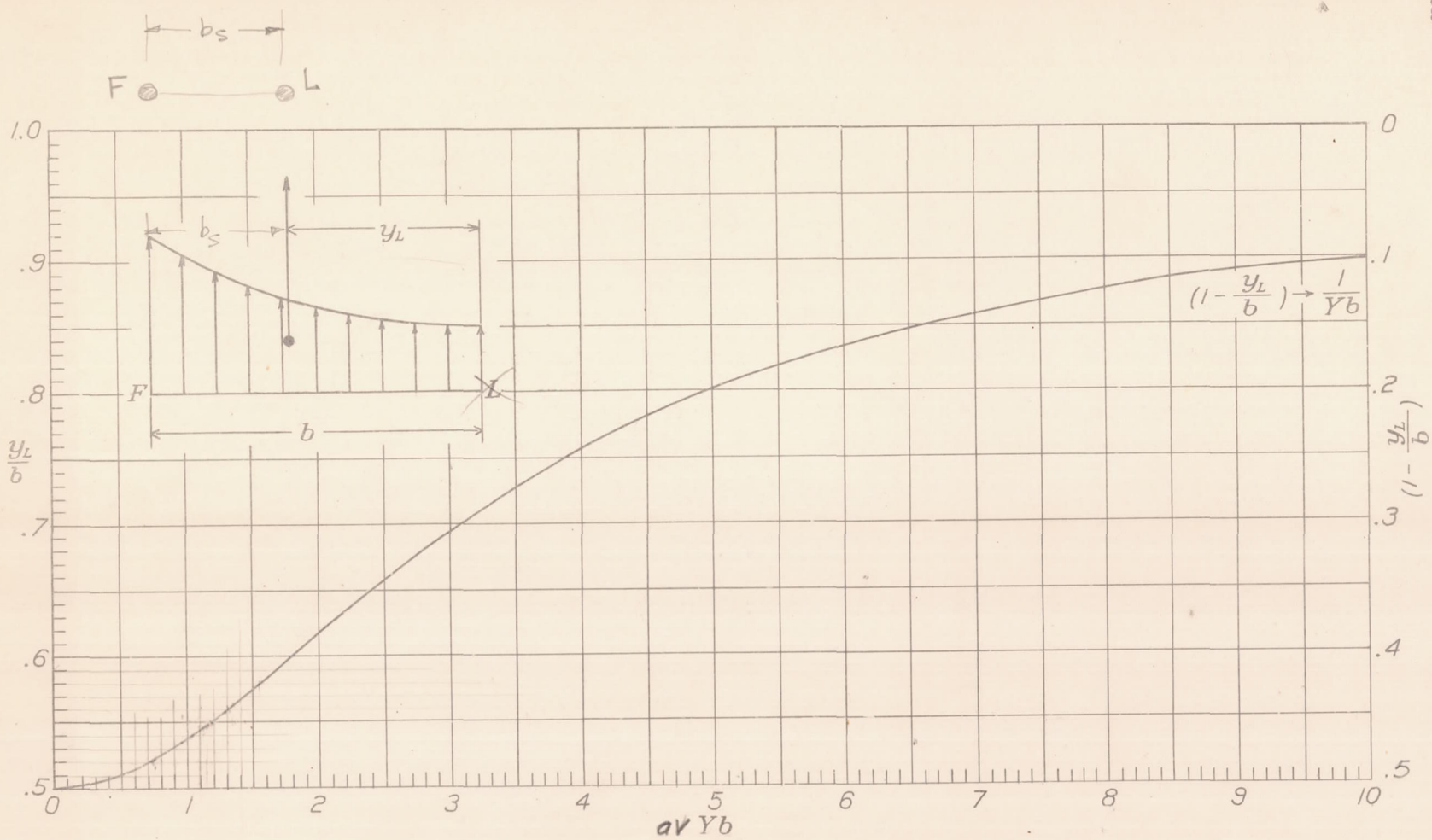



Figure 15.- Graph for locating resultant internal force.

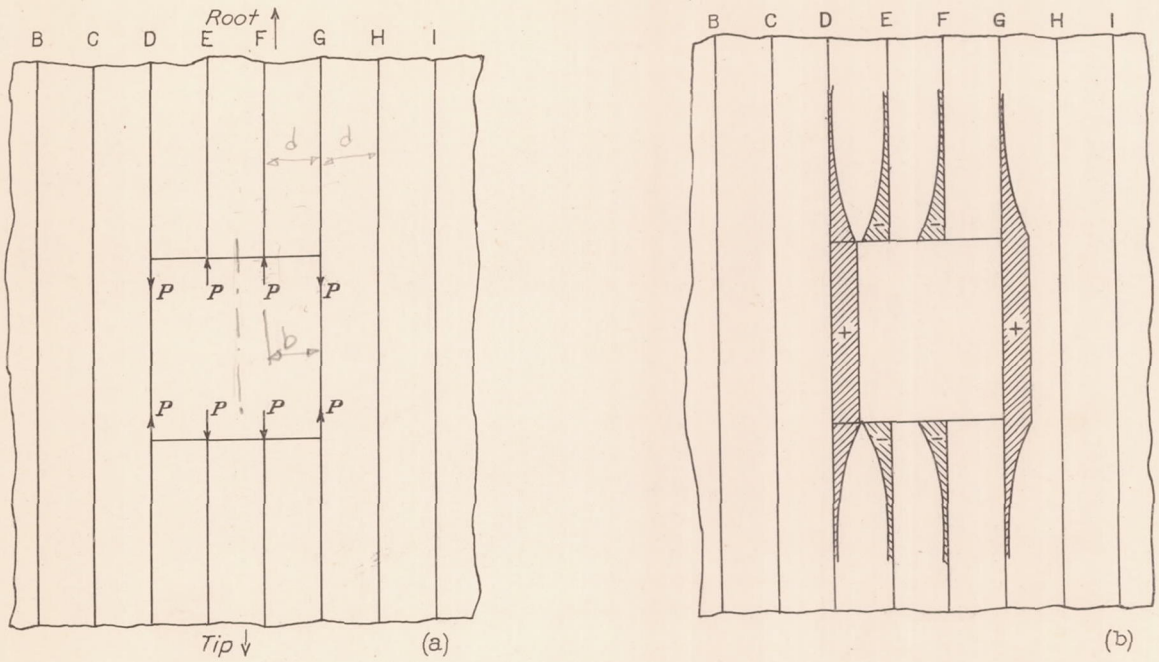



Figure 19.- Effects of cutting stringers.

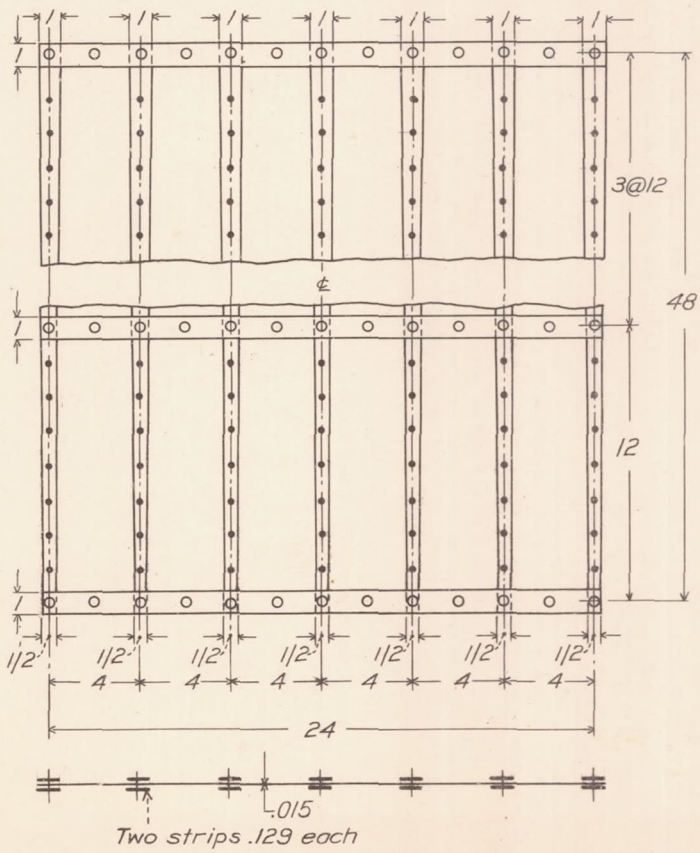



Figure 20.- Panel for tests with axial load. Sheet 178-T; Stringers 248-T; E = 10.8 x $10^6$.

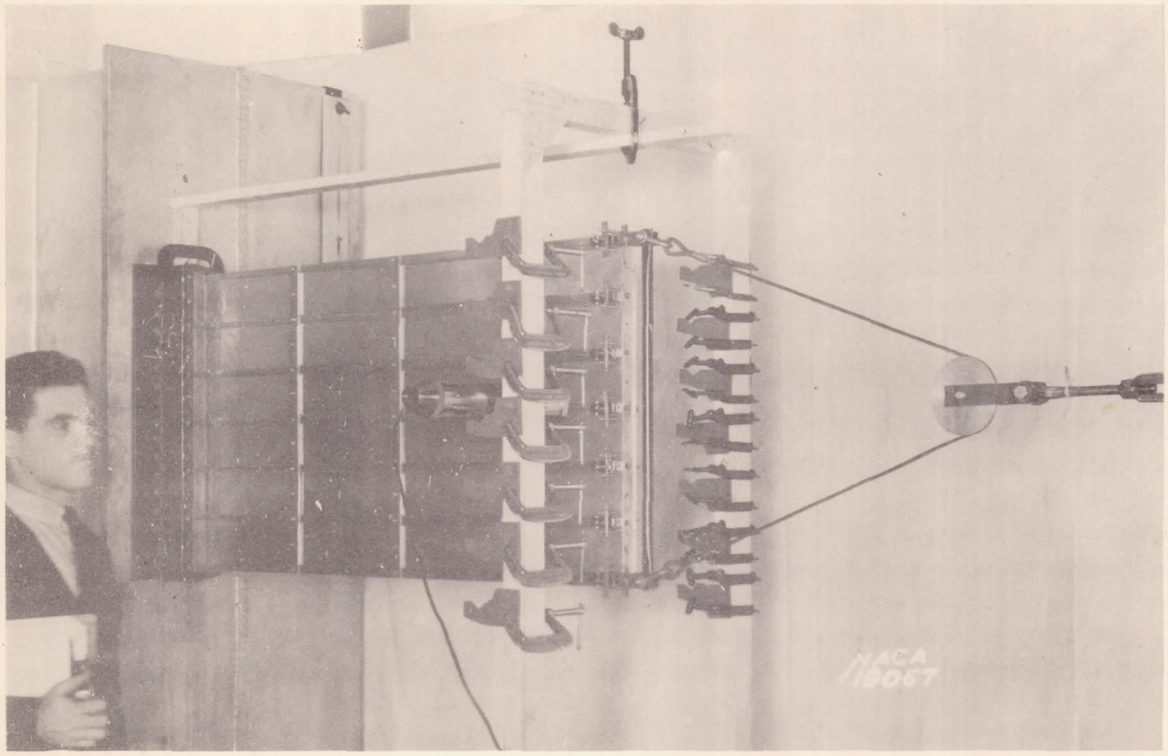



Figure 21.- Test set-up for panel.

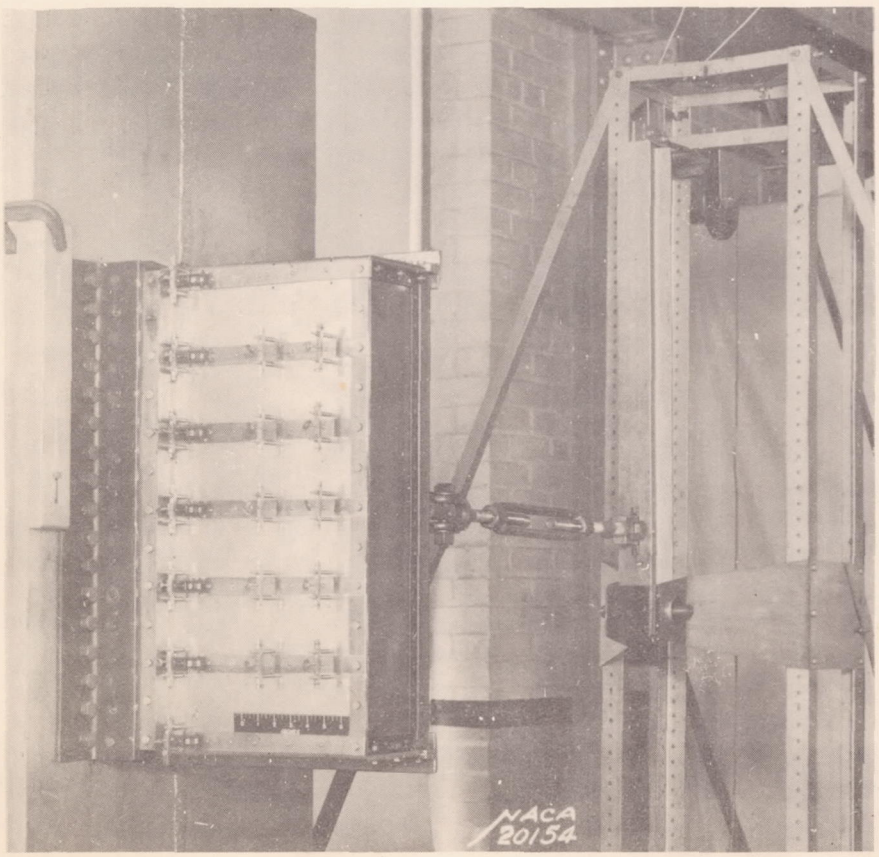



Figure 25.- Test set-up for beam 2.

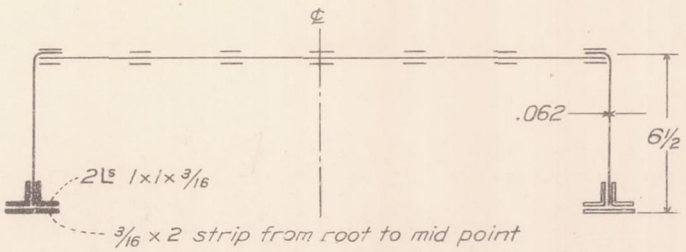
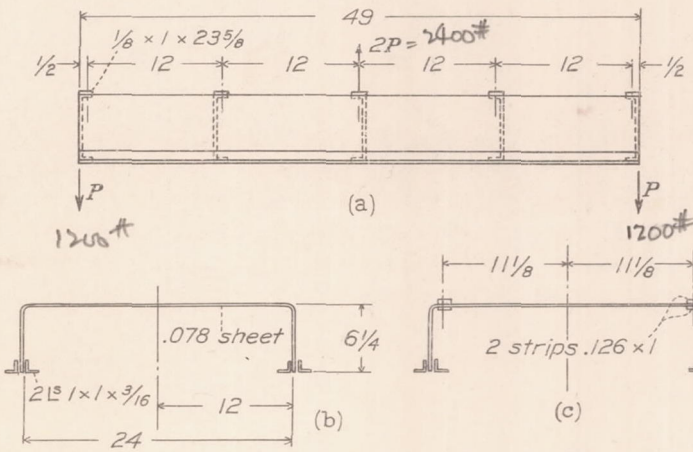



Figure 22.- Cross section of beam 1. Cover of beam is panel shown in figure 20.




(a) Side view. (b) Original cross section.
(c) Modified cross section.

Figure 26.- Beam 3. Sheet 24S-T, E = 10.6 x $10^6$; stringers 24S-T, E = 10.3 x $10^6$. Bulkheads not shown on cross sections.

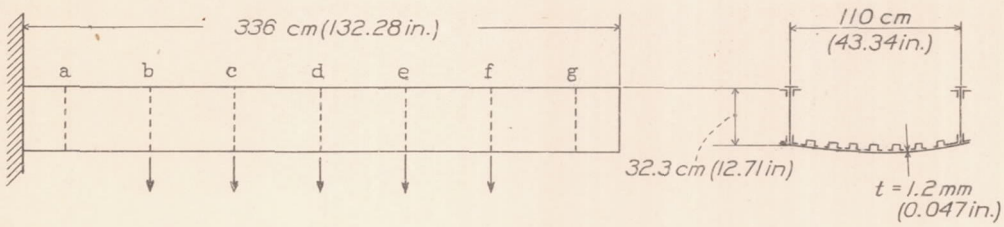



Figure 28.- Sketch of test beam from reference 5.

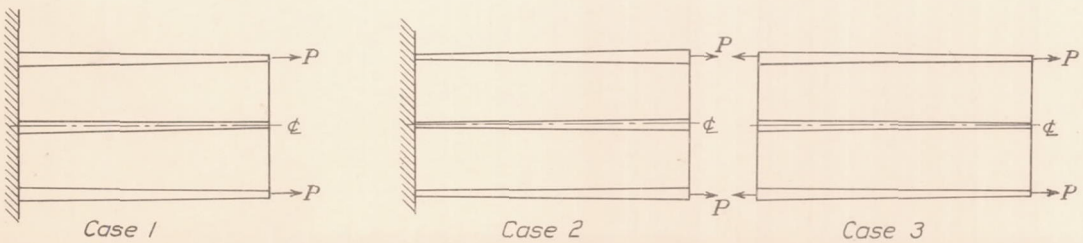



Figure 29.- Diagram of loading cases for panel. P = 1300 pounds.

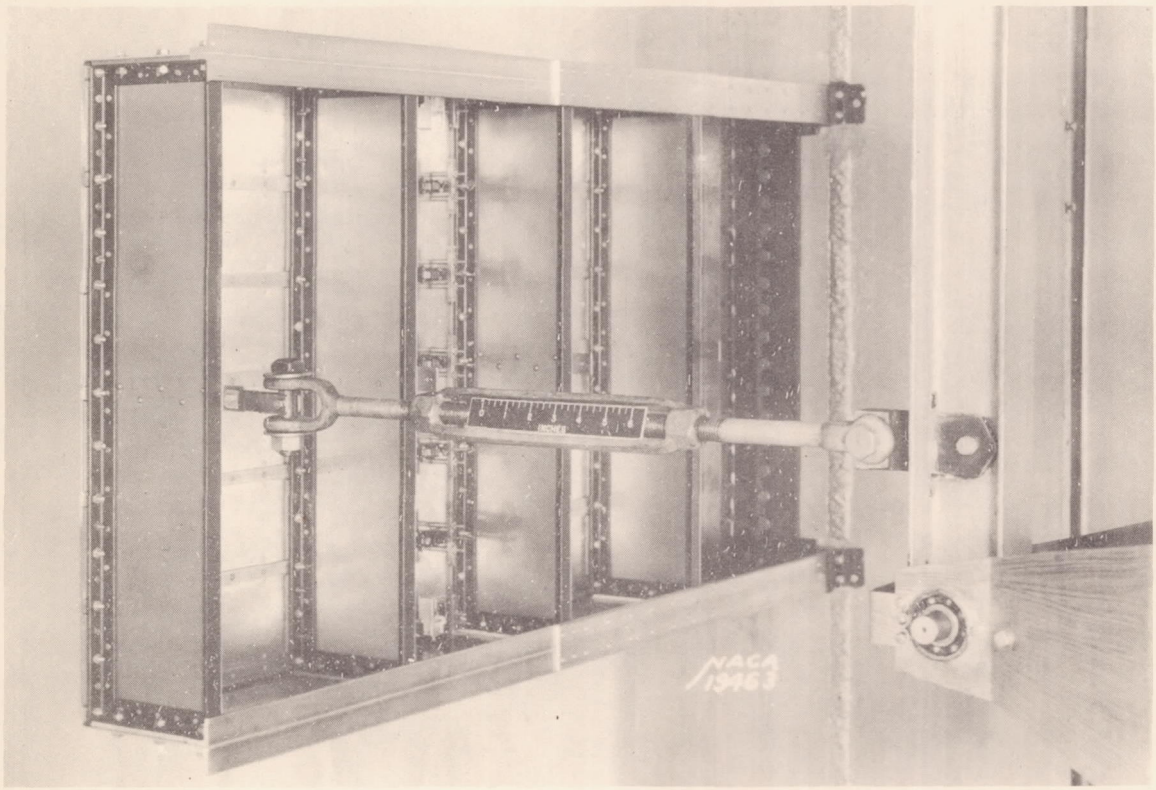



Figure 23.- Test set-up for beam 1.

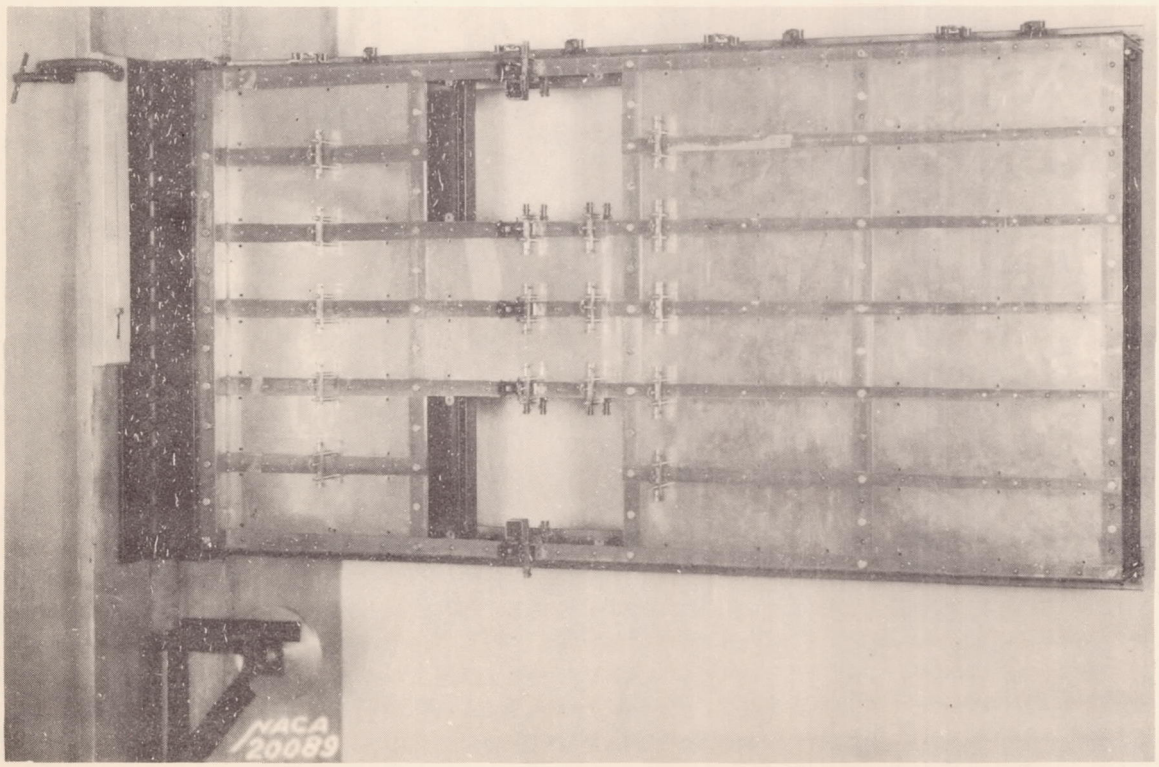



Figure 24.- Test set-up for beam 1 with cut-outs

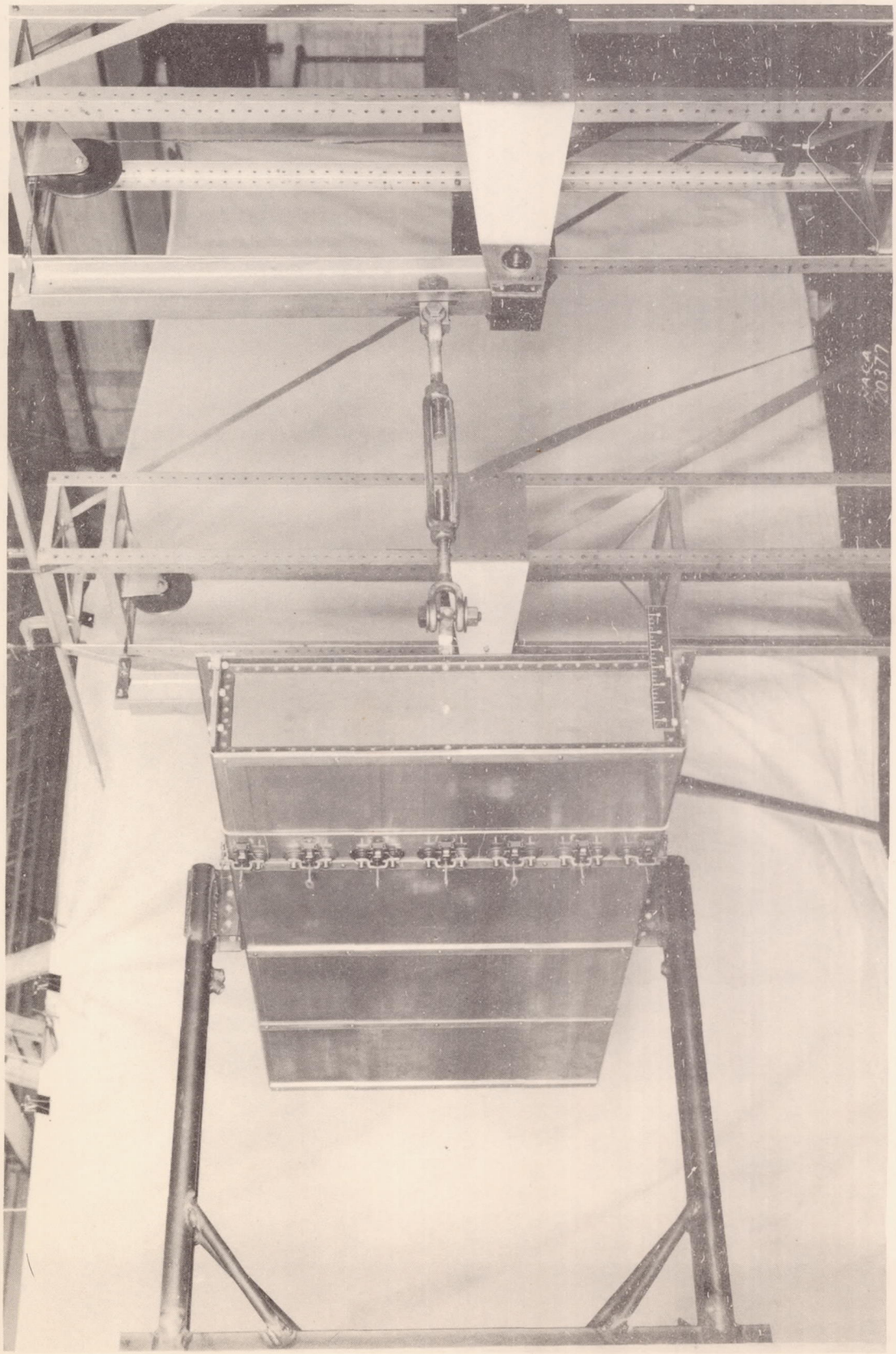



Figure 27.- Test set-up for beam 3.

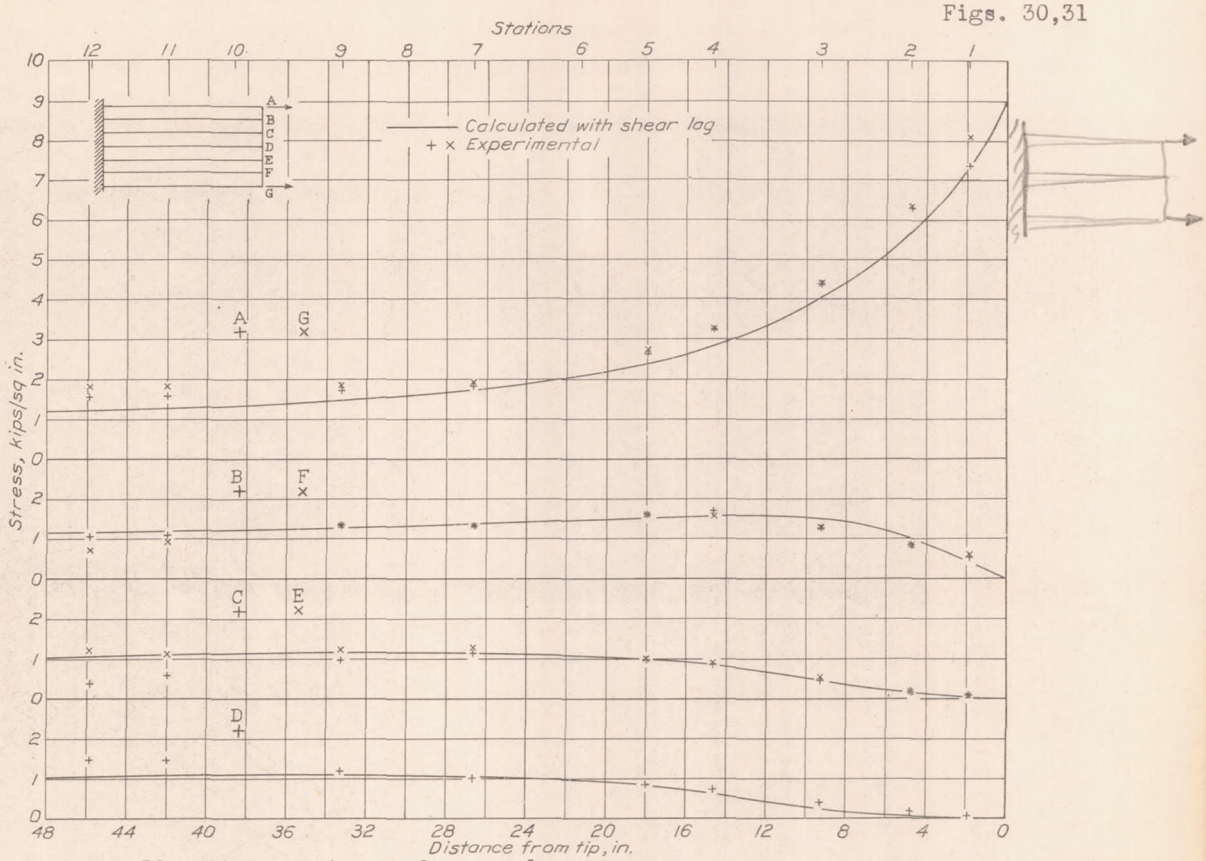



Figure 30.- Stresses in panel, case 1.

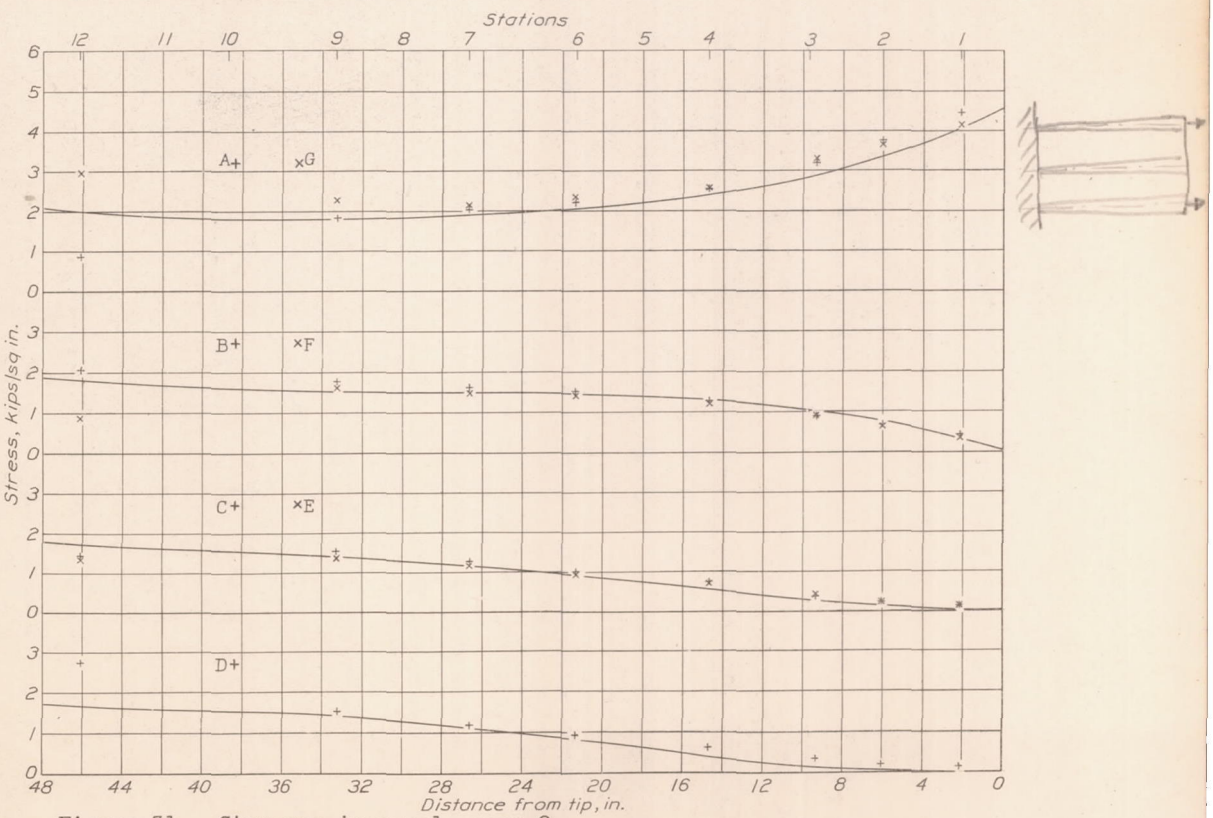



Figure 31.- Stresses in panel, case 2.

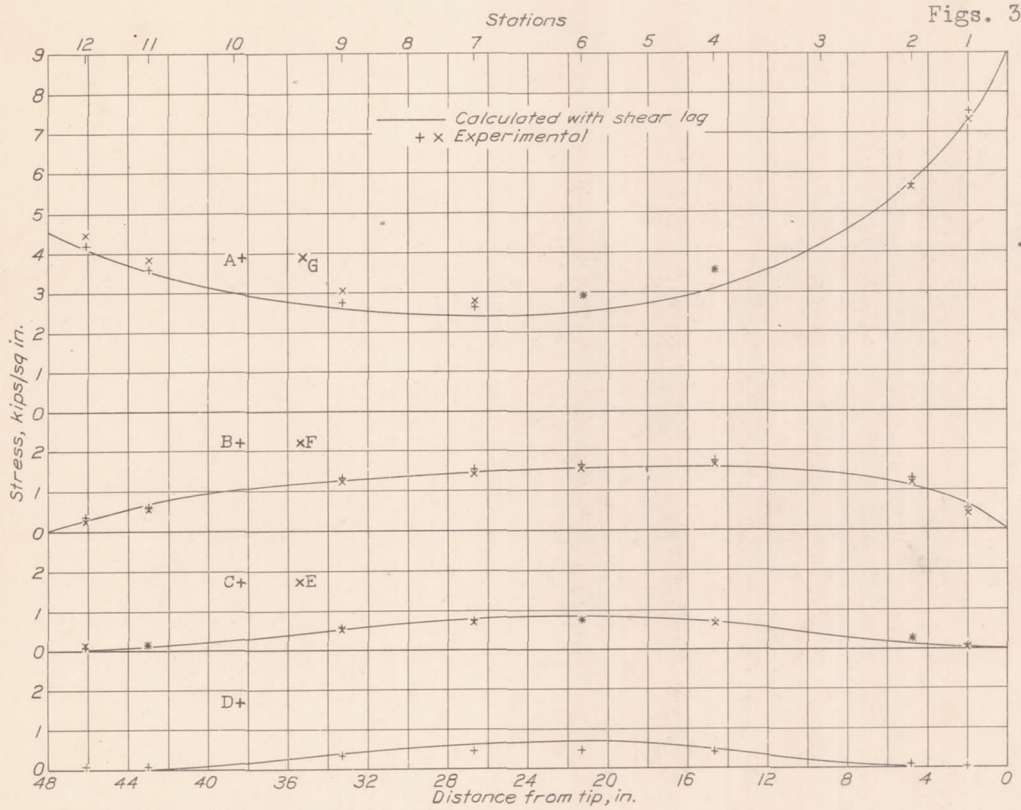



Figure 32.- Stresses in panel, case 3.

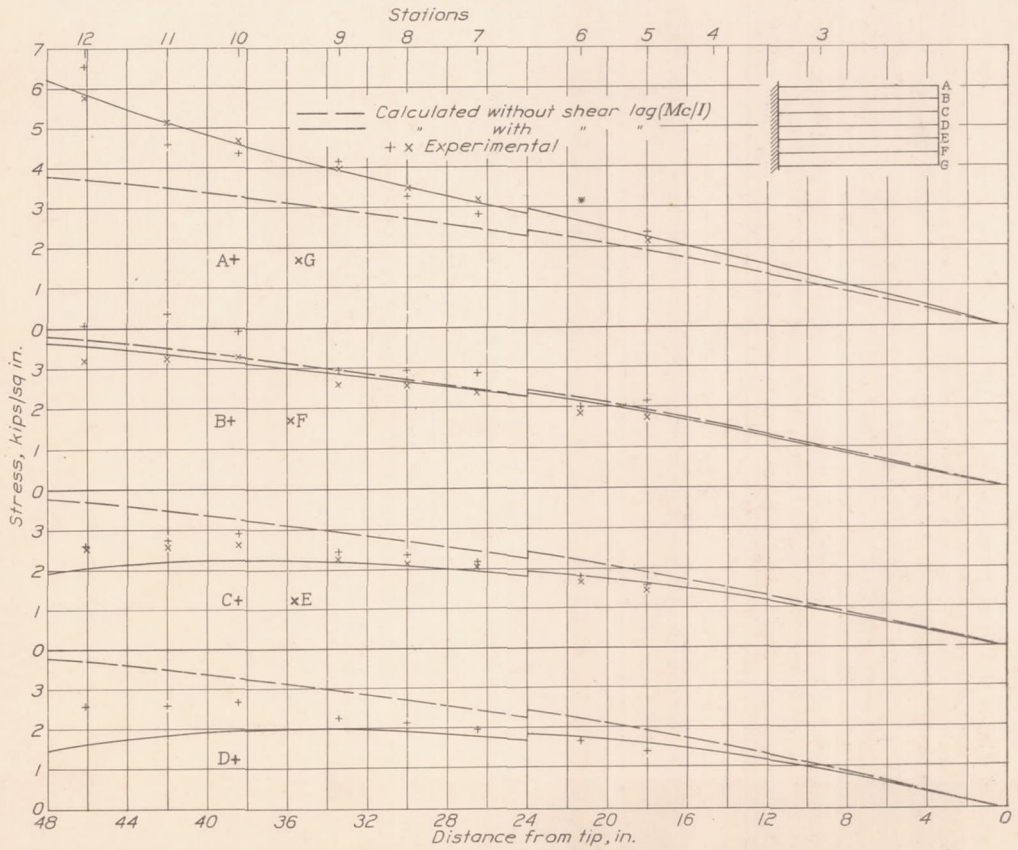



Figure 36.- Comparisons between calculated and experimental stresses in beam 1, case 1.

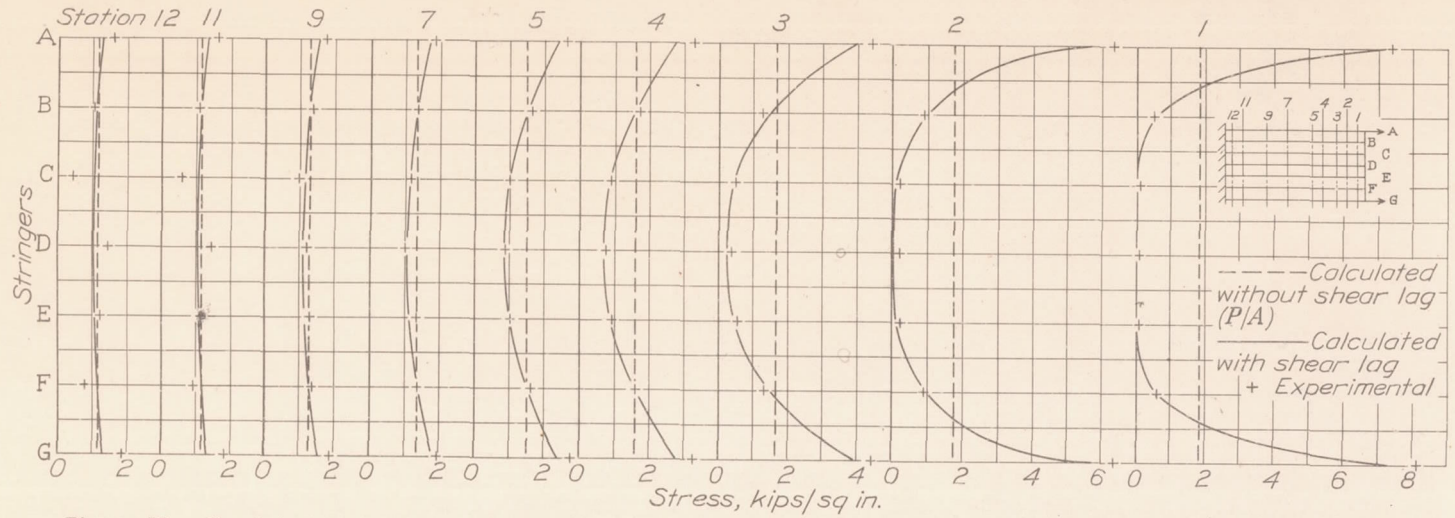



Figure 33.- Chordwise distribution of stresses in panel, case 1.

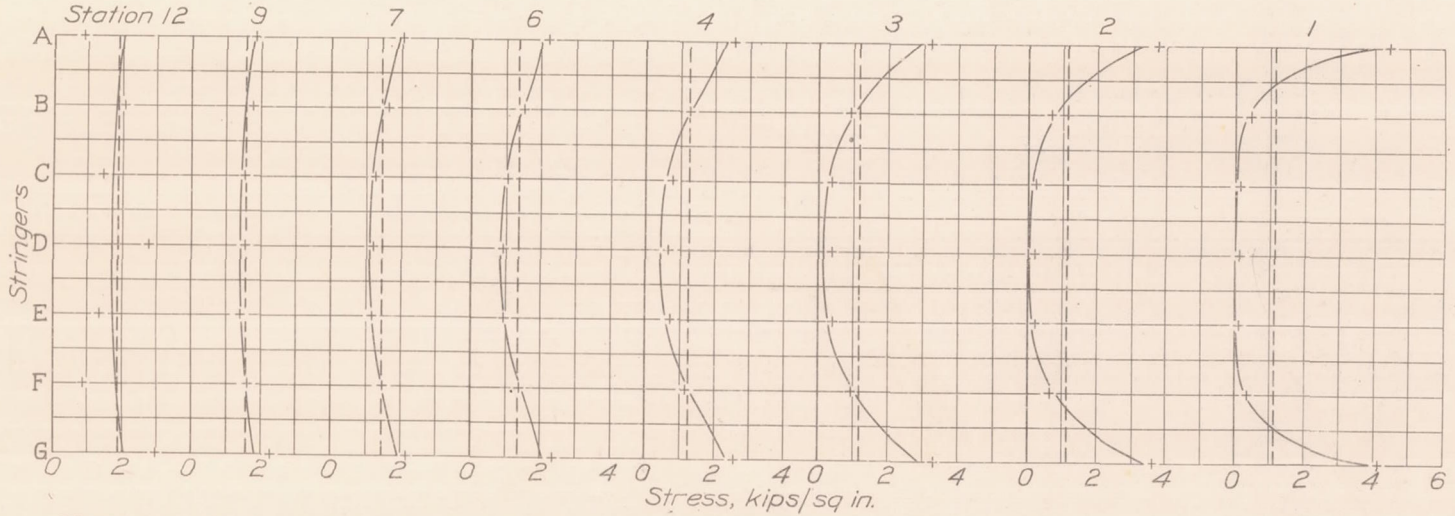



Figure 34.- Chordwise distribution of stresses in panel, case 2.

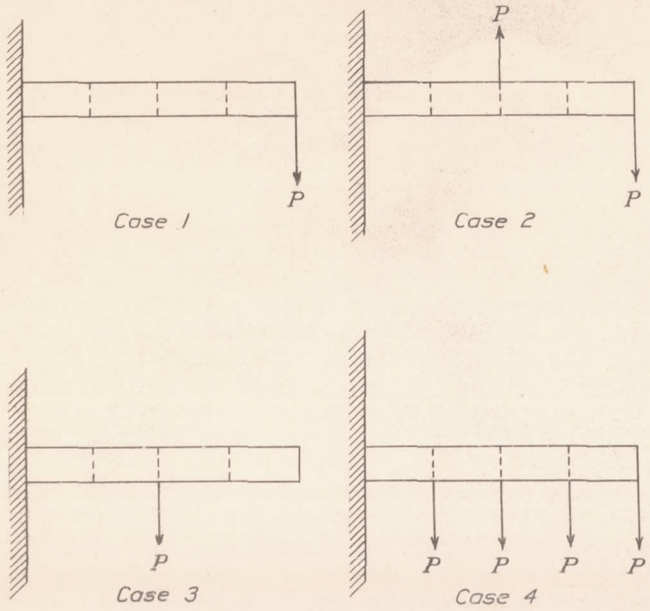



Figure 35.- Diagram of loading cases for beam 1. P = 600 pounds on each shear web for cases 1,2, and 3; P = 345 pounds on each shear web for case 4.

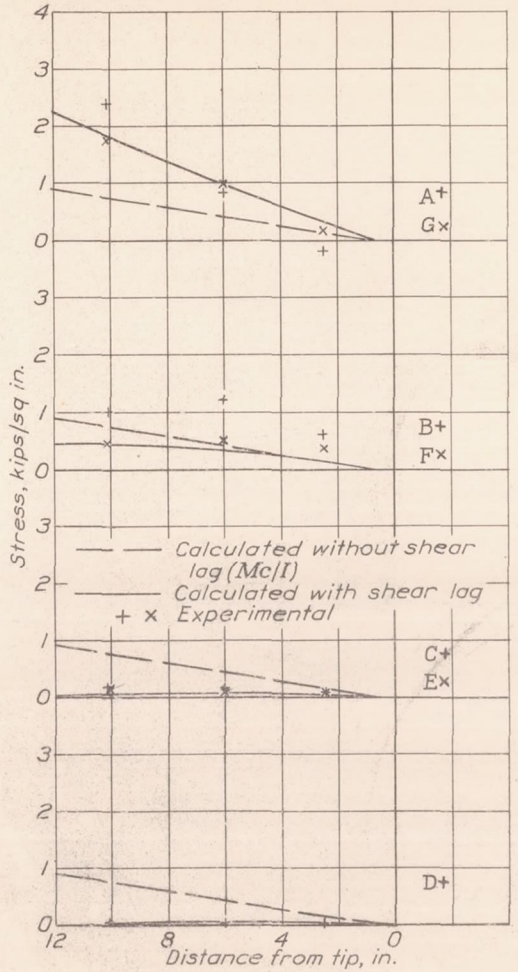



Figure 40.- Comparisons between calculated and experimental stresses in beam 2. Friction, 4 percent.

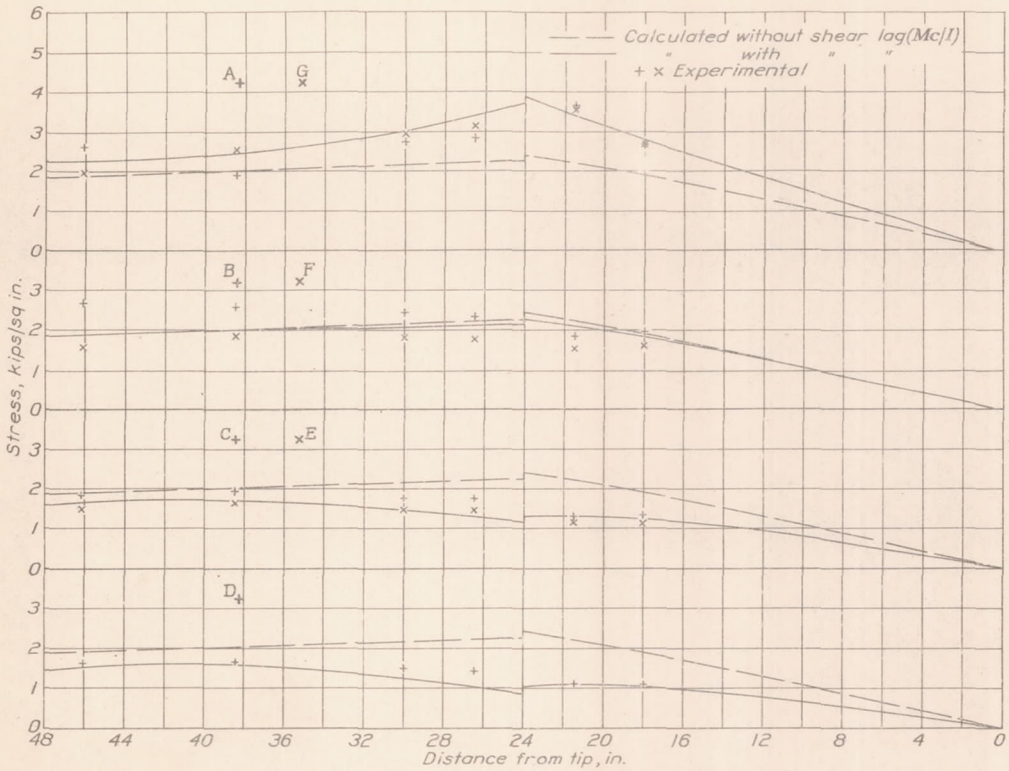



Figure 37.- Comparisons between calculated and experimental stresses in beam 1, case 2.

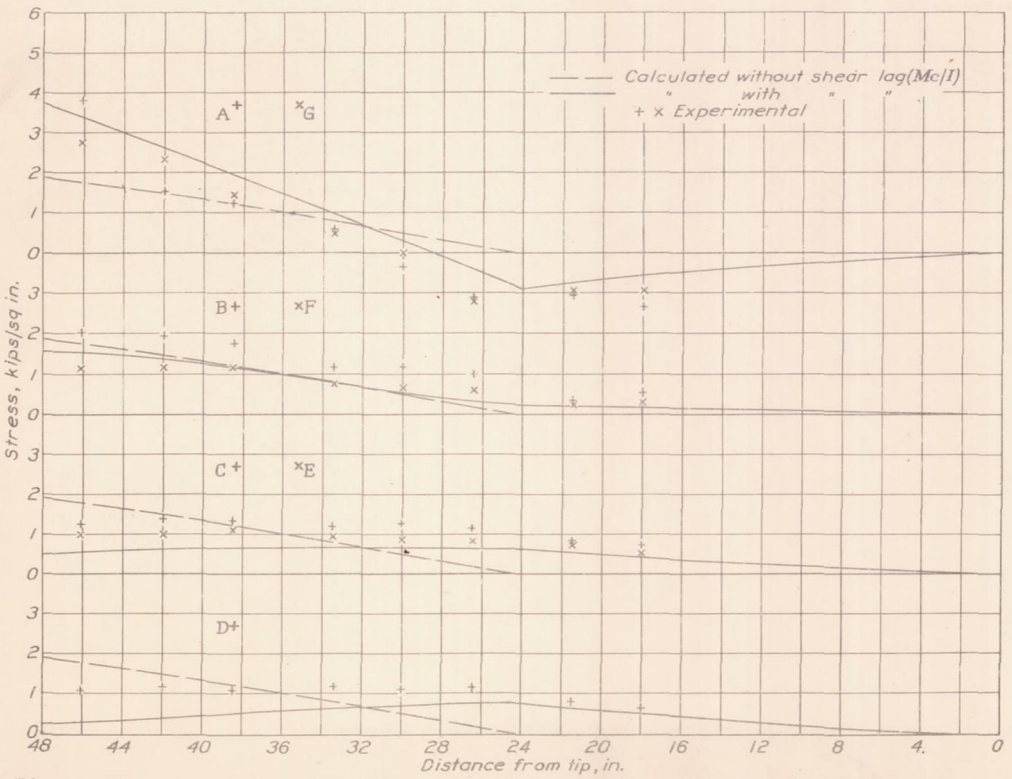



Figure 38.- Comparisons between calculated and experimental stresses in beam 1, case 3.

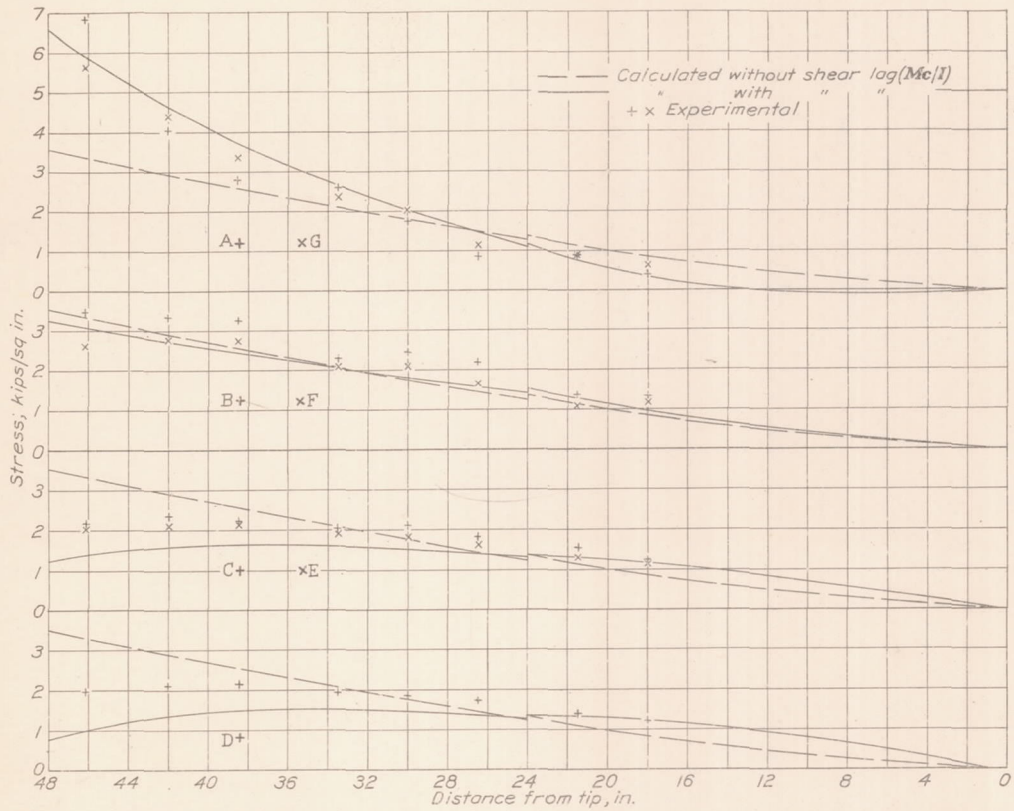



Figure 39.- Comparisons between calculated and experimental stresses in beam 1, case 4.

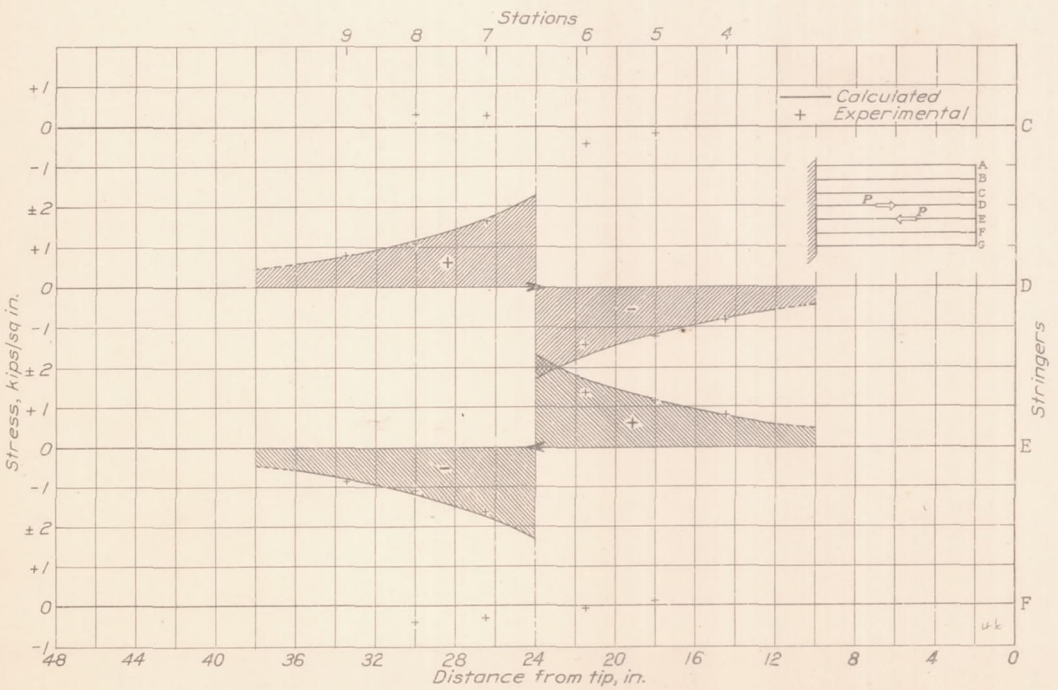



Figure 46.- Comparisons between calculated and experimental stresses for special tests on beam 1.

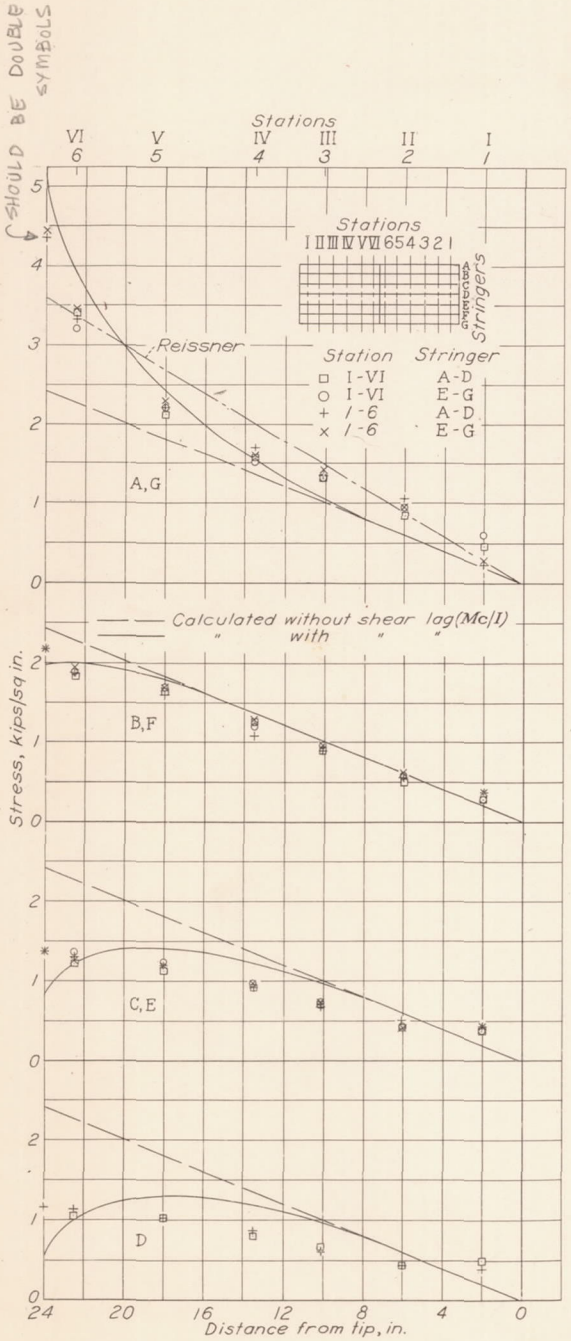



Figure 41.- Comparisons between calculated and experimental stresses in beam 3, case 1. Friction less than 1/2 percent.

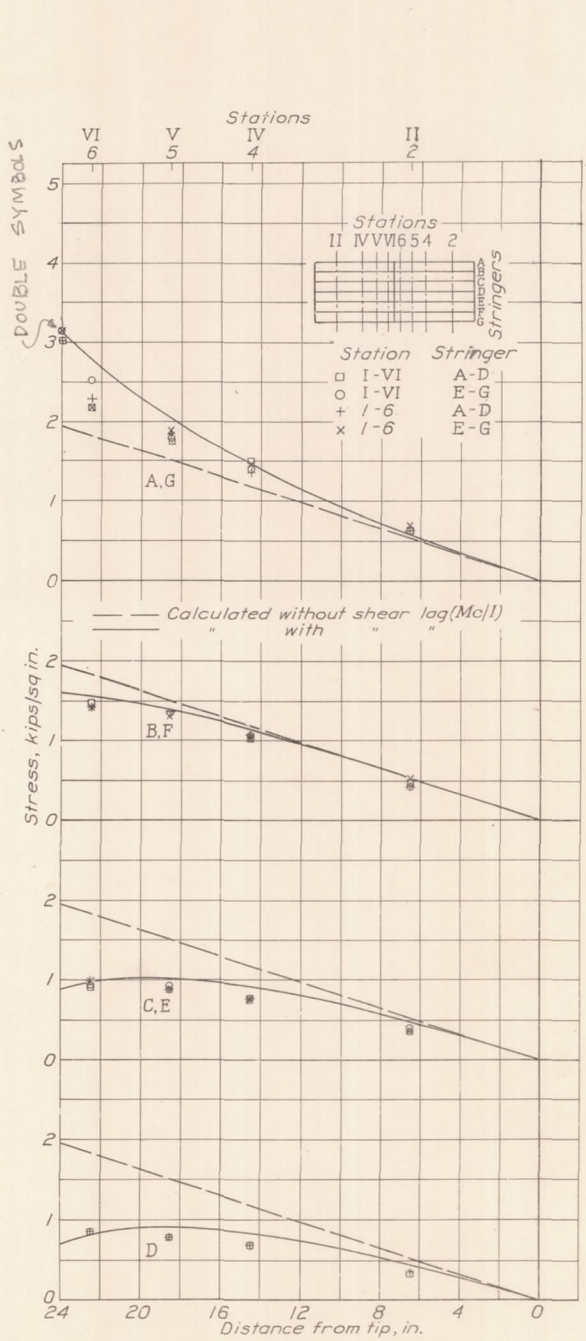
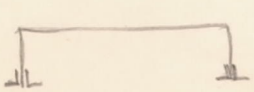
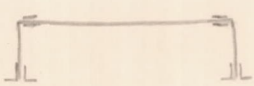



Figure 42.- Comparisons between calculated and experimental stresses in beam 3, case 2. Friction less than 1/2 percent. Third approximation.





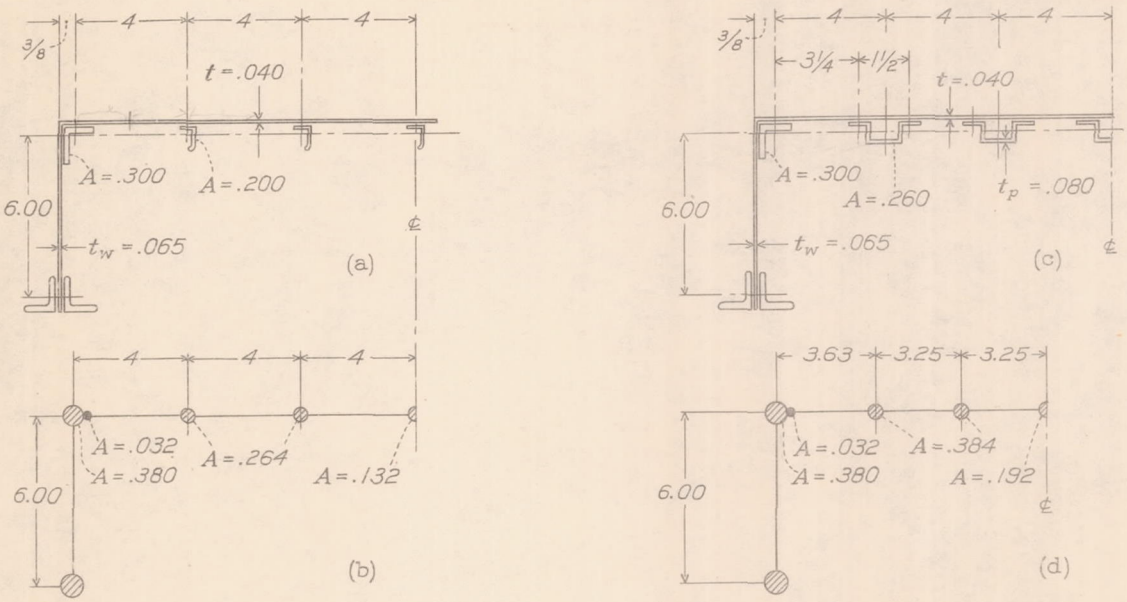



Figure 49.- Examples for idealization of cross sections.

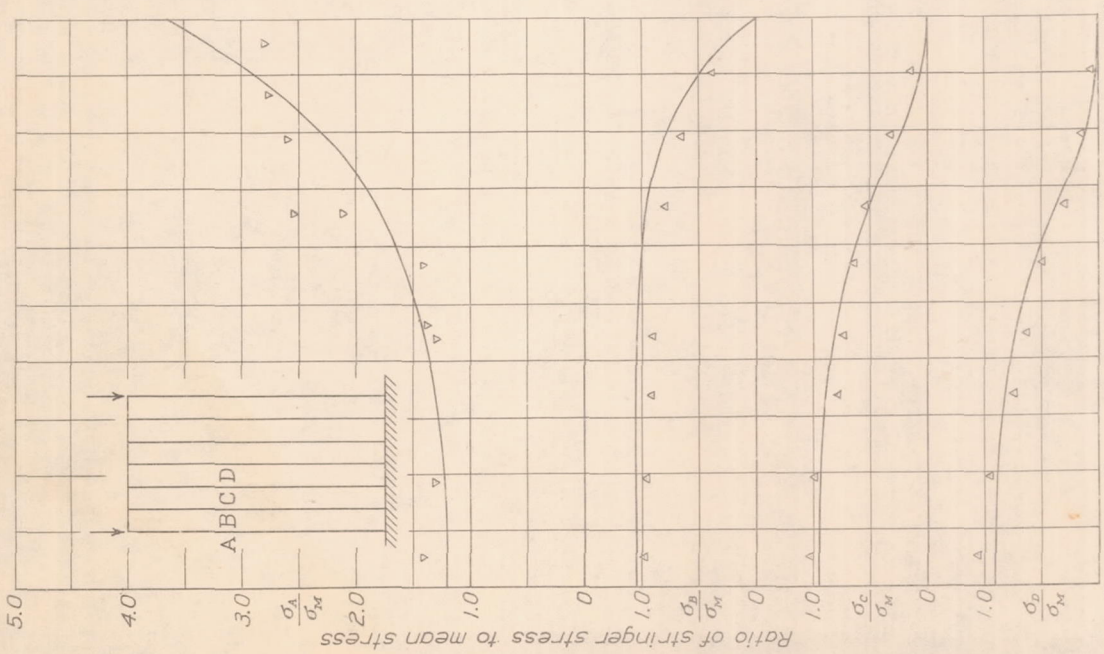
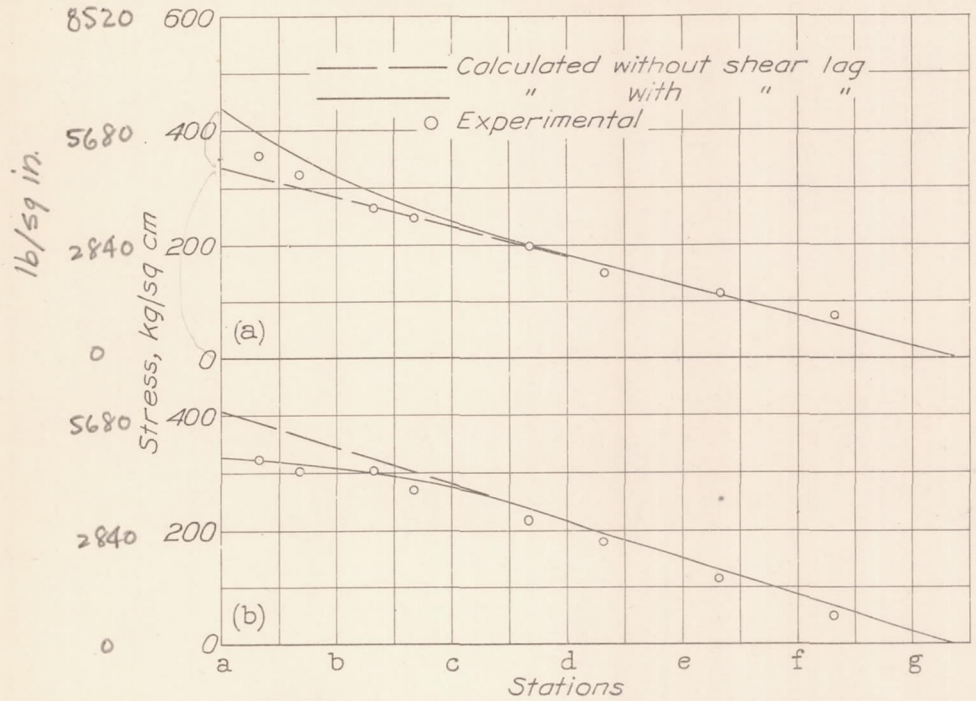
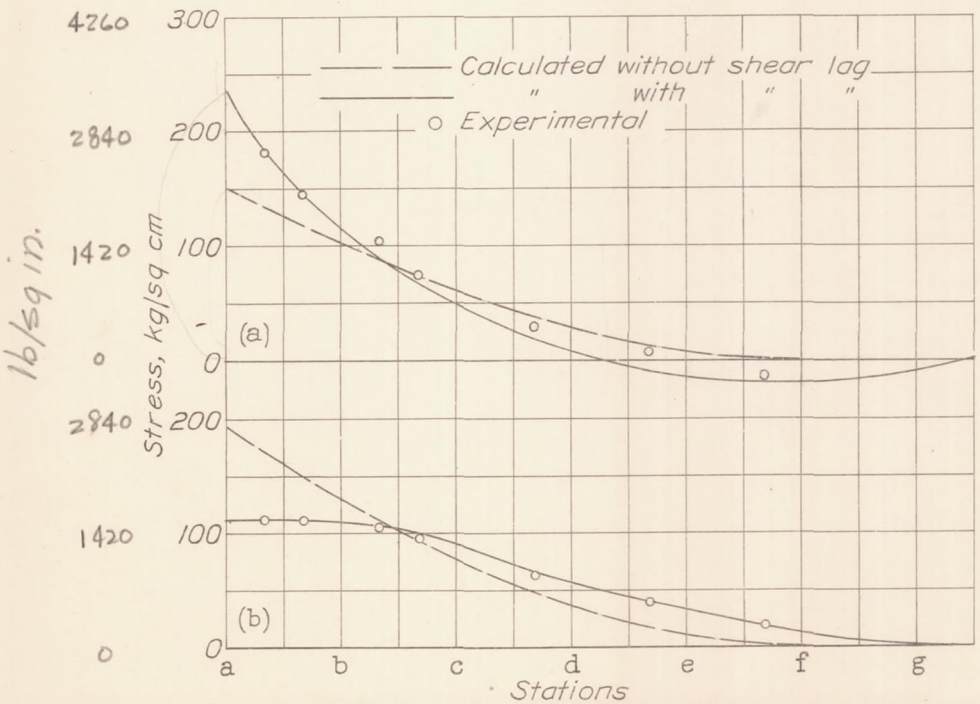



Figure 43.- Comparisons between calculated and experimental stresses in panel of reference 4.



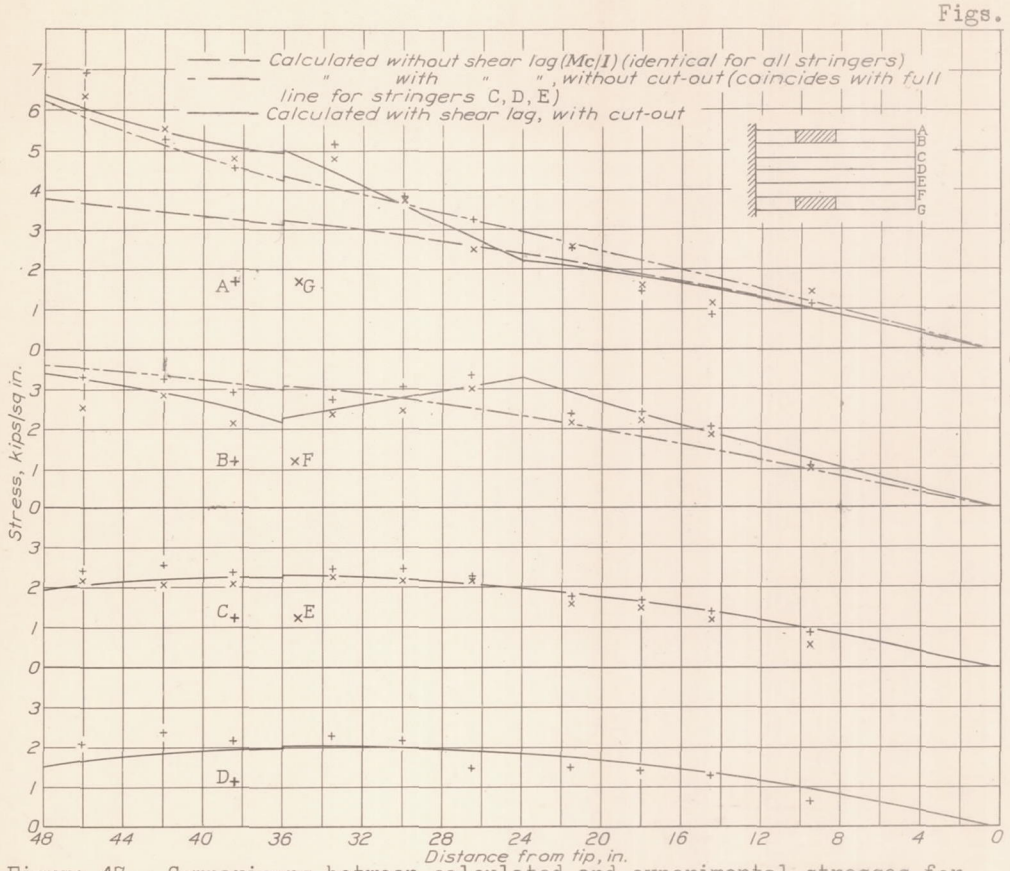

(a) Stress in flange. (b) Stress in center stringer.

Figure 44.- Comparisons between calculated and experimental stresses in beam of reference 5 for tip load.




(a) Stress in flange. (b) Stress in center stringer.

Figure 45.- Comparisons between calculated and experimental stresses in beam of reference 5 for distributed load.




Note- Break in Mc/I curve is counteracted by cover plate on tension flange at midspan.

Figure 47.- Comparisons between calculated and experimental stresses for beam 1, with small cut-outs.

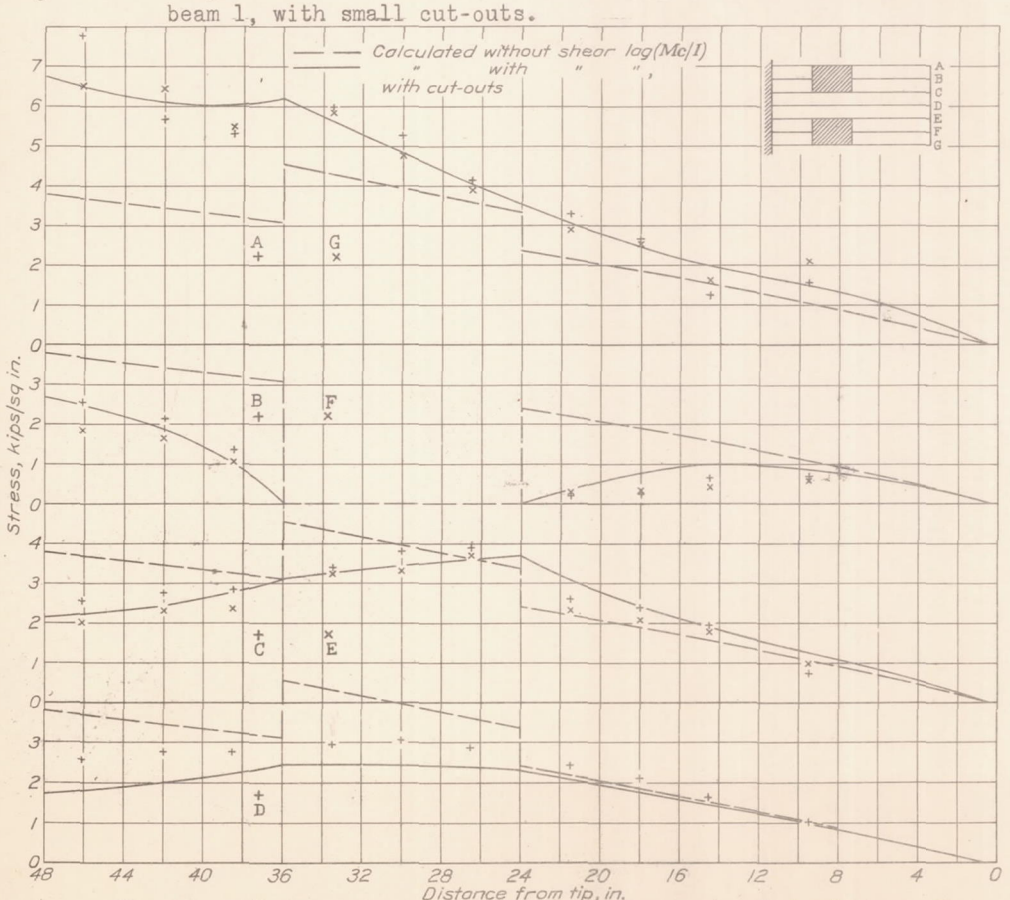



Figure 48.- Comparisons between calculated and experimental stresses for beam 1, with large cut-outs.

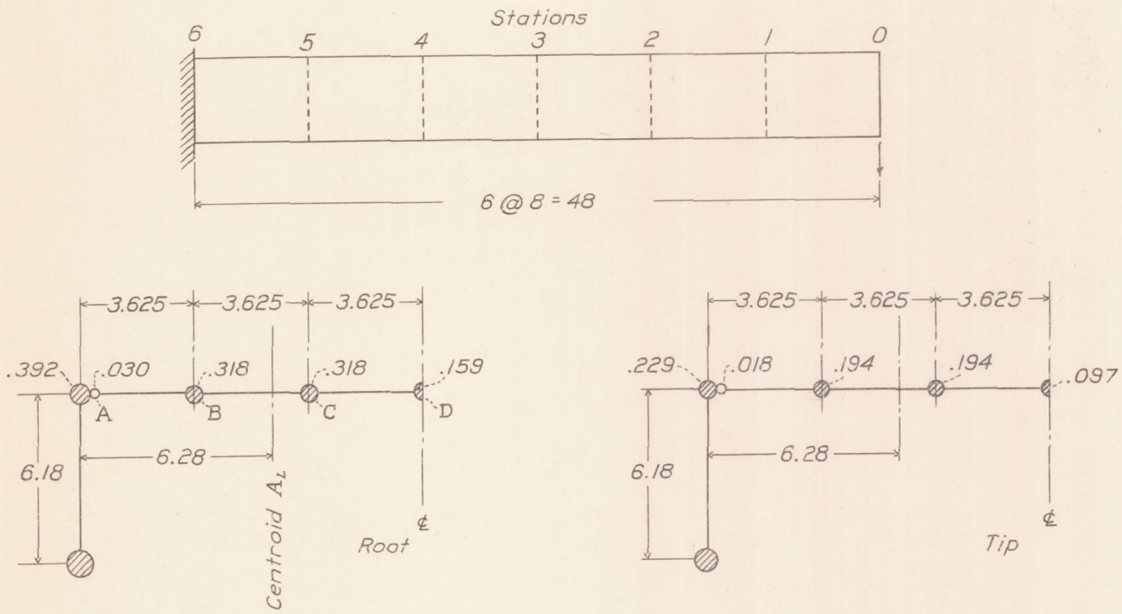



Figure 50.- Beam used for numerical examples.

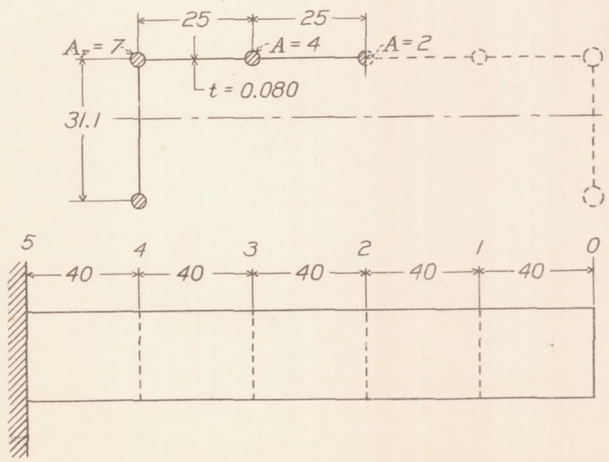


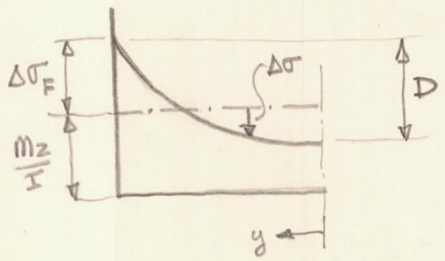

Figure 51.- Beam used by Ebner-Köller for numerical example (from reference 12). G/E = 0.385. Dimensions are in centimeter units.

For Conc. Load at tip:-

PANEL:- $\sigma_F = \frac{P}{A_T}\left[1 + \frac{A_L}{A_F}\frac{\cosh Kx}{\cosh KL}\right]$ $x = 0$ at root.

BEAM:- $\sigma_F = \frac{M}{hA_T}\left[1 + \frac{A_L}{A_F}\frac{\sinh Kx}{Kx \cosh KL}\right]$ $x = 0$ at tip.

---




$$\Delta\sigma = \Delta\sigma_F - D\left[1 - \left(\frac{y}{b}\right)^2\right]$$

where

$$D = \frac{4}{3} X \left(\frac{1}{A_F} + \frac{1}{A_L}\right)$$

---

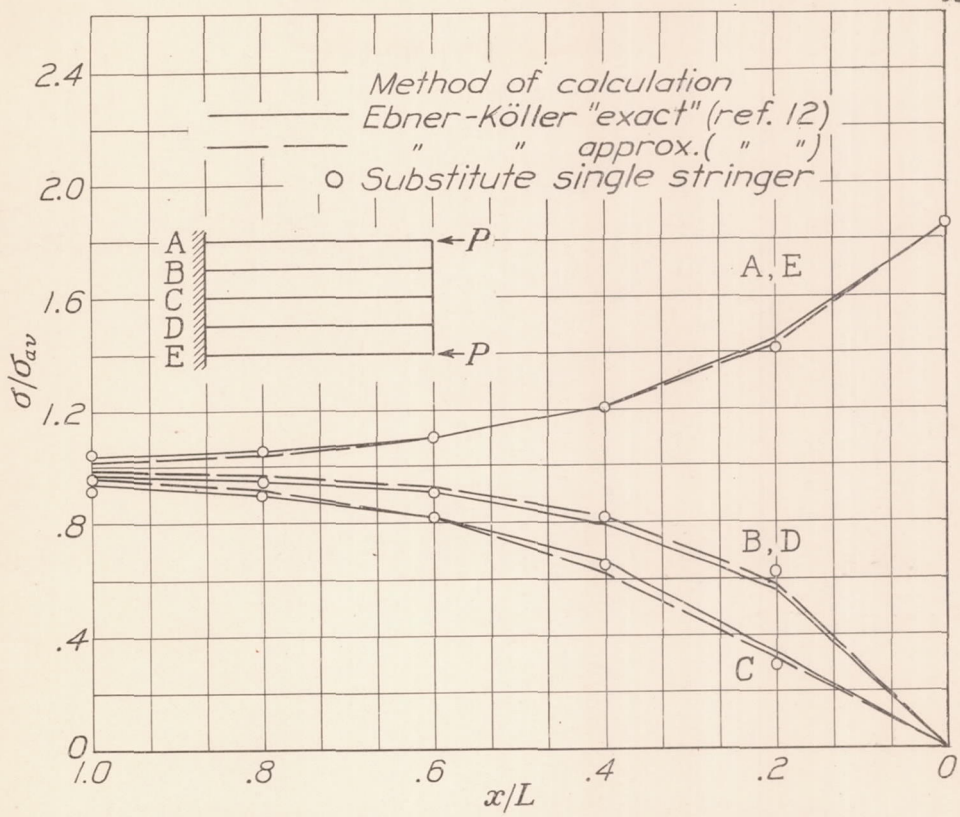



Figure 52.- Ebner-Köller beam, load case 1, analyzed by different methods.

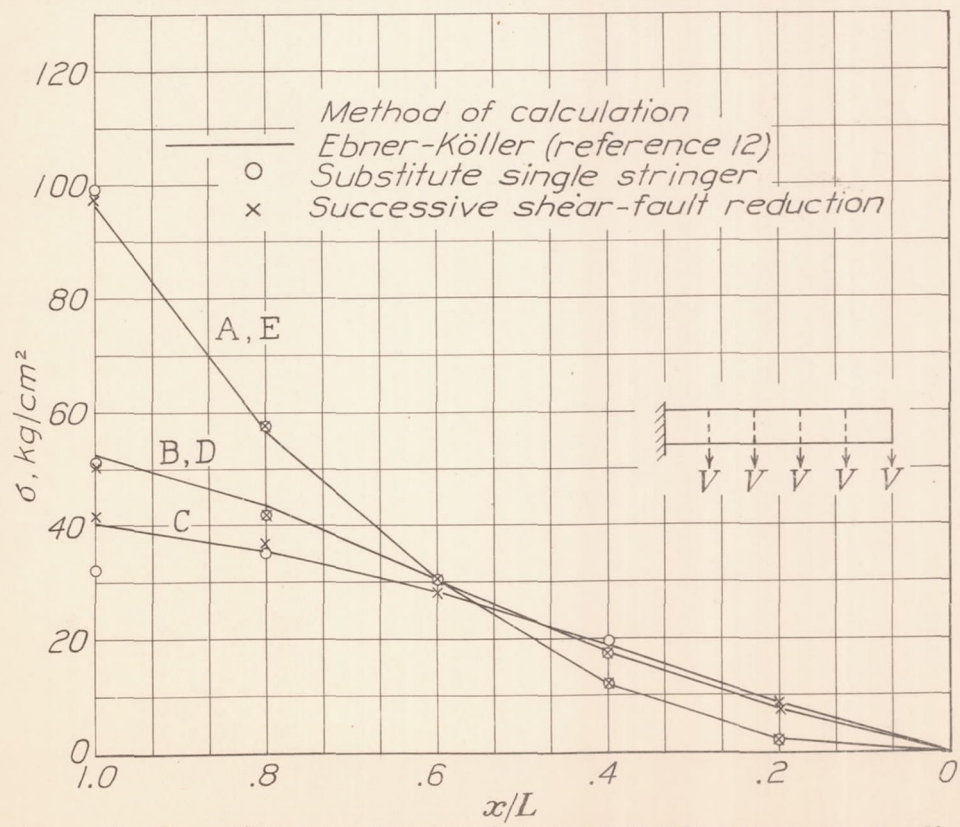
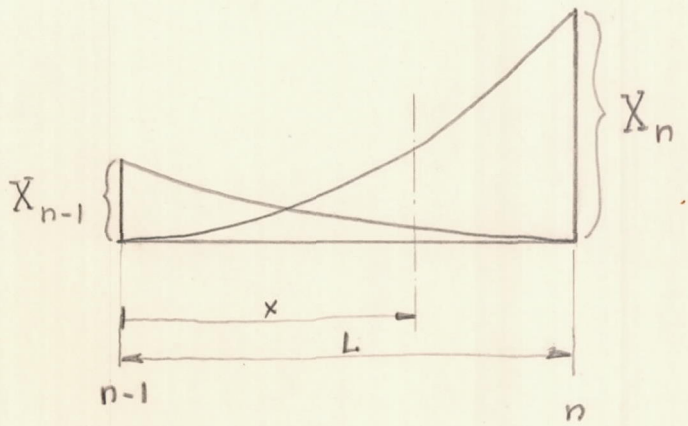



Figure 53.- Ebner-Köller beam, load case 2, analyzed by different methods. V = 50 kilograms on each shear web.

**BEAMS -**

Small ratio of $\frac{A_F}{A_L}$ and small $KL$ indicate large shear-lag effect. $\frac{A_F}{A_L}$ & $KL$ define the relative chordwise distribution; whereas, the loading defines the absolute magnitude [of $\Delta\sigma_F$ and $\sigma$]

---

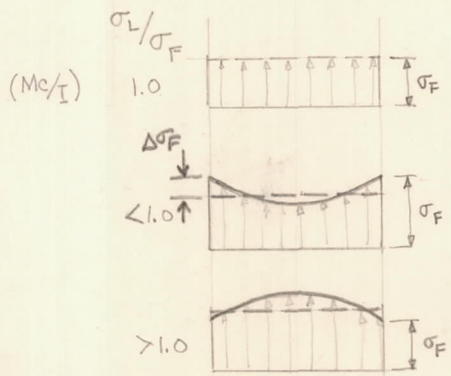



For interpolating within bay:

$$X_x = X_{n-1}\frac{\sinh K(L-x)}{\sinh KL} + X_n\frac{\sinh Kx}{\sinh KL}$$

[assuming shear is constant within bay, constant cross section, etc.]

---




SHEAR LAG EFFECT AT ROOT OF BEAM:-

CONC. LOAD $\Delta\sigma_F = \frac{Mc}{I}\left(\frac{A_L}{A_F}\frac{1}{KL}\right)$

DISTR. LOAD $\Delta\sigma_F = \frac{Mc}{I}\left(\frac{A_L}{A_F}\frac{2}{KL}\right)$